Novel experimental setup for coulometric signal transduction in ion-selective electrodes

Naela Villanueva Delmo

Master's programme in Excellence in Analytical Chemistry
Degree project in Analytical Chemistry, 30 credits

Laboratory of Molecular Science and Engineering
Faculty of Science and Engineering
Åbo Akademi University
Åbo, Finland
June 2022

Naela Villanueva Delmo

Co-funded by the
Erasmus+ Programme
of the European Union

Supervisor:

Docent Zekra Mousavi (Åbo Akademi University)

Co-supervisor:

Dr. Agnes Heering (University of Tartu)

Examiner:

Docent Tomasz Sokalski (Åbo Akademi University)

Date of the defense:

26 August 2022

TABLE OF CONTENTS

ABSTRACT

In this research work, a simple and versatile novel experimental setup for coulometric signal transduction in ion-selective electrodes was introduced and studied. It is based on a constant potential coulometry measurement carried out using a three-electrode electrochemical cell. Conventional potassium ion-selective electrodes (K^+-ISEs) and solid-contact potassium ion-selective electrodes (K^+-SCISEs) with either poly(3,4-ethylenedioxythiophene) doped with polystyrene sulfonate, *i.e.* PEDOT:PSS, or multi-walled carbon nanotubes as solid contacts were prepared and used in this work. In the setup, a K^+-ISE was connected as the reference electrode (RE). The potential difference between the RE (K^+-ISE) and a PEDOT:PSS-based working electrode (WE) was kept constant by using a potentiostat. The potentiometric response of K^+-ISE, which is due to change in the concentration (activity) of potassium ion in the sample, is transformed into amperometric and coulometric signals through the WE. Adding a non-selective dummy membrane to the structure of the WE and using a background electrolyte with high and constant concentration are significant steps in the regulation of the measured signal and equilibration time. These are also interesting strategies that helped ensuring the exclusive occurrence of analyte detection at the K^+-ISE and signal generation at the WE despite having a single-compartment configuration. Results from electrochemical impedance spectroscopy measurements showed that the time constant is heavily influenced by the dummy membrane thickness, and that the redox capacitance of the PEDOT:PSS film has a better correlation with the electrode area than the film thickness. Sequential addition/dilution experiments showed the improvement of current and cumulated charge signals in the new setup studied in this work compared to the setup used in the original coulometric signal transduction method. Furthermore, the responses were found to be reversible and reproducible across a variety of electrodes. Results from the calibration of different WEs with different K^+-ISEs used as RE presented a linear relationship between the cumulated charge and the logarithm of K^+ activity. It also confirmed the direct relationship between electrode area and electrode sensitivity. Lastly, measurements carried out using human serum sample showed that the new setup for coulometric signal readout could be used for detecting small concentration changes both in synthetic and real biological samples.

Keywords: coulometric signal transduction, solid-contact ion-selective electrodes, conventional ion-selective electrodes, potassium ion, PEDOT:PSS, MWCNT, chronoamperometry, chronocoulometry, electrochemical impedance spectroscopy

PREFACE

The research work presented in this thesis was done at the Analytical Chemistry Group in the Laboratory of Molecular Science and Engineering at Åbo Akademi University, in fulfillment of the requirements for the Erasmus Mundus joint master's degree programme Excellence in Analytical Chemistry (EACH), under the supervision of Docent Zekra Mousavi.

I would like to express my sincerest gratitude to my supervisor Docent Zekra Mousavi, for her experienced guidance and for being with me along the way as I make my first sensor up to the completion of this study. Thank you for your kindness, patience, and for motivating me during the toughest times of this journey. I would also like to thank Docent Tomasz Sokalski for his constant encouragement and for sharing his time and expertise for the improvement of this work. To Professor Johan Bobacka, thank you for suggesting this thesis topic and for all the help during our whole stay at ÅAU.

To Professor Ivo Leito and Dr. Anu Teearu-Ojakäär, thank you for this opportunity. Despite the unexpected circumstances that affected most of our stay in Tartu, we felt your genuine care and support to all of us. To my co-supervisor Dr. Agnes Heering, thank you for your help in writing this manuscript.

To my dearest EACH friends, especially to our group here at Åbo, I will forever cherish my experiences with you. I wish nothing but the best to all of us.

Finally, to my parents Nilo and Teresita, my sisters Nolissa and Nica Ann, my nieces Amanda and Mia, and to all my loved ones, thank you for being my inspiration and for supporting me in my dreams. Being away from home during some of the most unimaginable events in our lifetime is really difficult. But I am lucky to have people who truly believe that I can do it.

Åbo, June 2022

Written on a bright and warm summer evening,

with a grateful heart and unfaltering hope for the future.

Naela Villanueva Delmo

LIST OF SYMBOLS AND ABBREVIATIONS

AC	Alternating current
BGE	Background electrolyte
CE	Counter electrode
CP	Conducting polymer
CV	Cyclic voltammetry
CWE	Coated wire electrode
DC	Direct current
DM	Dummy membrane
DOS	Bis(2-ethylhexyl) sebacate
EDOT	3,4-ethylenedioxythiophene
EIS	Electrochemical impedance spectroscopy
ETH 500	Tetradodecylammonium tetrakis(4-chlorophenyl) borate
GC	Glassy carbon
ISE	Ion-selective electrode
ISM	Ion-selective membrane
KTFPB	Potassium tetrakis[3,5-bis(trifluoromethyl)phenyl] borate
MWCNTs	Multi-walled carbon nanotubes
NaPSS	Poly(sodium 4-styrene sulfonate)
OCP	Open circuit potential
PEDOT	Poly(3,4-ethylenedioxythiophene)
PEDOT:PSS	Poly(3,4-ethylenedioxythiophene) doped with polystyrene sulfonate
PPy	Polypyrrole
PVC	Poly(vinyl chloride)
RE	Reference electrode
SCISE	Solid-contact ion-selective electrode
WE	Working electrode
$Ø_{GC}$	Diameter of GC substrate
$Ø_{GC+PVC}$	Diameter of the GC substrate and the PVC disk
γ_i	Activity coefficient of species *i*

τ	Time constant
φ	Phase shift (angle)
ω	Angular frequency
a_i	Activity of species *i*
a_j	Activity of species *j*
A_{GC}	Area of the GC substrate
A_{GC+PVC}	Area of the GC substrate and the PVC disk
C	Molar concentration
C_{LF}	Low-frequency capacitance
E	Measured potential
$E°$	Standard potential
E_{cell}	Cell potential
E_{cp}	Potential of the conducting polymer
E_{ind}	Potential of the indicator (working) electrode
E_j	Liquid-junction potential
E_{pb}	Phase boundary potential
E_{ref}	Potential of reference electrode
$E(\omega)$	Angular frequency-dependent potential
f	Frequency
F	Faraday's constant (96485 C mol^{-1})
i	Primary ion (analyte)
I	Current
I_p	Current density
I_{polym}	Polymerization current
$I(\omega)$	Angular frequency-dependent current
J	Ionic strength
j_i	Interfering ion with respect to ion *i*
K_{ij}^{pot}	Selectivity coefficient
n	Number of electrons transferred during a redox reaction
Q	Cumulated charge
Q_{polym}	Polymerization charge

V_{DM}	Volume of the dummy membrane
V_{ISM}	Volume of the ion-selective membrane
r	Mean ionic radius
R	Universal gas constant (8.314 J $K^{-1}mol^{-1}$)
R_{DM}	Resistance of the dummy membrane
R_{ISM}	Resistance of the ion-selective membrane
s_d	Standard deviation
t	Measurement time
T	Absolute temperature
t_{polym}	Polymerization time
z_i	Charge of ion i
z_j	Charge of ion j
Z	Impedance
Z’	Real impedance
Z”	Imaginary impedance
$Z(\omega)$	Frequency-dependent impedance

1. INTRODUCTION

Detection and quantification of matter are among the most fundamental tasks in scientific research. With numerous instruments and techniques offering different analytical capabilities, it is important to consider what is the most suitable for the intended purpose. In environmental monitoring and clinical point-of-care diagnostics, robust, miniaturized, calibration and maintenance-free sensors are desirable for in-situ and long-term measurements[1–3]. Classical ion sensors are mostly potentiometric ion-selective electrodes (ISEs) that offer a wide linear range and good detection limits at optimized conditions[4,5] but the Nernst equation fundamentally restricts the relationship between potential and logarithm of the measured ion activity[4,6,7]. Conventional ISEs contain an internal filling solution essential to transform ionic to electronic conductivity, but it is also a major hindrance to achieving robustness and miniaturization[1,3,8]. The discovery of "solid contact" (SC) materials capable of replacing the internal filling solution enabled the fabrication of the so-called solid-contact ion-selective electrodes (SCISEs). Since then, numerous studies have been made towards developing electrode materials and new operational sensing mechanisms for improved sensitivity, stability, and overall performance[1,8,9].

In 2015, a novel coulometric signal transduction method for SCISEs was introduced by Bobacka's group. In this method, a three-electrode setup is used where the potential is kept constant between a conventional reference electrode (RE) and a conducting polymer-based SCISE connected as a working electrode (WE). A change in the primary ion activity alters the boundary potential at the ion-selective membrane/solution interface, which gives rise to the flow of a transient reducing/oxidizing current between the SCISE and the counter electrode (CE) until an opposite potential change is established at the conducting polymer-based solid contact. The total cumulated charge *(Q),* obtained from the integration of the transient current with time, was found to be linearly proportional to the change in the activity of the measured ion. Signal amplification and improved sensitivity can be achieved by increasing the electrode area, increasing the redox capacitance of the SC, and/or decreasing the membrane thickness[4,10,11].

Several configurations of this experimental setup have been investigated to provide alternative and versatile readout strategies alongside signal amplification and stabilization. Recently, the conversion of potentiometric responses to other signal readout mechanisms (*i.e.* current) by connecting the SCISE as the RE had provided promising results[7,12]. However, it uses a two-compartment electrochemical cell with a separate current-generating redox compartment connected by a salt-bridge; which, aside from some inherent instability[7,12], could also limit the possibility for miniaturization due to its complexity.

This thesis aims to study a simplified experimental setup for the coulometric signal transduction method in ISEs and to evaluate its analytical performance. For this purpose, the well-studied potassium ion-selective electrodes (K^+-ISEs) with valinomycin as ionophore, were chosen to carry out the study. Previous works have shown that vainomycin-based K^+-ISE is about 10000 times more selective for K^+ over Na^+, a common interfering ion[13]. Different electrochemical characterization techniques were used to gain a deeper understanding of the ion-to-electron transduction mechanism in the new experimental setup. The influence of parameters such as thickness of the dummy membrane and redox capacitance of the conducting polymer in the working electrodes were examined. Analytical performance characteristics such as linearity of the cumulated charge versus the analyte activity, sensitivity, and electrode-to-electrode reproducibility were assessed. The experimental setup was successfully used in measurements done using both synthetic samples and a real biological sample (human serum).

2. Chemical sensors

A chemical sensor is a device that selectively detects a certain analyte in a sample through a chemical reaction. It is composed of a recognition layer and a transducer (**Figure 1**). The analyte, which can be atoms, ions, or molecules in the solid, liquid, or even gaseous state, is detected at the recognition layer generating an input signal such as electron flow, change in color, or change in surface potential. The transducer transforms this input signal into an output signal related to the amount of analyte[14].

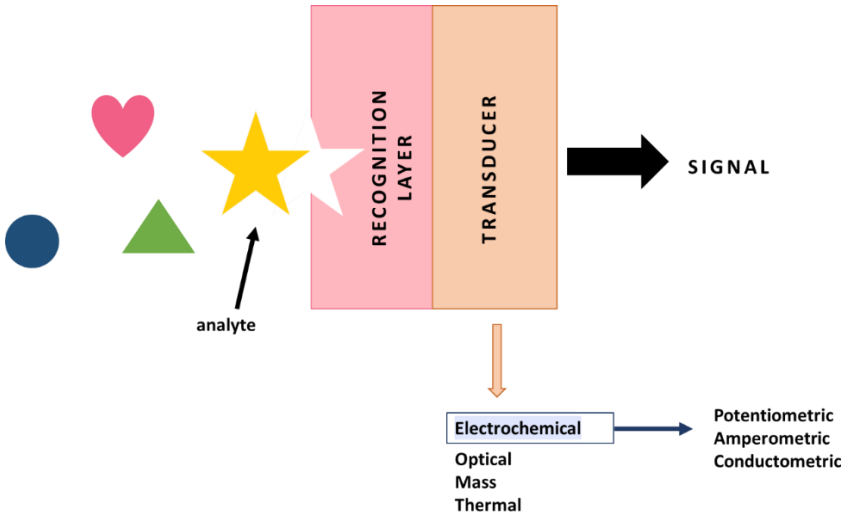

Figure 1. *A schematic representation of chemical sensor components and types of signal transduction.*

According to the type of signal transduction, chemical sensors can be divided into electrochemical, optical, mass, and thermal sensors. Electrochemical sensors are further classified into potentiometric, amperometric, and conductometric sensors based on the nature of the generated electrical signal. Potentiometric sensors, also called ion-selective electrodes, are studied in this thesis.

3. Ion-selective electrodes

Ion-selective electrodes are probably some of the most widely used electrochemical sensors. In terms of analytical performance, ISEs offer fast response, wide linear range, and good selectivity, making it an attractive analytical tool[15]. Over the years, potentiometric ISEs have become useful in a wide range of applications such as environmental, agricultural, and industrial analyses, but clinical application appears to be of the highest importance[16]. One successful example is the potassium ion-selective electrode (K^+-

ISE), which had since been broadly used in biological fluids instead of a flame photometer[14]. This wide range of analytical applications and increased scientific interest in ISEs is attributed to their small size, portability, low-energy consumption, little to no sample preparation, and relatively low cost compared to more complex instruments[8,14,16]. In addition, there have been continuous developments in terms of the improvement of the detection limit, membrane materials, and sensing concepts[5,8].

3.1. Conventional ISEs

A typical conventional ISE is composed of an ion-selective membrane (ISM), an internal reference electrode, internal filling solution, and an electronic wire conductor **(Figure 2**) The internal solution must contain the ion of interest for stable and reproducible potentials[16]. Both the ISM and the internal solution are ionic conductors. For instance, in a potassium ion-selective electrode (K^+-ISE), the charge is transferred by K^+ ions in the membrane and the internal solution. However, the external wire is an electronic conductor. Therefore, an internal reference electrode, most often Ag/AgCl wire, is needed for a reversible ion-to-electron transduction. Conventional ISEs give stable and reproducible potential and have been used for routine analyses for a long time.

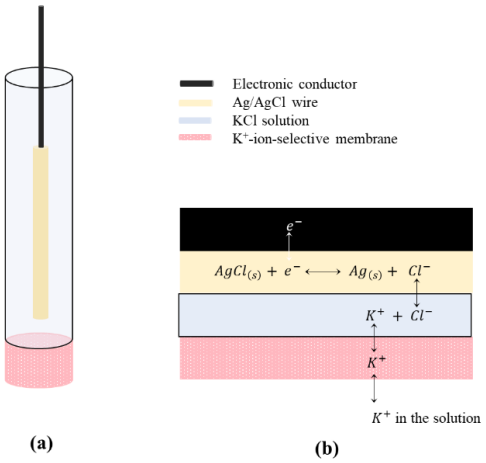

Figure 2. *A schematic illustration of a conventional K^+-ISE* ***(a)*** *and the ion-to-electron transduction mechanism in it* ***(b)****.*

However, the need for an internal reference electrode and filling solution also comes with several limitations. The internal filling solution must always be in contact with the inner surface of the ISM and the internal reference electrode for the ion-to-electron transduction, limiting the positioning of

conventional ISEs when in use. Moreover, evaporation of the filling solution must be prevented to avoid breaking the electrical circuit[17]. In some cases, additives and complexing agents are added to prevent freezing or to control the activity of the measured ion[16]. One of the most significant disadvantages of a conventional ISE is the difficulty of miniaturization, which limits the ISE's practical applications in environmental monitoring, biological, and clinical analyses [8,14,16].

3.2. Solid-contact ISEs

The above-mentioned drawbacks related to the configuration of conventional ISEs led to the increased interest in solid-state ion-selective electrodes. In 1971, Cattrall proposed the first all-solid-state ISE in the form of a coated wire electrode (CWE)[8], in which the ISM is directly coated on an electronic conductor (**Figure 3a**). However, due to the absence of a transducer between the purely ionic (ISM) and purely electronic conductors, difficulties in obtaining stable potential readings were encountered[5]. To solve this problem, the so-called solid-contact ion-selective electrode (SCISE) was introduced. In this type of sensor, a solid intermediate layer (solid contact) between the ISM and the electronic conductor serves as an ion-to-electron transducer, whereas the ISM determines the sensor's selectivity for a particular ion[18]. Different materials such as conducting polymers (CPs), carbon-based nanomaterials, and redox couples have been used as solid contact in fabricating all-solid-state ISEs[8]. The difference between a CWE and a SCISE with a redox-active solid-contact (SC) layer in terms of composition and ion-to-electron transduction mechanism is shown in **Figures 3a** and **3b**, respectively.

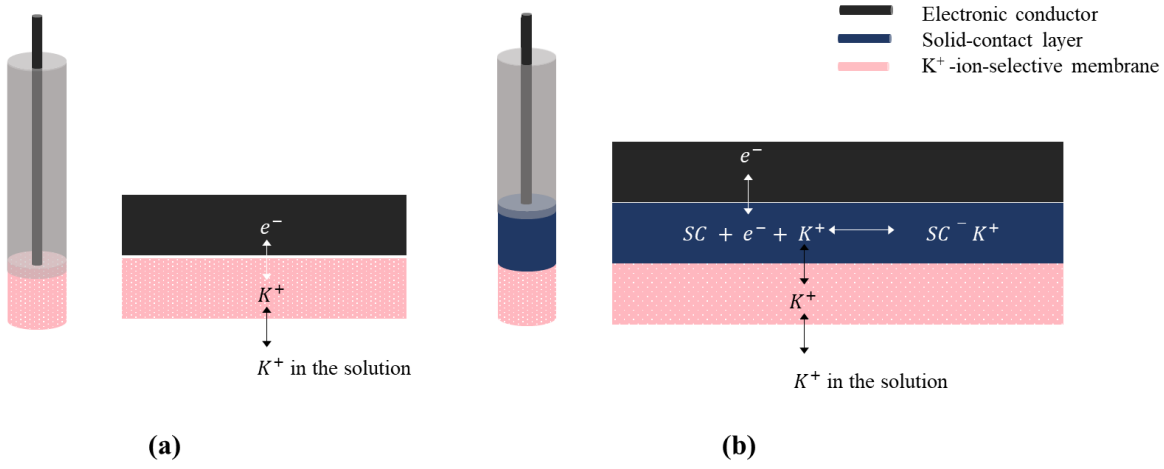

Figure 3. *Schematic illustration of the composition and the ion-to-electron transduction mechanism in K^+-selective CWE* ***(a)*** *and SCISE with a redox-active solid-contact (SC) layer* ***(b)***.

3.2.1. Conducting polymers as ion-to-electron transducers

A conjugated polymer consists of carbon chain with alternating single (σ) and double (π) carbon-carbon bonds that form extended π-conjugated system. Some of the commonly studied conjugated polymers include polyacetylene, polypyrrole (PPy), and polythiophene (**Figure 4**). In the pure form, the conductivity of conjugated polymers lies between an insulator to a conventional semiconductor, but doping drastically enhances the conductivity value up to that of metallic conductors[19]. Chemical doping is the introduction of chemical dopants (oxidizing and reducing agents)[20,21], but doping can also be performed by electrochemical oxidation and reduction[23] and can be coupled with polymerization, leading to a simultaneous and reversible oxidation (p-type)/reduction (n-type) of the polymer film. The reversible redox process of doping and undoping enables the migration of electric charges in the conjugated double bonds in the polymer structure with highly delocalized π electrons and gives the material its redox capacitance[8]. The delocalization of π electrons along the polymer backbone is responsible for the unusual electronic and optical properties of this type of polymers.

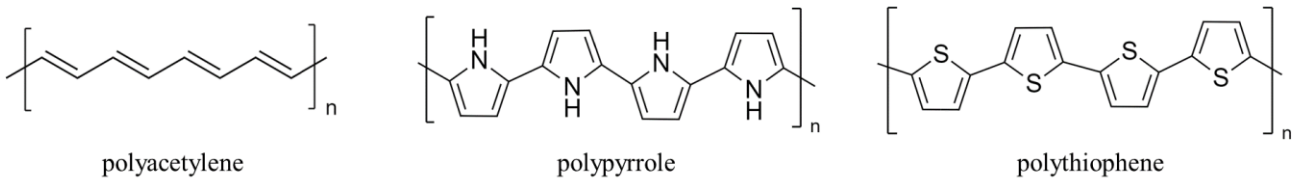

Figure 4. *Molecular structures of some common conducting polymers.*

Synthesis of CPs can also be done by various methods, typically by chemical and electrochemical means. Chemical polymerization by oxidation is a common route for redox polymers. It is a direct polymerization reaction in a monomer solution in the presence of an oxidizing agent and could be assisted by a catalyst[19]. One historically significant example is the serendipitous synthesis of polyacetylene with a halogen dopant and Zeigler-Natta catalyst. Further studies led to producing a material with excellent conductivity, and was eventually awarded by a Nobel prize in 2000[22].

The electrochemical polymerization can be performed either potentiodynamically (by potential cycling), potentiostatically, or galvanostatically. In the galvanostatic electrochemical polymerization method, a

constant current is applied for a certain time to achieve a specific polymerization charge and film thickness. Studies have shown that the capacitance of the electrochemically synthesized conducting polymer film is linearly related to the polymerization charge[23], so one can easily tune the polymerization parameters to achieve the desired properties. Those parameters include polymerization current (I_{polym}) and polymerization time (t_{polym}). For instance, if one wishes to double the thickness of the conducting polymer film, the t_{polym} must be doubled at constant I_{polym}. Moreover, if the same film thickness is to be deposited on a different area (*A)*, the current density (I_{polym}/A) must be kept constant by adjusting the I_{polym}, then the polymerization can be done at the same t_{polym}. The ease of control in the polymerization process is one significant advantage of electrochemical synthesis of CPs for electrodes and sensors compared to the chemical route, unless a large amount of polymer is needed[24].

CPs are interesting materials to be used as ion-to-electron transducers in the fabrication of SCISEs because of their ionic and electronic conductivity combined with outstanding mechanical properties and processability. A variety of monomer precursors and suitable electrolytes can be used to prepare conducting polymers. Because of this, there are many possibilities for functionalization, doping, and receptor immobilization (for biosensors)[20]. As shown in **Eq 1** and **Eq 2**, the choice of dopant can influence the ionic response of the polymer film. Oxidized conducting polymers are generally positively charged and have anion exchange sites, though it does not offer much selectivity[20]. If the dopant is a small anion (A^-), its movement in and out of the polymer film can be easily achieved during the oxidation/reduction process, giving the material an anionic response. On the other hand, a bulky anion (B^-) has restricted movement in the polymer film, resulting in the excess of negative charges. Small and mobile positively charged counterions move in and out of the film to compensate for these charges, giving it a cationic (C^+) response.

$$(CP^+ A^-)_{film} + e^- \longleftrightarrow (CP^0)_{film} + A^-_{solution} \qquad \textbf{Eq 1}$$

$$(CP^+ B^-)_{film} + C^+_{solution} + e^- \longleftrightarrow (CP^0 B^- C^+)_{film} \qquad \textbf{Eq 2}$$

Among the listed CPs, poly(3,4-ethylenedioxythiophene) (PEDOT) has a relatively wide potential window even in aqueous environments, is highly stable in its p-doped form, and has a high redox-capacitance and electronic conductivity, making it a suitable candidate as solid-contact[8]. When deposited onto an electronic conductor, it shows significantly less sensitivity to the presence of O_2 and CO_2

(changes in pH) in the sample solution compared to other CPs such as PPy, especially with a layer of polymer-based ion-selective membrane placed on top of the CP (solid contact) layer[25]. In this thesis, PEDOT doped with polystyrene sulfonate (PSS^-), *i.e.* PEDOT:PSS (**Figure 5**), was used as the ion-to-electron transducer in the fabrication of the studied electrodes.

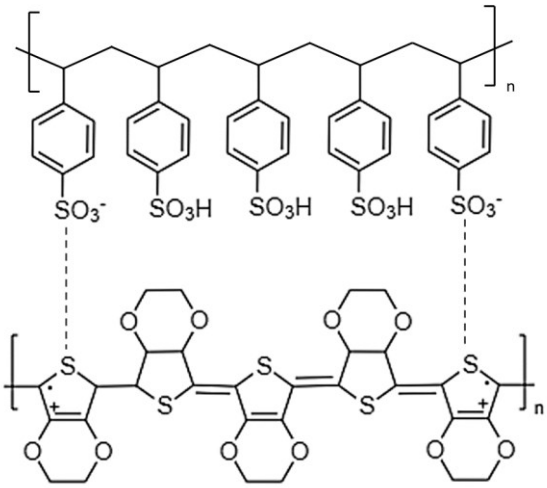

Figure 5. *The molecular structure of poly(3,4-ethylenedioxythiophene) (PEDOT) doped with polystyrene sulfonate (PSS^-).*

The PEDOT:PSS layer deposited on a glassy carbon substrate is electrochemically synthesized using the galvanostatic method. The bulky PSS^- anion has limited mobility in the PEDOT film, inducing the movement of positively charged ions to compensate for the resulted charge in the polymer backbone, giving the material a cationic response[23]. The process of ion-to-electron transduction is illustrated in **Figure 6**.

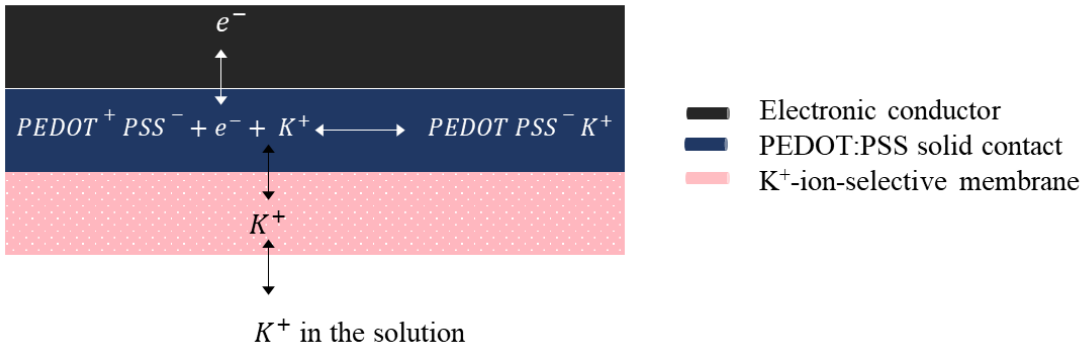

Figure 6. *A schematic illustration of the ion-to-electron signal transduction with PEDOT:PSS as solid contact.*

3.2.2. Carbon-based nanomaterials as ion-to-electron transducers

Carbon-based nanomaterials have attracted remarkable scientific and commercial interest in the past years, not only in the field of electrochemical sensing but also in other practical applications. Examples of these materials are fullerenes, porous carbon, carbon nanotubes, graphene, and carbon black with high surface areas[8]. The ability of these nanomaterials to function as ion-to-electron transducers originates from the formation of an electrical double layer (**Figure 7**) – one layer is formed by the accumulation of electronic charge on the nanomaterial layer, and the other is from the accumulation of ions in the ISM[26]. Compared to conducting polymers, the transduction mechanism in this case is purely capacitive as there is no redox reaction at the nanomaterial solid-contact layer/ISM interface. This can be an advantage as it reduces the possibility of interfering side reactions and offering greater stability[26].

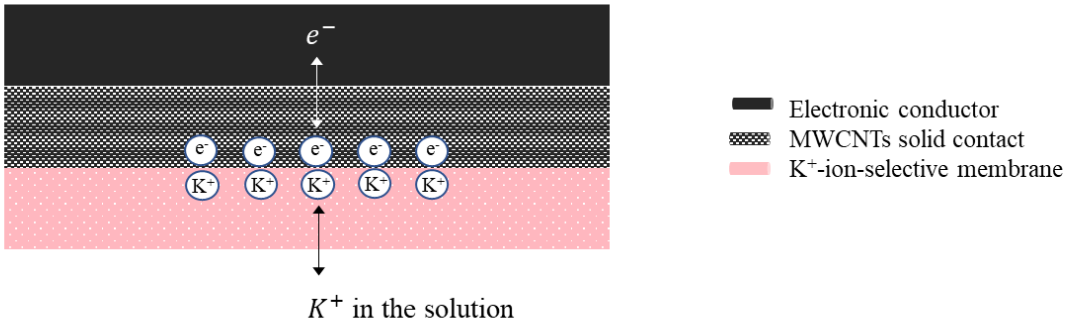

Figure 7. *A schematic illustration of the ion-to-electron signal transduction with a carbon-based nanomaterial as solid contact.*

The utilization of these materials as solid contacts is attributed to their high double-layer capacitance, insensitivity to light and oxygen, hydrophobicity which prevents the formation of a water layer between the ISM and the solid-contact layer, ease of handling, and relatively low cost[27,28]. In this study, multi-walled carbon nanotubes (MWCNTs) were used as solid contact in the preparation of K^+-SCISEs. MWCNTs, commonly synthesized by chemical vapor deposition, laser ablation, and carbon arc discharge, can be loosely described as graphene sheets that are seamlessly rolled into a hollow tube with a diameter of several nanometers and variable lengths of up to several micrometers (**Figure 8**)[29]. With

its fibrous nature, it carries properties such as elasticity, rigidity, and strength that are desirable for many practical applications.

Electrochemical impedance spectroscopy and cyclic voltammetry measurements carried out on electrodes with MWCNTs as solid contact showed high double-layer capacitance, making them excellent materials for ion-to-electron transduction[27]. different studies have been done utilizing single-walled[26,27], multi-walled[28,30,31], and functionalized[32] carbon nanotubes, on their own or in combination with other materials, as solid contact for ISEs.

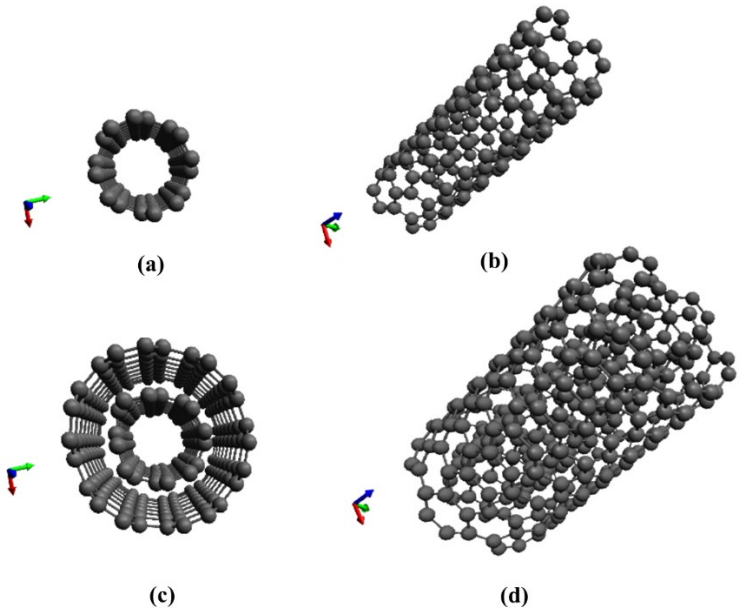

Figure 8. *Structures (top-view, side-view) of single-walled* ***(a, b)*** *and multi-walled* ***(c, d)*** *carbon nanotubes.*

3.3. Plasticized poly(vinyl chloride)-based ion-selective membranes

The possibility of immobilizing the components of ion-selective membranes into a polymer film was discovered in 1970 and has led to a cascade of advancements in the development of ISEs for various commercial applications[14]. The membranes used for the fabrication of ion-selective electrodes are prepared from a mixture of different reagents, which comprise the “membrane cocktail”. Poly(vinyl chloride) (PVC) is one of the main components of a membrane cocktail and is one of the most commonly used matrices in ISMs. High molecular weight PVC is used to reduce the ionic impurities in the ISM.

PVC-based membranes require plasticizers to ensure the flexibility of the membrane which is an important mechanical feature that allows the mobility of ions and ionophores[16].

Plasticizers are non-volatile organic liquids that exhibit certain lipophilicity. Its compatibility and suitability with PVC are of great importance – it must contain several branched alkyl chains to avoid crystallization. Still, certain functional groups should be avoided as well because they could influence the selectivity of the ISE[33]. In the case of ISM for monovalent cations, bis(butylpentyl)adipate, and bis(2-ethylhexyl)sebacate (DOS) **(Figure 9)** are used. Most of the PVC-based membranes contain PVC and plasticizers in a 2:1 ratio[16].

The component responsible for the selectivity of K^+-ISEs fabricated in this thesis is the ionophore valinomycin **(Figure 9)**. It consists of twelve alternating amino acids and esters that form a macrocyclic molecule. The excellent selectivity of this ionophore to K^+ ion is attributed to its cavity that closely matches the size of K^+ ion and the six carbonyl ester oxygen atoms capable of forming stable but reversible valinomycin-K^+ complex[14]. Because of this, valinomycin-based K^+-ISEs have been extensively used especially in biomedical applications, *e.g.,* on-site determination of K^+ concentration in blood and urine[1,9].

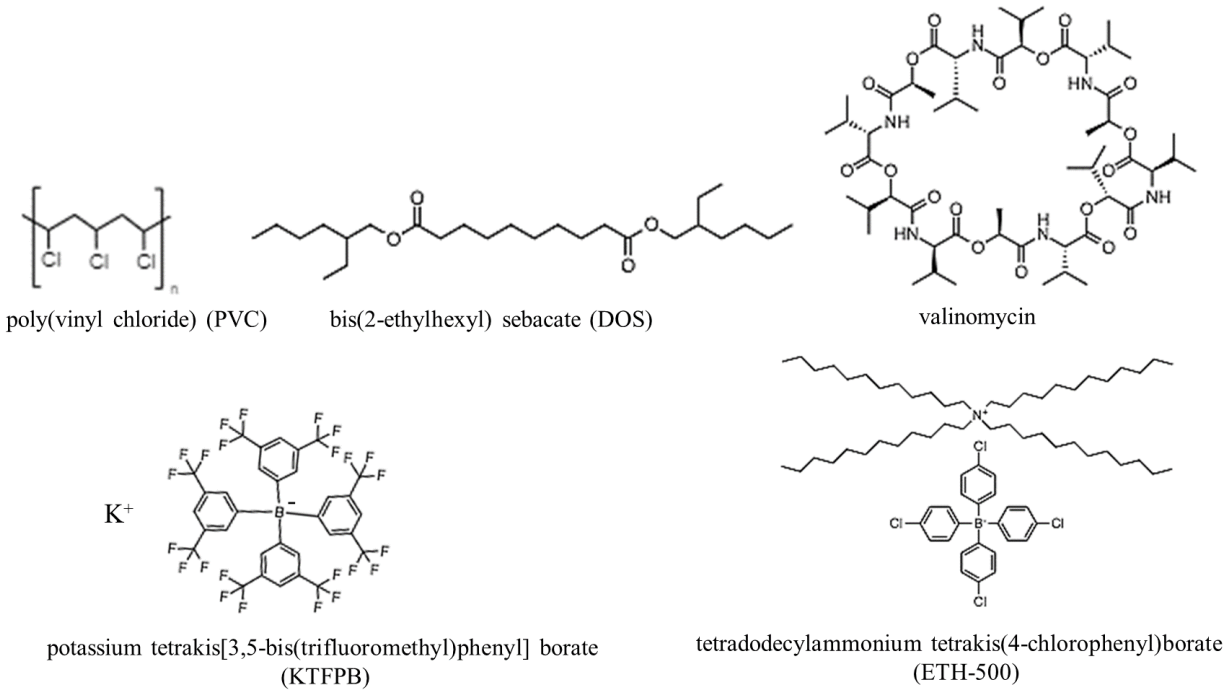

Figure 9. *Molecular structures of the different components of K^+-ISM.*

Lastly, a small amount of lipophilic salt is needed to preserve electroneutrality and reduce the membrane resistance. A lipophilic salt composed of a lipophilic anion and a hydrophilic cation (same as the primary ion) is suitable for cation-selective electrodes. The lipophilic anion stays in the membrane while the hydrophilic cation is free to move between the plasticized PVC membrane and solution interface[34]. Lipophilic anionic additives such as tetraphenylborates are good examples of this. The negative charge of the lipophilic anion reduces the possible anionic interferences in cationic ISEs. Still, despite being anionic, the charged sites are highly sterically hindered and would not interfere with the selectivity of the membrane[35].

Despite its great contribution to achieving desirable membrane properties, the amount of added salt must not surpass that of the ionophore. Moreover, salts with high lipophilicity such as tetrakis[3,5-bis(trifluoromethyl)phenyl] borate ($TFPB^-$) **(Figure 9)** which is also used in this study, are preferred to slow down the eventual and unavoidable leaching process that reduces the lifetime of the membrane, even without the ionophore[35]. In more recent ISE fabrication, tetradodecylammonium tetrakis(4-chlorophenyl) borate (ETH 500) **(Figure 9)**, which has lipophilic cation and anion, is also typically incorporated in the membrane cocktail to reduce the resistance of the membrane[36].

4. Principles of ion-to-electron signal transduction

4.1. Potentiometric signal transduction method

In a classical perspective, ISEs are considered as potentiometric sensors. An electrical potential is developed when the sensing element at the electrode surface selectively recognizes the target ion[14]. A typical two-electrode electrochemical cell used in potentiometric measurements is shown in **(Figure 10).** It consists of a RE with an accurately known and stable potential (E_{ref}) that is independent of the measured analyte and an indicator or ion-selective electrode which responds to changes in the concentration (activity) of the measured analyte and has the potential E_{ind}. Another important parameter that should be considered in potentiometric measurements is the liquid-junction potential (E_j) which develops at the interface between two dissimilar solutions, usually between the inner filling solution in the RE and the sample solution[15].

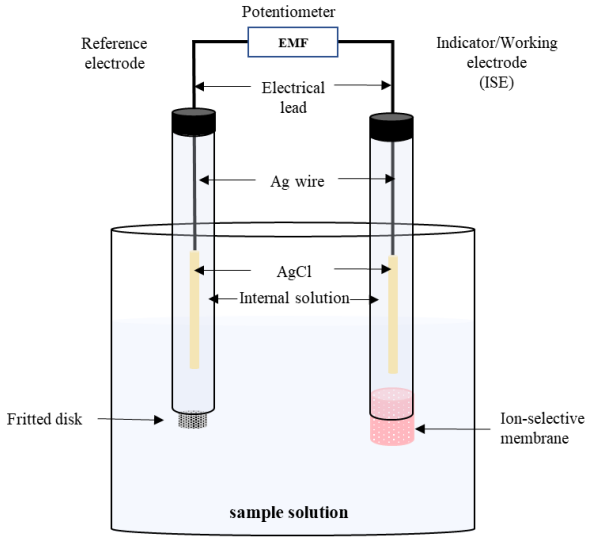

Figure 10. *A schematic representation of the setup used in potentiometric measurements.*

Considering all the above-mentioned potential values, the overall cell potential E_{cell} is calculated **(Eq 3)**. If E_{ref} and E_j are maintained constant throughout the measurement, then the measured potential depends solely on E_{ind}.

$$E_{cell} = E_{ind} - E_{ref} + E_j \qquad \textbf{Eq 3}$$

In potentiometry, the term activity (a_i) is used to indicate the effective concentration of the measured ion i. It is calculated as the product of the activity coefficient (γ_i) and the molar concentration (C_i) of the ion of interest **(Eq 4)**. The parameter γ_i depends on the ionic strength (J) of the solution **(Eq 5)** and can be estimated using the Debye-Hückel equation **(Eq 6)**, where A and B are constants depending on the solution and temperature, and r is the mean ionic radius of the hydrated ion. In this approach, the electrostatic interactions caused by the charge of the ions (z_i) are taken into consideration[37].

$$a_i = \gamma_i . C_i \qquad \textbf{Eq 4}$$

$$J = \frac{1}{2}\sum_i C_i z_i^2 \qquad \textbf{Eq 5}$$

$$log(\gamma_i) = \frac{A z_i^2 \sqrt{J}}{1 + rB\sqrt{J}} \qquad \textbf{Eq 6}$$

The relationship between the measured potential of the electrode (E) and the activity of the analyte i (a_i) is described in Nernst equation. Two forms of the equation are shown in **Eq 7** and **Eq 8** where $E°$ is the

standard potential, R is the universal gas constant (8.314 J·mol^{-1}·K^{-1}), T is the absolute temperature, z_i is the charge of the primary ion, and F is the Faraday constant (96485 C·mol^{-1}). Following the equation, a plot of E vs log a_i is a straight line with a slope of 2.303 $RTz_i^{-1}F^{-1}$. For instance, the slope of the calibration curve for a monovalent cation and anion-selective electrode conforming to the Nernst equation would be 59.2 mV decade^{-1} and −59.2 mV decade^{-1} at 25 °C, respectively [38], as shown in **Figure 11.**

$$E = E^o + \frac{RT}{z_i F} ln(a_i) \qquad \textbf{Eq 7}$$

$$E = E^o + \frac{2.303RT}{z_i F} log(a_i) \qquad \textbf{Eq 8}$$

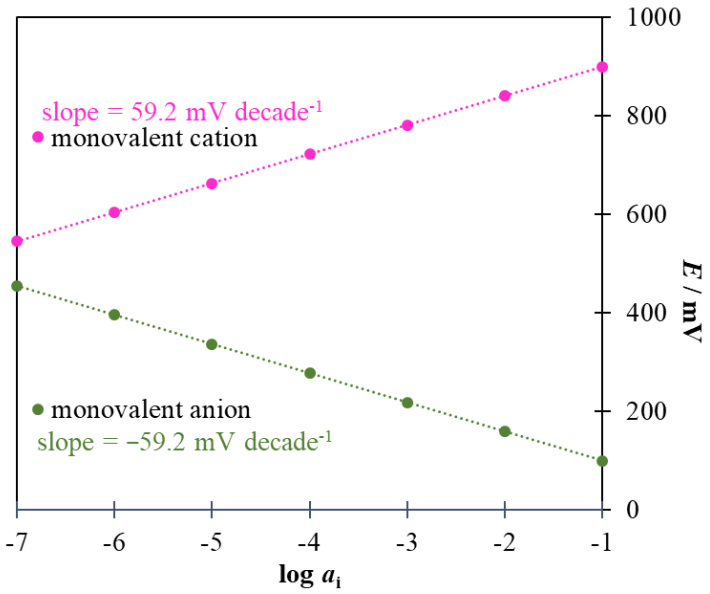

Figure 11. *A schematic representation of the Nernstian reponse of cationic and anionic ISEs.*

Under ideal conditions, the recognition element in an ISE should respond specifically and solely to the measured analyte. However, it is important to note that it is not the case in practical applications. Interfering species in the solutions, especially in more complex ones, will also contribute to the overall response of the sensor. The extent at which the interfering ions influence the potentiometric response of the ISE is quantified by the parameter selectivity coefficient (K_{ij}^{pot}), mathematically described by the Nikolskii-Eisenmann equation **(Eq 9)**, where a_i and a_j are the activities of the primary and interfering

ions with charges z_i and z_j, respectively. If K_{ij}^{pot} is equal to one, then a_i and a_j have equal contributions to the potentiometric response and the sensor is not selective. Typically, ISEs have extremely low values of K_{ij}^{pot} which means they are, by a big magnitude, more responsive towards the primary ion, making ion- "selective" a more appropriate term[14]. However, the effect of a_j can be more pronounced at very low a_i, near the detection limits.

$$E = E^{o} + \frac{2.303RT}{z_i F}\log(a_i + K_{ij}^{pot} a_j^{z_i/z_j}) \qquad \textbf{Eq 9}$$

4.2. Coulometric signal transduction method

Despite the recent advances in potentiometric SCISEs, obtaining stable and reproducible standard potentials is still a challenge. Solving this problem could potentially lead to the development of calibration-free sensors. The limitation due to the logarithmic relationship between analyte activity and measured potential as governed by the Nernstian equation also reduces the sensitivity of the potentiometric ion-to-electron transduction method[6]. Moreover, the signal produced from potentiometric measurements have poor resolution, only down to the mV range[12].

This is especially problematic in clinical analysis where the measured concentration intervals are very small. For example, maintaining the normal potassium homeostasis (3.5 mmol L^{-1} to 5.3 mmol L^{-1} K^+) in extracellular fluids is critical and needs to be monitored in some patients[39]. For this reason, non-conventional electrochemical readout protocols have been studied, such as coulometry[11,40], amperometry[12,41], and voltammetry[42], with the first two being the focus of this study.

In 2015, Bobacka et al.[40] introduced a novel transduction principle based on the redox capacitance of the conducting polymer solid contact in ISEs. It employed a three-electrode electrochemical cell with a potentiostat to maintain a constant potential difference between the WE and the RE. As shown schematically in **Figure 12**, a change in the activity of the primary ion (Δa_{K+}) **(1)**, results in a change in the phase boundary potential (ΔE_{pb}) at the ISM/solution interface **(2)**. Since the potential between K^+-SCISE and RE is kept constant by the potentiostat, a transient current (I) will flow between the counter

electrode (CE) and the K^+-SCISE **(3)**. The generated current causes oxidation/reduction of the conducting polymer layer and it will stop when the change in potential of the conducting polymer (ΔE_{cp}) exactly compensates for the potential difference at the ISM/solution interface and a new state of equilibrium is reached **(4)**. The generated current-time curve is integrated to obtain the cumulated charge (Q) **(5)** which is proportional to $\log\Delta a_{K+}$ and to the redox capacitance of the CP as solid contact[40].

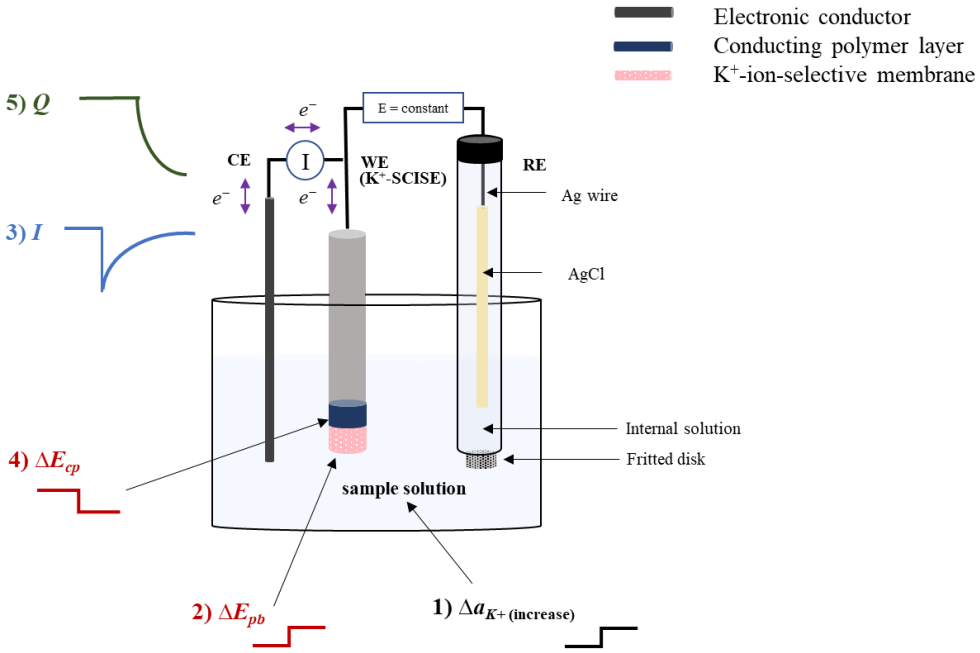

Figure 12. *A schematic illustration of the principle of coulometric signal transduction method in a three-electrode setup with a K^+-SCISE connected as the WE. The parameter ΔE_{pb} is the change in phase boundary potential at the ISM/solution interface and ΔE_{cp} is the change in potential at the conducting polymer solid contact. The small graphs show the change of the corresponding signal in time.*

Increasing the capacitance of the solid contact results in the magnification of the signal readout, which is significantly useful for applications such as clinical analysis and environmental monitoring that require quantification of minute changes in ion activity[43]. However, this signal amplification was obtained at the expense of the response time. Increasing the electrode area at constant electrode capacitance significantly shortened the response time, suggesting that the distribution of the same redox capacitance over a larger area allowed better accessibility and faster equilibration time[10]. Moreover, lowering the membrane resistance was found to produce sharper transient current and cumulated charge peaks, improve the

SCISE sensitivity, and shorten the coulometric response time[4,11]. The studied transduction method also worked well with cationic and anionic SCISEs, using different solid-contact materials such as conducting polymers[4,11,40,43,] and nanomaterials[6], and in measurements done using real samples such as seawater and blood serum samples [4].

The constant potential coulometric transduction method paved the way for multiple studies where the potentiometric response of the ISE is used to produce another electrochemical response, which could be in the form of current and/or charge and is related to the amount of analyte. Yin et al.[7] proposed a new strategy based on the oxidation of H_2O_2, employing a two-compartment electrochemical cell connected by a salt bridge **(Figure 13)**. In one compartment (sample cell), there is an SCISE, serving as a potentiometric ion sensor, that is connected as the RE. The other compartment (detection cell) contains a glassy carbon rod as the WE and a platinum (Pt) wire as the CE, both submerged in H_2O_2. An amperometric response (oxidation current of H_2O_2) is induced when a potential change in the SCISE is detected due to a change in primary ion activity. This signal readout setup showed good sensitivity, even better than the classical potentiometric method, but the instability of H_2O_2 limited its practical applications. Under the same principle, Sun et al.[12] utilized redox probes that offer more stability, such as ferrocyanide/ferricyanide ($Fe(CN)_6^{3-/4-}$), for translating the potentiometric response of the SCISE connected as the RE into amperometric signals that are related to change in the analyte activity.

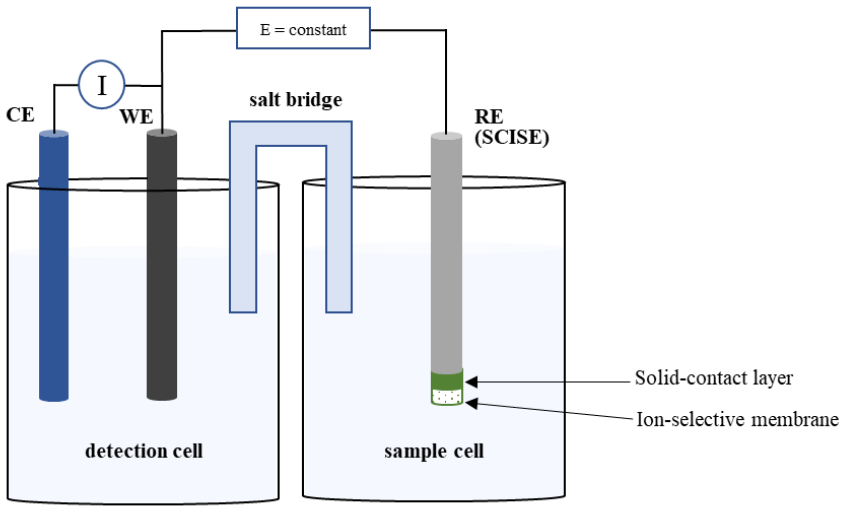

Figure 13. *A general schematic illustration of a two-compartment electrochemical setup for an alternative coulometric signal readout method.*

In the work done in this thesis, a novel experimental setup was used and studied which is simpler and more convenient compared to those used in the previous works mentioned earlier[7,12]. In this case, the general principle of operation and the signal transduction is still based on the constant potential coulometry described above. In the setup studied in this work, an ISE is used as a potentiometric ion sensor where the analyte detection takes place. Moreover, this ISE is connected as the RE that has a fixed potential difference with the WE, where the signal transformation takes place. The new configuration offers an alternative approach in compartmentalizing analyte-dependent potentiometric response from signal transformation and readout.

The WE was capable of generating transient currents by depositing a CP (PEDOT: PSS) layer on GC disk electrode. As it is well known, PEDOT:PSS is cationic sensitive, but not selective. Therefore, a possible problem could be that the WE (GC/PEDOT:PSS) would also respond to changes in the (cationic) analyte activity. This defeats the goal of having the potentiometric detection occurring only at the ISE and weakens the validity of the whole setup. To address this problem, a high concentration of background electrolyte (BGE) was used to mask the relatively smaller changes in analyte activity that could be detected at the WE. Thus, despite having the RE (ISE) and WE in the same compartment, the WE is not directly affected by changes in the analyte activity. The response time and signals generated at the GC/PEDOT:PSS electrode with high-redox capacitance was regulated by the addition of a non-selective dummy membrane (DM), containing all the components used in a K^+-ISM except valinomycin, to impart resistance to the electrode without affecting its sensitivity. The amperometric and coulometric responses in the WE were fine-tuned by preparing GC/CP/DM electrodes with different thicknesses of the CP layer and DM.

The mentioned strategies permitted the merging of the sample recognition and signal readout compartments into a single electrochemical cell, eliminating the need for a salt bridge[7,12], and reducing the overall complexity of the setup. A good feature of the novel setup presented in this work is that in principle it could work with any potentiometric ISE (conventional or solid-contact) connected as the RE. In this study, the compatibility of the setup with both solid-contact ISEs and conventional ISEs (with inner filling solution) was investigated, whereas only solid-contact ISEs can be utilized when using the original coulometric signal transduction method[4,6,10,43]. This gives the new setup versatility to a wider range of applications.

The signal transduction mechanism in this novel experimental setup is illustrated in **Figure 14** with K^+-SCISE, as an example for a K^+-ISE, connected as RE and GC/CP/DM as the WE. Following the principles of constant potential coulometry, the potential between the working and reference electrodes is kept constant by a potentiostat throughout the whole measurement. Any change in the analyte concentration **(1)** leads to a change in the phase boundary potential (ΔE_{pb}) at the ISM/solution interface in the K^+-SCISE connected as RE **(2)**, and thus a new potential difference is established between the WE and RE. As the potential between the WE and RE is forced to stay constant by a potentiostat, any change in the potential of the RE (K^+-SCISE) will cause the same potential change at the WE. This results in a transient current that flows between the WE and CE **(3)** causing the oxidation/reduction of the conducting polymer layer in the WE untill a new state of equilibrium is reached **(4)** to maintain a constant potential difference with the RE. Integration of the current-time transient gives the cumulated charge (Q) **(5),** which is proportional to the change in the activity of the measured ion and can be used as the analytical signal.

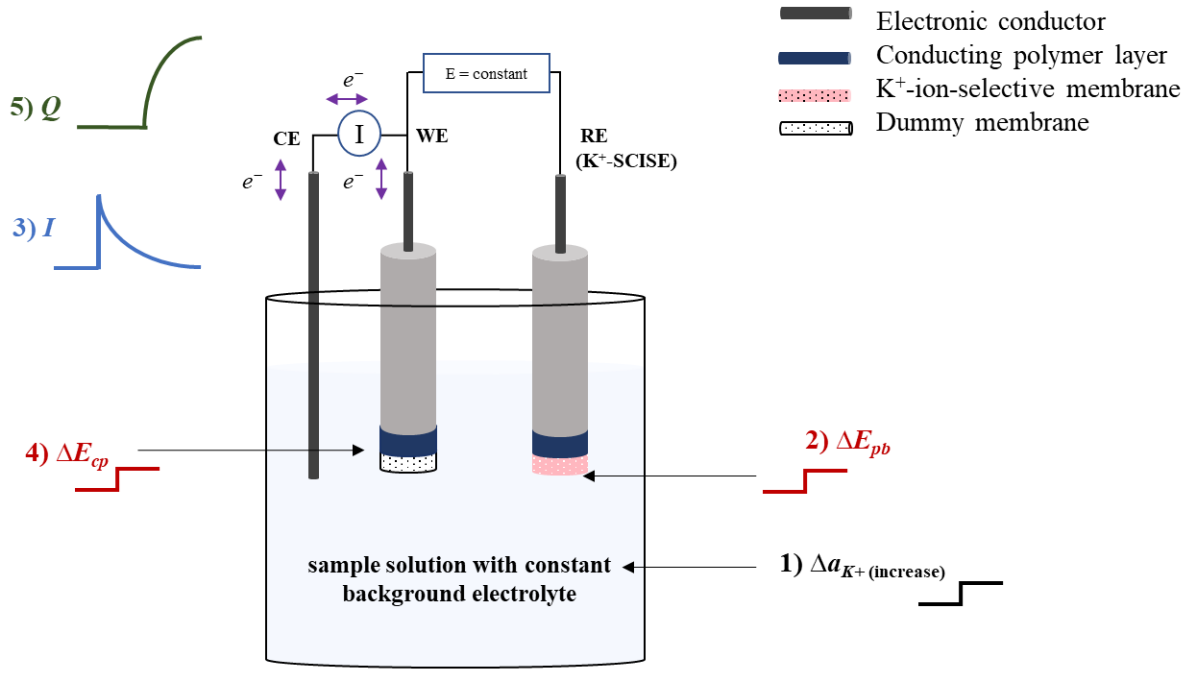

Figure 14. *Schematic illustration of the novel experimental setup studied in this thesis with a GC/CP-based K^+-SCISE connected as the RE. A GC/CP/DM electrode and GC rod are connected as the WE and CE, respectively. The parameter ΔE_{pb} is the change in phase boundary potential at the ISM/solution interface and ΔE_{cp} is the change in potential at the CP layer in the WE. The small graphs show the change of the corresponding signal in time.*

5. Characterization techniques

5.1. Cyclic voltammetry

Voltammetry is defined as a collection of electroanalytical methods based on current measurement as a function of applied potential[44]. As a characterization technique, CV is often the first test performed on an electrode[2]. For a cyclic voltammetric measurement, a three-electrode electrochemical cell is used composed of RE, WE, and CE. The potential is changed between the working and the reference electrodes, while the current flowing between the working and the counter electrodes is measured. The total current response is the sum of the faradaic and non-faradaic charging background (capacitive) currents. Faradaic current is produced from change in the oxidation states of redox species at the electrode surface and can be used to measure the rate of a redox reaction[45].

Current response is recorded as the potential is linearly cycled between two (or more) set of values. The starting potential is typically the open circuit potential (OCP) where there are no faradaic processes happening due to the absence of redox-active species at the electrode surface[45]. Once the upper limit of the range or the switching potential is reached, the potential direction is reversed, ultimately going back to the initial value[37]. The potential-time profile during CV has a triangular appearance, indicating one full cycle/sweep **(Figure 15)**. A plot of current against applied potential is called a voltammogram. As per the IUPAC convention, anodic currents are taken to be positive, whereas cathodic currents are negative[46]. If there are no faradaic species at the set potential range, symmetrical anodic and cathodic waves without peaks are expected, which means that the current recorded is purely capacitive. As previously mentioned, io-to-electron transducer materials with high capacitance are beneficial for SCISEs.

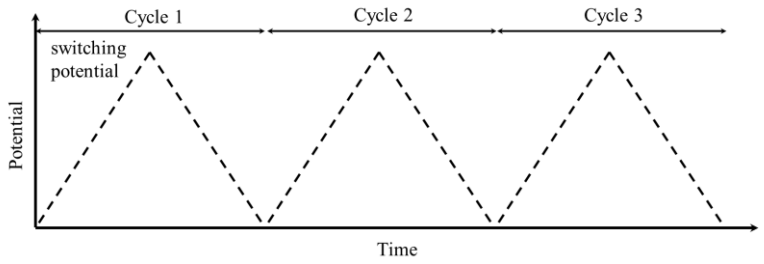

Figure 15. *Potential-time profile in cyclic voltammetry.*

Cyclic voltammetric measurement was used in this thesis for (i) checking the polished bare GC electrodes, (ii) checking the deposition of the PEDOT:PSS and MWCNTs solid contacts on GC substrates, and (iii) having an insight on the capacitive behavior of the said ion-to-electron transducers.

5.2. Electrochemical impedance spectroscopy

Electrochemical impedance spectroscopy (EIS) is another informative technique used for the characterization of the properties and mechanism of the charge transfer kinetics at the bulk of the membrane, the membrane/solution boundary, and the boundary layers[16,23]. An EIS measurement is performed in a three-electrode electrochemical cell containing a RE, WE, and CE. When a constant potential (E_{DC}) is applied to a system with a certain resistance R, a corresponding constant current will be generated with a value equal to the ratio of the potential and resistance according to Ohm's law[44] (**Eq 10**). Similarly, when the cell is perturbed with small and alternating sinusoidal excitation potential ($E(\omega)$), the output signal ($I(\omega)$) produced is a sinusoidal alternating current (AC) of the same frequency but with a corresponding shift in phase. The applied alternating potential ($E(\omega)$) and the response signal ($I(\omega)$) are described in **Eq 11** and **Eq 12**. In the equations, E is the amplitude of applied potential, and I is the amplitude of the measured signal, ω is the angular frequency equal to $2\pi f$, f is the frequency in Hz, t is the time, and φ is the phase shift (angle) between the $E(\omega)$ and the $I(\omega)$. In an EIS experiment, the input and output signals are applied and measured at a broad range of frequencies, typically 10^{-6} – 10^{-2} Hz [37, 44].

$$E_{DC} = IR \qquad \textbf{Eq 10}$$

$$E(\omega) = E \sin(\omega t) \qquad \textbf{Eq 11}$$

$$I(\omega) = I \sin(\omega t + \varphi) \qquad \textbf{Eq 12}$$

Looking back at Ohm's law in **Eq 10**, impedance (Z) is said to be analogous to resistance, but for an AC instead of a DC[44] and is equal to the ratio of $E(\omega)$ and $I(\omega)$ as shown in **Eq 13**. As a frequency-dependent complex quantity, the complete electrochemical impedance ($Z(\omega)$) is expressed as the sum of the real and imaginary portions (**Eq 14**) where Z' is the real impedance representing the frequency-dependent

resistance, and Z'' is the imaginary impedance representing the frequency-dependent reactance, with $j = \sqrt{-1}$[47].

$$Z(\omega) = E(\omega)/I(\omega) \quad \textbf{Eq 13}$$

$$Z(\omega) = (Z') - j(Z'') \quad \textbf{Eq 14}$$

One way to represent impedance graphically is by a Nyquist plot, in which the real impedance (Z') is plotted on the x-axis and the imaginary impedance, commonly a negative value, is plotted as $-Z''$ on the y-axis[37]. Though not explicitly shown in the plot, the frequency decreases from left to right. During experiments, it is also a common practice to start at higher frequencies. The resulting Nyquist plot can be seen as a schematic representation of different processes occurring within the electrochemical cell and can be used to build an equivalent circuit.

The concept of an equivalent circuit is one of the most important aspects of impedance analysis, where an electrochemical cell is assumed to be approximated or represented by an array of electrical components such as resistors and capacitors. For instance, the phase angle describes the behavior of an electrochemical system in terms of the capacitive and resistive properties. More specifically, the system is said to act as a pure resistor if $\varphi = 0$, a pure capacitor if $\varphi = \pi/2$, and a mixture of both if $0 > \varphi > \pi/2$ [38].

An ideal Nyquist plot for a conducting polymer film is shown in **Figure 16**, divided into four regions. The first one is a high-frequency offset on the x-axis (i) caused by the resistance of the solution. This is followed by a high-frequency semi-circle (ii) representing the charge transfer at the CP/solution interface in combination with the charging of the double-layer. A linear plot at an angle of around 45° (iii) called the Warburg impedance represents the diffusion of the ions through the polymer film. Lastly, a near vertical spike at the low-frequency region (iv) is attributed to the charge build-up at the CP/solution interface, resembling a capacitor[44]. For solid-contact materials with high capacitance such as conducting polymers, it is expected that this capacitive line would be distinct with minimal deviation[23].

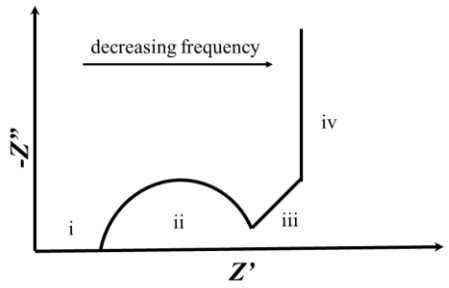

Figure 16. *Ideal Nyquist plot of a conducting polymer.*

Figure 17 shows the Randles equivalent circuit, frequently used in impedance studies. The solution resistance represented by the element R_s, connected in series with a double-layer capacitor C_{dl}., then connected in parallel with a charge-transfer resistor R_{ct}. Lastly, is the Warburg impedance Z_W connected in series[38].

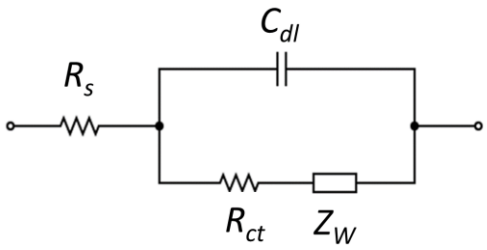

Figure 17. *A Randles equivalent circuit.*

In this thesis, EIS measurements were performed to determine the capacitance of the deposited PEDOT:PSS film or MWCNTs layer as transducer materials and the resistance of the plasticized PVC-based membrane in the prepared electrodes. The Nyquist plots and the calculated capacitance and resistance values were used to understand and explain the mechanism behind the novel experimental setup for the coulometric signal transduction method.

5.3. Potentiometry

Potentiometry is an electroanalytical technique based on measuring the potential difference between a reference electrode and one (or more) indicator electrode in an electrochemical cell. The basic principles of potentiometric ion-to-electron signal transduction in ISEs are explained in **Section 4.1**. Potentiometric

measurements are done using a high-input impedance potentiometer to achieve a zero to near-zero current condition[3,12].

In this thesis, potentiometric measurements were performed to verify the Nernstian behavior of the prepared K^+-ISEs (SCISEs and conventional ISE) to be connected as the RE in the studied setup. Potentiometry was alsoused to assess the non-selectivity of the PEDOT:PSS-based electrodes with a layer of dummy membrane (WEs) to ensuring the validity of the proposed novel experimental setup. Lastly, potential readings were taken to monitor the sensitivity of the prepared electrodes to O_2 and CO_2 gases present in the sample solution.

5.4. Chronoamperometry and chronocoulometry

Chronoamperometry is a three-electrode technique used to monitor current-time dependence. It begins with current measurement at the OCP, which is the cell potential recorded where no appreciable amount of current flowing between the electrodes. Then, an instantaneous potential step is applied, and the current response is recorded[38]. This step can be generated by a sudden change in the concentration of electroactive species at the electrode surface, which gradually decreases with time as the redox reaction continues to take place. Consequently, this is reflected in the current-time curve which illustrates current decay with time, until equilibrium is reached[45].

During a potential step, the array of charged species at the electrode/solution interface, called the electrical double layer, behaves as a capacitor. The charging of this double layer in the absence of electron transfer produces the non-faradaic (capacitive) current[45]. The time constant, τ, which is the product of cell resistance and the capacitance of the double layer, describes the exponential decay of the non-faradaic current with time[11,48]. In the experiment, the bulk resistance of the SCISE is attributed to the added layer of dummy membrane with resistance R_{DM}, while the capacitance of the electrical double-layer is attributed to the low-frequency capacitance of the conducting polymer layer C_{LF}.

One practical significance of τ is that it provides an estimate of the minimum amount of time needed to perform a potential step[11,38]. It has been estimated that the whole duration of a potential step takes about $5C_{LF}R_{DM}$, and in principle, the measurement must last until *ca.* 10 $C_{LF}R_{DM}$ to ensure that the current has decayed to the equilibrium state[38]. It can also be thought of as the required time for charging/discharging

or a capacitor[37]. The study of the current-time response to a potential step can be extended through additional steps, usually the reverse of the initial one, and is called the chronoamperometric reversal technique[38]. In this work, this technique is used to assess the reversibility of the electrode response.

Chronocoulometry is the study of charge-time dependence, carried out by integrating the current produced with respect to time. During the process of integration, the charge signal is accumulated with time (Q), resulting in a better signal-to-noise ratio[38]. The coulometric signal transduction method is in principle, and is also referred to as, a constant potential coulometry technique because the integrated current response is recorded at constant applied potential between the reference and working electrodes. Since the measurements are performed at the OCP, it is expected that a near zero to zero current and cumulated charge readings will be recorded in the absence of any potential step. Once optimized to constantly give zero current and charge readings at the OCP, constant potential coulometry is a good technique to address the irreproducibility of the E^{o} in potentiometry.

In this work, chronocoulometry and chronocoulometry were performed to (i) compare the current and Q signals resulting from the original and the novel experimental setup, (ii) determine the capability of the novel experimental setup to detect small changes in concentration, (iii) check if the setup can be used in real biological samples, and (iv) establish the relationship between Q and the logarithm of analyte activity. The first three were characterized by stepwise addition/dilution experiments while the last one was achieved by sequential dilution.

6. EXPERIMENTAL WORK

6.1. Materials

Potassium ionophore I (valinomycin), potassium tetrakis[3,5-bis(trifluoromethyl)phenyl)] borate (KTFPB), tetradodecylammonium tetrakis(4-chlorophenyl) borate (ETH-500), bis(2-ethylhexyl) sebacate (DOS), polyvinyl chloride (PVC), and tetrahydrofuran (THF, ≥ 99.5%) were Selectophore reagents purchased from Sigma-Aldrich. Poly(sodium 4-styrenesulfonate) (NaPSS, average Mw ~70,000), 3,4-Ethylenedioxythiophene (EDOT, 97%) sodium chloride (NaCl, ≥ 99.9995%), potassium chloride (KCl, ≥ 99.999%), and MWCNTs (≥ 95%, O.D x L: 6-9 nm x 5 μm) were purchased from Sigma-Aldrich. Human control serum (Abtrol, REF 981044) and ISE calibrator 3 (REF 984035) were obtained from Thermo Fisher Scientific Oy. Distilled and deionized water (ELGA Purelab Ultra; resistivity 18.2 MΩ cm) was used to prepare the aqueous solutions.

6.2. Cleaning the bare electrodes

The used electrodes consist of GC rods (3 mm or 5 mm diameter) mounted in PVC cylinders. The bare GC electrodes were polished with sandpaper with decreasing level of coarseness (180, 240, 600, 800, 1000, 1200), followed by diamond paste (15 μm, 9 μm, 3 μm, 1 μm), then with 0.3 μm alumina slurry, and lastly with a clean wet cloth. After all the polishing steps, the electrodes were ultra-sonicated for 15 minutes in ethanol and then in deionized water.

6.3. Cyclic voltammetry

Cyclic voltammetric measurements were performed to check that the GC electrodes were properly cleaned and later to confirm the formation of the solid-contact layer (conducting polymer film or MWCNTs) deposited on the GC substrate. The Autolab general purpose electrochemical system (AUT30.FRA2-Autolab, Eco Chemie, B.V., The Netherlands), with a three-electrode electrochemical cell, was used. A Metrohm single-junction Ag/AgCl/3 M KCl electrode was used as the RE and a GC rod as the CE. The electrolyte used was a 10^{-1} M KCl solution de-aerated with N_2 gas for 15 minutes before starting the measurement, and the gas flow was kept above the solution throughout the experiment. The OCP was used as the starting potential, the potential range was set from −0.5 V to 0.5 V, and the scan rate was 0.1 V/s.

6.4. Electrochemical impedance spectroscopy

The same three-electrode electrochemical cell and electrolyte used in the cyclic voltammetric measurements (**Section 6.3)** were used for carrying out the electrochemical impedance spectroscopic measurements. The measurements were done using the Autolab Frequency Response Analyzer System (AUT20.FRA2-Autolab, Eco Chemie, B.V., The Netherlands). The impedance spectra were recorded at the OCP, in the frequency range of 100 kHz - 10 mHz and excitation amplitude of 10 mV.

6.5. Electrode preparation

6.5.1. Preparation of GC/PEDOT:PSS electrodes

For the electrochemical synthesis of PEDOT:PSS, a polymerization solution containing 10^{-2} M of the monomer 3,4-ethylenedioxythiophene and 10^{-1} M sodium polystyrene sulfonate as supporting electrolyte was prepared, covered with aluminum foil, and stirred overnight to ensure the dissolution of the monomer. The polymerization solution was de-aerated with N_2 gas for 15 minutes, and the gas flow was kept above the solution throughout the process. A Metrohm double-junction Ag/AgCl/3 M KCl/0.1 M NaPSS was used as the RE, GC rod as the CE, and the bare GC electrode was connected as the WE.

The Autolab general purpose electrochemical system (AUT30.FRA2-Autolab, Eco Chemie, B.V., The Netherlands), with a three-electrode electrochemical cell, was used. Using the galvanostatic polymerization method, a constant current (I_{polym}) was applied between the WE and CE for a certain time (t_{polym}) to achieve the desired polymerization charge (Q_{polym}). For instance, electrodes with the same $Ø_{GC}$, a 2 times increase in the PEDOT:PSS film thickness was achieved by doubling t_{polym}. The same film thickness was obtained in electrodes with different $Ø_{GC}$ by adjusting I_{polym} to get the same current density at the given area. **Table 1** summarizes the galvanostatic polymerization parameters used for preparing electrodes of varied sizes to achieve the desired thickness of the formed conducting polymer poly(3,4-ethylene dioxythiophene) doped with polystyrene sulfonate, *i.e.* PEDOT:PSS. Afterwards, the resulted electrodes (GC/PEDOT:PSS) were rinsed thoroughly with deionized water and soaked in a 10^{-2} M KCl conditioning solution for at least 24 hours. Similar to the bare GC electrodes, CV was performed to check

the GC/PEDOT:PSS electrodes. Moreover, EIS was performed to determine the capacitance of the deposited conducting polymer layer.

Table 1. *Parameters used for the electrochemical deposition of PEDOT:PSS on GC electrodes of different sizes.*

$Ø_{GC}$ / mm	A_{GC} / mm^2	I_{polym} / µA	t_{polym} / s	Q_{polym} / mC
3	7.07	14.14	142	2
3	7.07	14.14	707.2	10
3	7.07	14.14	1414.4	20
5	19.6	39.26	707.2	27.8
5	19.6	39.26	1414.4	55.5

$Ø_{GC}$ = diameter of the GC substrate, A_{GC} = area of the GC substrate,
I_{polym} = polymerization current, t_{polym} = polymerization time, Q_{polym} = polymerization charge

6.5.2. Preparation of GC/MWCNTs electrodes

A MWCNTs dispersion was prepared by adding 1 mL of tetrahydrofuran to 0.005 g of MWCNTs to achieve a final concentration of 0.5 wt%. The mixture was vortexed at 2500 rpm for two minutes and ultra-sonicated for two hours. A silicon sheet with a hole of the same size as the glassy carbon disk ($Ø_{GC}$ = 3 mm) was used to deposit the MWCNTs only on the GC part of the electrode. A 5 µL of the MWCNTs dispersion was drop-cast on top of the bare GC electrode. After five minutes, another 5 µL of the dispersion was added, resulting in a total volume of 10 µL MWCNTs dispersion. The GC/MWCNTs electrodes were covered with a beaker and left to dry overnight. The dried GC/MWCNTs electrodes were then conditioned in 10^{-2} M KCl overnight before performing CV and EIS measurements using the previously mentioned experimental parameters.

6.5.3. Preparation of the plasticized PVC-based membranes

Different plasticized PVC-based membranes were prepared in this study. In the case of the K^+-ISEs, the K^+-ISM cocktail contained the following components: the ionophore valinomycin, KTFPB, ETH-500, DOS, and PVC, all dissolved in THF. The final dry mass content is calculated as the mass ratio of the sum of all components (except THF) to the sum of all components (with THF). The K^+-ISM cocktails prepared for the solid-contact and conventional ISEs had a final dry mass content of 15% and 9.76%, respectively. A PVC-based cocktail for the dummy membrane (DM) was made using all the previously

mentioned membrane components except the ionophore valinomycin, and had a final dry mass content of 14.88%.

All the dry components were weighed in a 5 mL glass vial, followed by the addition of THF. The corresponding mixture was vortexed, wrapped with aluminum foil, and left on a rocker until all the components were completely dissolved. The dry mass composition of the different plasticized PVC-based membrane cocktails is summarized in **Table 2**.

Table 2. *Dry mass composition of the different PVC-based membrane cocktails.*

Dry membrane components	**Ion-selective membrane**				**Dummy membrane**	
	for solid-contact K^+-ISEs		**for conventional K^+-ISEs**			
	wt. %	**mass / g**	**wt. %**	**mass / g**	**wt. %**	**mass / g**
valinomycin	1	0.0024	1	0.0024	-	-
KTFPB	0.5	0.0012	0.5	0.0012	0.52	0.0012
ETH-500	1	0.0024	1	0.0024	1.03	0.0024
DOS	65	0.1527	65	0.1560	65.62	0.1527
PVC	32.5	0.0764	32.5	0.0780	32.83	0.0764
Total	100	0.2351	100	0.2400	100	0.2327

6.5.4. Drop-casting the membranes

The conditioned GC/PEDOT:PSS and GC/MWCNTs electrodes were washed with deionized water, and then dried for at least 24 hours before applying the membrane. The electrodes were kept upside down on a plastic holder, and the prepared PVC-based membrane cocktail was carefully drop-cast on top of the electrode, covering both the GC substrate (with a solid-contact layer) and the PVC disk. All of the GC/PEDOT:PSS and GC/MWCNTs electrodes that were later used as K^+-ISEs were drop-cast with 50 µL of the K^+-ISM cocktail.

The working electrodes with the same $Ø_{GC}$ and PEDOT:PSS film thickness were drop-cast with either a thin or a thick layer of the dummy membrane (DM). For instance, one 3 mm GC/10 mC PEDOT:PSS electrode was drop-cast with 25 μL DM, and another one with 100 μL DM. Furthermore, the volume of the added dummy membrane cocktail (V_{DM}) was calculated so that the electrodes with $Ø_{GC}$ = 5 mm will have the same membrane thickness as the electrodes with $Ø_{GC}$ = 3 mm considering the total area of the GC substrate and the PVC disk (A_{GC+PVC}) (**Table 3**). As an example, a 25 μL DM cocktail in the 3 mm

GC electrodes is equivalent to 41.7 µL in the 5 mm GC electrodes. In some places of the succeeding parts of the manuscript, V_{DM} = 25 µL and its equivalent is referred to as the thin membrane, while V_{DM} = 100 µL and its equivalent is referred to as the thick membrane. Due to practical reasons, the 5 mm GC/55.5 mC PEDOT:PSS electrode was prepared only with a thin membrane.

Table 3. *Volumes of the dummy membrane cocktail drop-cast on electrodes of different sizes.*

$Ø_{GC}$ / mm	A_{GC} / mm^2	$Ø_{GC+PVC}$ / mm	A_{GC+PVC} / mm^2	Q_{polym} / mC	V_{DM} / µL
3	7.07	8.40	55.42	10	25, 100
3	7.07	8.40	55.42	20	25, 100
5	19.6	10.85	92.46	27.8	41.7, 166.8
5	19.6	10.85	92.46	55.5	41.7

$Ø_{GC}$ = diameter of the GC substrate, A_{GC} = area of the GC substrate, $Ø_{GC+PVC}$ = diameter of the GC substrate and the PVC disk, A_{GC+PVC} = area of the GC substrate and the PVC disk, Q_{polym} = polymerization charge, V_{DM} = volume of the dummy membrane cocktail (composition in **Table 2**)

The prepared electrodes were covered with a glass beaker to protect the membranes from contaminants and were left to dry for *ca*. 48 hours. Afterwards, they were conditioned in 10^{-2} M KCl solution for at least 24 hours before further use.

6.5.5. Preparation of the conventional K^+-ISEs

The membrane cocktail (composition in **Table 2**) was poured into a glass cylinder fixed on top of a glass plate. The whole setup was kept under a glass cover, and a small open vial with THF was placed inside to saturate the air with the solvent vapor. The membrane was left to dry for *ca*. 48 hours. Meanwhile, the sensor body (Philips 1S561, Möller glasbläserie, Zürich, Switzerland) with Ag/AgCl wire and the screw cap with the hole for the ISM were thoroughly rinsed with deionized water and then with 10^{-1} M KCl. Once dried, smaller disks with 8 mm diameter were punched from the main membrane to be used as the ISMs. The conventional K^+-ISE was assembled as follows: the K^+-ISM was placed at the bottom of the screw cap, ensuring it covers the hole, while the main cylinder holding the Ag/AgCl wire was filled with the 10^{-1} KCl solution up to the brim. Lastly, the screw cap containing the K^+-ISM was connected to the main body, avoiding the formation of any air bubbles inside the tube.

The assembled conventional K^+-ISEs were placed in a 10^{-1} M KCl solution and their potential response was checked. Finally, the electrodes were soaked in a 10^{-2} M KCl conditioning solution before further use and in-between measurements.

6.6. Potentiometric measurements

A 16-channel millivoltmeter (Lawson Labs. Inc., Malvern, PA, USA) and a two-electrode electrochemical cell composed of the K^+-ISEs and a Metrohm double junction Ag/AgCl/3 M KCl/1 M LiOAc RE was used for the potentiometric measurements carried out using different K^+-ISEs (GC/PEDOT:PSS/K^+-ISM, GC/MWCNTs/K^+-ISM, and conventional K^+-ISE). In addition, the potentiometric response of the electrodes with dummy membrane (GC/PEDOT:PSS/DM) was also checked.

For calibrating the different K^+-ISEs, a 50.0 mL starting solution of 10^{-1} M KCl was pipetted into the measuring cell. Sequential dilution was performed automatically using a Metrohm Dosino 700 instrument equipped with two 50-mL burettes (Herisau, Switzerland). The calibration was performed from 10^{-1} to 10^{-7} M KCl. In each dilution step, 45 mL of the starting solution was removed from the cell and was replaced with 45 mL of deionized water, corresponding to one decade change in concentration ($\Delta \log C_{K+}$ = 1 decade step^{-1}). The solutions were allowed to equilibrate for five minutes for potential stabilization before the next dilution step, and the potential measurements were taken every 0.2 seconds. The activity coefficients were calculated using the extended Debye-Hückel equation, followed by the determination of potassium ion activity (a_{K^+}) per dilution step. A calibration curve was prepared using the average of the last five stable potential values per dilution step versus the corresponding log a_{K^+}. The slope and standard potential values were calculated from the linear part of the calibration curve (10^{-1} M to 10^{-5} M). The same procedure was performed in the presence of a background electrolyte (BGE). For this purpose, a 10^{-1} M KCl with 10^{-1} M NaCl as BGE was used as the starting solution and a 10^{-1} M NaCl solution was used as the diluent.

The potentiometric response of the prepared PEDOT:PSS-based working electrodes before and after adding the dummy membrane were determined by potentiometric measurements. The potentiometric response of the 3 mm GC/10 mC PEDOT:PSS and 3 mm GC/10 mC PEDOT:PSS/25 µL DM electrodes to changes in K^+ concentration was measured. With 50.0 mL of 10^{-2} M KCl as the starting solution, dilution was performed with 1 decade change in K^+ concentration per step. The measurements were done

in KCl solutions without and with BGE. For the latter, 50.0 mL of 10^{-2} M KCl with 10^{-1} M NaCl as BGE was used as the starting solution, and 10^{-1} M NaCl was used as the diluent.

The sensitivity of the GC/PEDOT:PSS electrodes with and without the dummy membrane to O_2 and CO_2 gases present in the sample was studied in KCl solutions. A starting solution of 10^{-3} M KCl was placed in the measuring cell, and the potential of the electrodes was measured as a function of time. First, equilibration was done in the starting solution for 30 minutes. Then the solution was purged with N_2 gas for an hour with consistent potential measurements. Afterwards, the solution was purged with other gases in the following order: O_2, N_2, CO_2, and N_2, allotting one hour per gas. Lastly, the potential was measured for another 30 minutes without purging any gas. The same experiment was done in 10^{-2} M KCl with 10^{-1} M NaCl as BGE.

6.7. Chronoamperometric and chronocoulometric measurements

The chronoamperometric and chronocoulometric experiments were performed using IviumCompactStat (Ivium Technologies, The Netherlands). Each of the K^+-ISEs (GC/PEDOT:PSS/K^+-ISM, GC/MWCNTs/K^+-ISM, or conventional K^+-ISE) in the three-electrode electrochemical cell was connected as the RE. The GC/PEDOT:PSS/DM and a GC rod were connected as working and counter electrode, respectively.

Since the measurement was done in one cell instead of using separate sample and detection cells, several factors were considered to ensure that the analyte recognition only takes place at the ISE connected as the RE. As explained in **Section 3.2.1**, the PEDOT:PSS film itself has a cationic response that is relatively non-selective. A BGE with high and constant concentration was used to suppress the detection of changes in analyte concentration by the WE (GC/PEDOT:PSS/DM). As it was mentioned earlier, the dummy membrane in the WE contains all the components present in K^+-ISM except the ionophore (valinomycin) to eliminate the selectivity of the membrane to K^+ ion.

The setup was placed in a Faraday cage to reduce the background noise. Prior to the actual experiment, chronopotentiometric measurement (using the IviumCompactStat) was done for 15 minutes with

constant stirring to determine the OCP, which was then used as the applied potential for the succeeding addition/dilution and calibration experiments.

6.7.1. Addition/Dilution experiments

Sequential addition/dilution steps were done starting with 50.0 mL of 10^{-3} M KCl solution with 10^{-1} M NaCl as BGE using the electrochemical cell described above. An addition step refers to increasing the concentration of K^+ ions in the sample solution by adding a proper volume of a solution with higher K^+ concentration. On the contrary, a dilution step refers to decreasing the concentration of K^+ ions in the sample solution, accomplished by adding a proper volume of the 10^{-1} M NaCl solution. In the experiment, the starting solution was allowed to equilibrate at the OCP for *ca.* 5 minutes until a stable current baseline with drifts within ± 1 nA was achieved. Then, 25.0 µL of the 10^{-1} M KCl solution with 10^{-1} M NaCl was added to the starting solution, followed by the addition of 2.50 mL of 10^{-1} M NaCl solution to constitute a single addition/dilution step. This corresponds to a 5 % change in K^+ concentration, from 1 mM to 1.05 mM and back to 1 mM. A five-minute equilibration time was given after each step under constant stirring. For the second addition/dilution step, 26.0 µL of 10^{-1} M KCl solution with 10^{-1} M NaCl was added to the solution followed by 2.60 mL of 10^{-1} M NaCl. Since the increase/decrease in concentration was manually performed, a magnetic stirrer was incorporated into the setup.

Smaller concentration changes (2.5 % and 1 %) were also checked using 10^{-2} M KCl solution with 10^{-1} M NaCl for the addition steps and 10^{-1} M NaCl for the dilution steps. Volumes of solutions used in the addition/dilution steps are summarized in **Table 4**.

Table 4. *Protocol for chronoamperometric and chronocoulometric addition/dilution experiment.*

Step	Concentration change, %	
	1	2.5
	Volume added, µL	
1st addition (a)	55.6	139.2
1st dilution (b)	500	1250
2nd addition (a)	56.2	143.2
2nd dilution (b)	506	1280

a = 10^{-2} M KCl with 10^{-1} M NaCl, b = 10^{-1} M NaCl

6.7.2. Calibration experiments

Various working electrodes (GC/PEDOT:PSS/DM) with dummy membranes of equivalent thickness were calibrated using different K^+-ISEs connected as the RE in the electrochemical cell described in **Section 6.7**. A 50.0 mL starting solution of 10^{-2} M KCl solution with 10^{-1} M NaCl as BGE was pipetted into the measuring cell. Sequential dilution was performed automatically, using the Metrohm Dosino 700 instrument equipped with two burettes of 50 mL volume (Herisau, Switzerland). The calibration was carried out from 10^{-2} M to $10^{-3.4}$ M KCl. In each dilution step, 18.5 mL of the starting solution was removed from the cell and replaced with 18.5 mL of 10^{-1} M NaCl, corresponding to $\Delta\log C_{K+} = 0.2$ decade per step. Current (and cumulated charge) measurements were made for 10 minutes after each concentration change. Only the electrodes with thin DM were chosen for this experiment upon considering the equilibration time from the addition/dilution experiments. For the same reason, a smaller $\Delta\log C_{K+}$ and longer measurement time were used compared to the potentiometric measurements.
A calibration curve was prepared using the average of five stable cumulated charge Q values towards the end of the step against $\Delta\log a_{K+}$. The calibration parameters (slope, intercept, and correlation coefficient R^2) were calculated for the whole calibration range.

6.7.3. Measurements in a biological sample

The ability of the proposed coulometric setup to detect small changes in potassium ion concentrations in a human serum sample, as a real biological sample, was studied. The electrochemical cells employed for chronoamperometric/chronocoulometric measurements were described **Section 6.7**. The human serum Abtrol (C_{K+} = 6.8 mM) was used as the sample, a 30 mM KCl with 10^{-1} M NaCl BGE solution was used in the addition steps, and an ISE calibrator 3 standard solution (C_{K+} = 3 mM) was used for the dilution steps.

Starting from a 5 mL control serum sample solution, the first and second addition steps were done by adding 44 µL and of 81 µL of 30 mM KCl with 10^{-1} M NaCl BGE corresponding to a K^+ concentration increase of 2.5 % (6.8 mM to 7.0 mM) and 5 % (6.8 mM to 7.15 mM), respectively. Alternating with the addition steps are the dilution steps, performed by the addition of 265 µL and 496 µL of the ISE calibrator 3, corresponding to a K^+ concentration decrease of 2.5% (7.0 mM to 6.8 mM) and 5% (7.15 mM to 6.8 mM), respectively. A five-minute equilibration time was allotted for each step under constant stirring.

7. RESULTS AND DISCUSSION

7.1. Cyclic voltammetric measurements

The cyclic voltammograms of GC electrodes ($Ø_{GC}$ = 3 mm) with 2 mC PEDOT:PSS and 10 µL of 0.5 wt% MWCNTs as solid contact, later used in the fabrication of K^+-SCISEs, are shown in **Figure 18**. Measurements were done in 10^{-1} M KCl solution, and the potential range used in the linear scans is 0.5 V to −0.5 V, which matches the potential stability window for PEDOT in aqueous solutions[43]. In the absence of faradaic processes at the used potential range, near-rectangular current-voltage shapes were obtained for both cases, confirming the successful electrochemical synthesis of PEDOT:PSS or the deposition of MWCNTs as a solid-contact layer. The absence of distinct oxidation and/or reduction peaks is indicative of the capacitive-like current being measured[23].

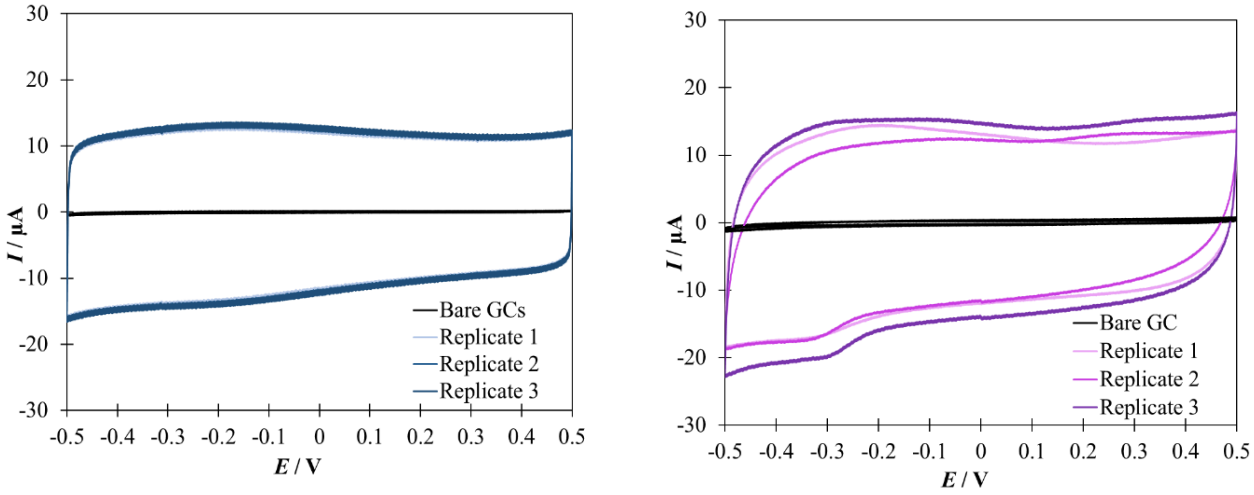

(a) GC/2 mC PEDOT:PSS **(b)** GC/10 µL 0.5 wt% MWCNTs

Figure 18. *Cyclic voltammograms of GC electrodes with PEDOT:PSS* ***(a)*** *and MWCNTs* ***(b)*** *as solid contact measured in 10^{-1}M KCl with 0.1 V/s scan rate.*

However, there seems to be some deviation from the rectangular shape as the scan goes from 0 V to −0.5 V, which is most likely caused by the reduction of oxygen[6], despite the deaeration of the solution and keeping of the flow of N_2 gas over the solution during the measurements. This observation is more pronounced in the case of GC/MWCNTs electrodes and is found to be common for carbon-based nanomaterials used as solid contacts[6]. Moreover, the electrodes with galvanostatically electropolymerized PEDOT:PSS films **(Figure 18a)** showed a more symmetrical voltammogram shape and better electrode-to-electrode repeatability than the electrodes with a manually drop-cast layer of

MWCNTs **(Figure 18b)** as solid contact. This is because there is better experimental control during the electrochemical synthesis of the conducting polymer layer[24].

Several electrodes were prepared with varying PEDOT:PSS film thickness to further examine the influence of capacitance on the coulometric signal transduction. The polymerization parameters (t_{polym} and I_{polym}) were adjusted to achieve a specific Q_{polym} which corresponds to a certain film thickness. The cyclic voltammograms of GC electrodes with $Ø_{GC}$ = 3 mm deposited with 10 mC and 20 mC PEDOT:PSS films are shown in **Figure 19a**, while GC electrodes with $Ø_{GC}$ = 5 mm deposited with equivalent PEDOT:PSS film thickness are shown in **Figure 19b**. Since the signal (cumulated charge) generated in the coulometric signal transduction method depends on the solid contact's charging and discharging, the solid-contact layer's capacitance is important[4, 10]. From the graphs, one can see that the increase in the PEDOT:PSS film thickness at constant $Ø_{GC}$ resulted in an increase in the recorded capacitive-like current responses. Similarly, the increase in $Ø_{GC}$ from 3 mm to 5 mm at constant PEDOT:PSS film thickness produced larger capacitive-like currents. The shape of the voltammograms remained consistent in all of the electrodes, indicating the absence of a faradaic process at different Q_{polym}. The redox capacitance of the PEDOT:PSS films were later confirmed with EIS measurements.

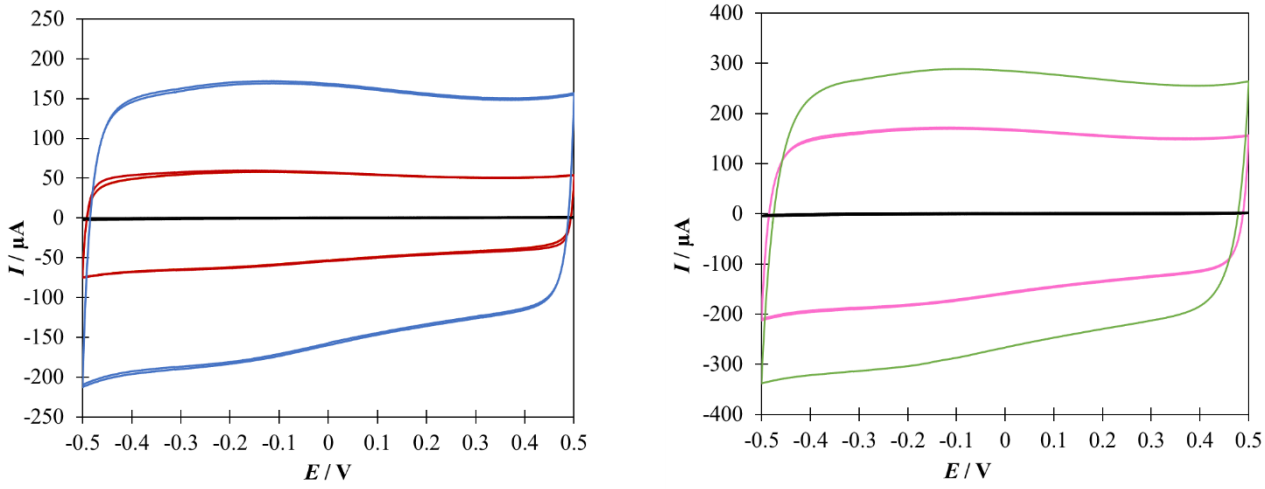

(a) Electrodes: Bare GCs
3 mm GC/10 mC PEDOT:PSS
3 mm GC/20 mC PEDOT:PSS

(b) Electrodes: Bare GCs
5 mm GC/27.8 mC PEDOT:PSS
5 mm GC/55.5 mC PEDOT:PSS

Figure 19. *Cyclic voltammograms of 3 mm GC/PEDOT:PSS* ***(a)*** *and 5 mm GC/PEDOT:PSS* ***(b)*** *electrodes measured in 10^{-1}M KCl with 0.1 V/s scan rate.*

7.2. Electrochemical impedance spectroscopic measurements

To gain a deeper understanding of the electrochemical properties and processeses in the solution and at the prepared electrode interface, EIS experiments were performed. The impedance spectra of the K^+-SCISEs before and after drop-casting the K^+-ISM are shown in **Figure 20.** A close to vertical line can be seen in the impedance spectra of both GC/PEDOT:PSS **(Figure 20a)** and GC/MWCNTs **(Figure 20c)**, which is typical for electrodes with PEDOT:PSS[23] and MWCNTs[28] as solid-contact. This indicates a purely capacitive mechanism[28], with a fast charge transfer at the GC/SC and SC/solution interface, related to the bulk redox and double-layer capacitance of the PEDOT:PSS and MWCNTs films, respectively.

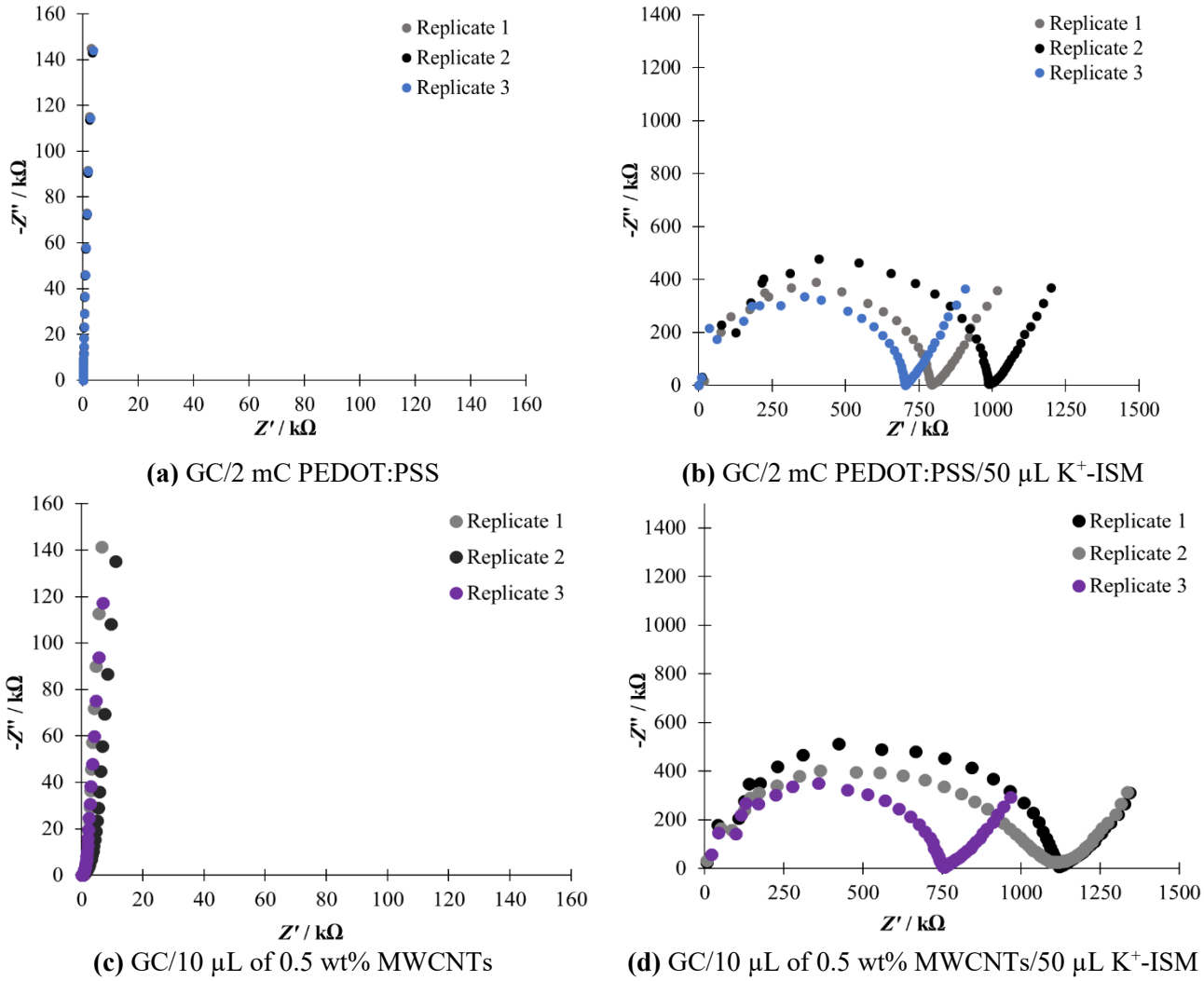

(a) GC/2 mC PEDOT:PSS

(b) GC/2 mC PEDOT:PSS/50 µL K^+-ISM

(c) GC/10 µL of 0.5 wt% MWCNTs

(d) GC/10 µL of 0.5 wt% MWCNTs/50 µL K^+-ISM

Figure 20. *Electrochemical impedance spectra of PEDOT:PSS-based (**a** and **b**) and MWCNT-based (**c** and **d**) electrodes recorded in 10^{-1} M KCl at the open circuit potential (OCP), in the frequency range of 100 kHz - 10 mHz, and excitation amplitude of 10 mV.*

While the 90° capacitive line in the GC/PEDOT:PSS electrodes **(Figure 20a)** extends to the low-frequency region of the spectra, a slight deviation is noticeable for the GC/MWCNTs **(Figure 20c)**. This indicates that there is a small diffusion contribution in the transduction process, which can be attributed to the inhomogeneous quality of the MWCNTs film due to manual deposition[28]. Moreover, good repeatability was observed in the impedance spectra of the electrodes with galvanostatically polymerized PEDOT:PSS, compared to the manually added MWCNTs film.

A low-frequency line with an angle of *ca.* 45° (Warburg impedance) was seen in the impedance spectra of the electrodes after adding the K^+-ISM *i.e.* GC/PEDOT:PSS/K^+-ISM **(Figure 20b)** and GC/MWCNTs/K^+-ISM **(Figure 20d).** This corresponds to the diffusion-limited ion-to-electron transduction mechanism in the electrodes and it can be used to estimate the low-frequency capacitance (C_{LF}) of the solid-contacts using **Eq 15** below, where f is the lowest frequency value used in the EIS measurement (0.01 Hz) and Z'' is the corresponding imaginary impedance.

$$C_{LF} = 1/(2\pi f Z'') \qquad \textbf{Eq 15}$$

Compared to the spectra shown in **Figures 20a** and **20c**, which are dominated by a capacitive spike, the spectra in **Figures 20b** and **20d** are dominated by a high-frequency semicircle. This is related to the geometric capacitance and the bulk resistance of the ISM (R_{ISM}), determined by estimating the diameter of the semicircle[4,10]. The poor repeatability of the calculated R_{ISM} for the prepared K^+-SCISEs is caused by the manual drop-casting of the K^+-ISM. The calculated values from the EIS measurements are summarized in **Table 5**.

Table 5. *The low-frequency capacitance and bulk resistance values calculated from the EIS spectra of K^+-SCISEs. s_d = standard deviation (n=3)*

$Ø_{GC}$ / mm	Solid-contact layer	V_{ISM} / µL	$C_{LF} \pm s_d$ / µF	$R_{ISM} \pm s_d$ / kΩ
3	2 mC PEDOT:PSS	50	43.69 ± 0.64	820 ± 141.64
3	10 µL 0.5 wt% MWCNTs	50	52.11 ± 1.99	998.06 ± 206.31

Similar to the previous results, the impedance spectra of the GC/PEDOT:PSS electrodes in **Figures 21a** and **21c** are dominated by the 90° capacitive line while a high-frequency semicircle dominates after the

deposition of the dummy membrane as seen in **Figures 21b** and **21d**. This means that the electrochemical properties of the cell, including the redox capacitance of the CP film was greatly affected by the interfacial ion movement at the DM/solution boundary, especially on the electrodes with thicker DM.

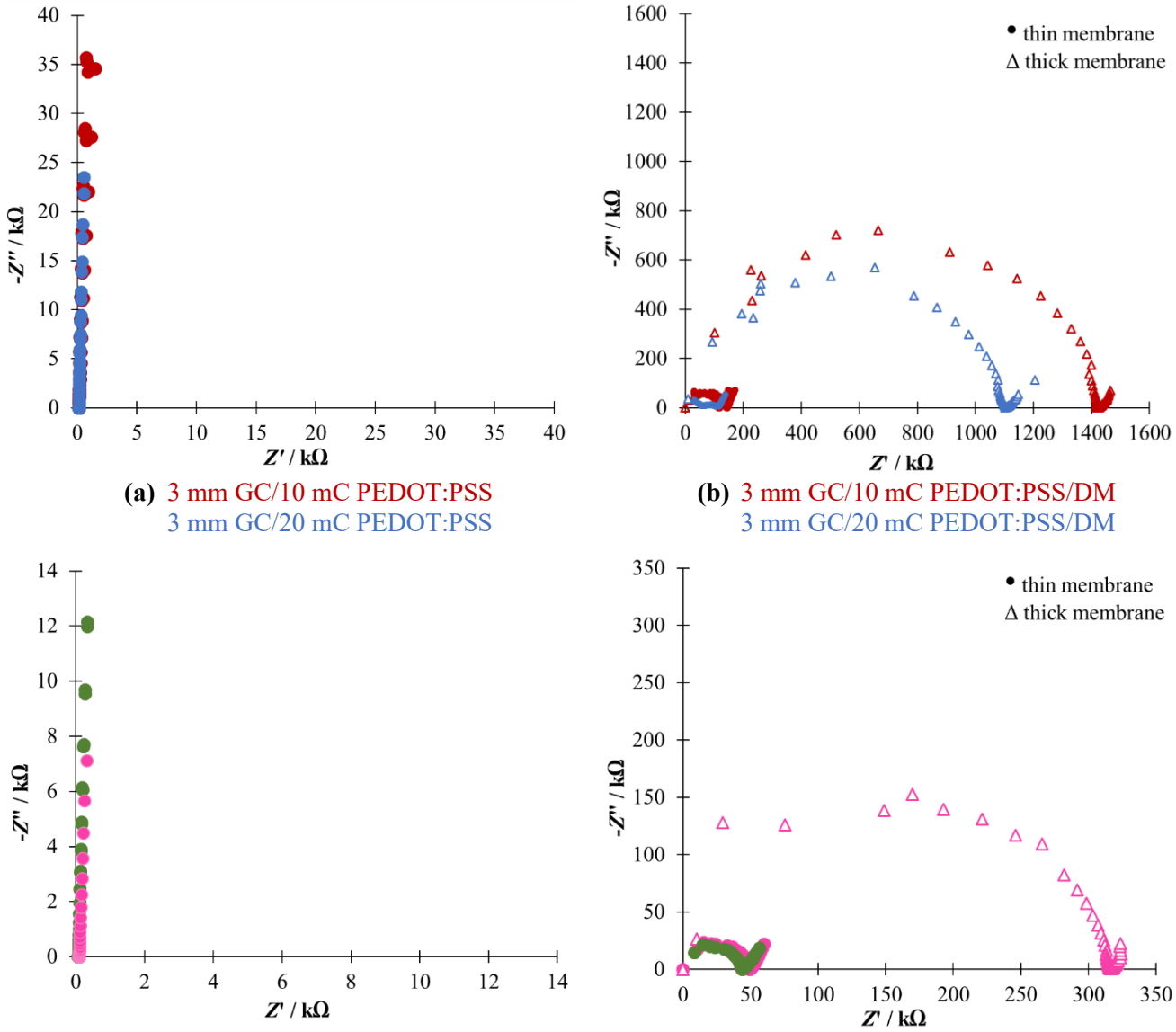

(a) 3 mm GC/10 mC PEDOT:PSS
3 mm GC/20 mC PEDOT:PSS

(b) 3 mm GC/10 mC PEDOT:PSS/DM
3 mm GC/20 mC PEDOT:PSS/DM

(c) 5 mm GC/27.8 mC PEDOT:PSS
5 mm GC/55.5 mC PEDOT:PSS

(d) 5 mm GC/27.8 mC PEDOT:PSS/DM
5 mm GC/55.5 mC PEDOT:PSS/DM

Figure 21. *Electrochemical impedance spectrum of GC/ PEDOT:PSS electrodes with different $Ø_{GC}$, Q_{polym}, and V_{DM}, recorded in in 10^{-1}M KCl at the open circuit potential (OCP), in the frequency range of 100 kHz - 10 mHz, and excitation amplitude of 10 mV. The plots in* ***(a)*** *and* ***(c)*** *were measured prior to drop casting the membrane while plots* ***(b)*** *and* ***(d)*** *were obtained after adding the membrane.*

It is also clearly depicted in **Figures 21b** and **21d** that the diameter of the high-frequency semicircle increases with DM thickness, as expected. Given the same $Ø_{GC}$, increasing the DM thickness which

corresponds to a larger R_{DM} value that heavily influences the time constant τ. It is expected that the same R_{DM} values will be obtained for electrodes with equivalent DM thickness, but the values were found to decrease as the C_{LF} increases. It appears that for thinner membranes combined with high capacitance of the inner CP layer, the contribution of the geometric capacitance in the diameter of the semicircle becomes more apparent.

The C_{LF} and R_{DM} values shown in **Table 6** were also estimated in the same way as for the K^+-SCISEs. The redox capacitance of the PEDOT:PSS film was varied in two ways: one is by increasing the film thickness and another is by using electrodes with larger $Ø_{GC}$ (and corresponding A_{GC}). Ideally, the redox capacitance of the film is directly proportional to Q_{poly} and film thickness[25], which was generally observed in the results of the EIS experiments. As shown from the results in **Table 6**, doubling the Q_{polym} (and the PEDOT:PSS film thickness) at constant $Ø_{GC}$ and DM thickness resulted in less than 2 times (*ca.* 1.4 times) increase in C_{LF}. Interestingly, *ca.* 2.8 times increase in electrode area (A_{GC}) while keeping the thickness of the PEDOT:PSS film and the dummy membrane constant, resulted in *ca.* 2.8 times increase in C_{LF}. This shows that there is a better correlation between A_{GC} and C_{LF} compared to Q_{polym} and C_{LF}.

Table 6. *The low-frequency capacitance and bulk resistance values calculated from the EIS spectra of the fabricated GC/PEDOT:PSS/DM working electrodes.*

$Ø_{GC}$/mm	A_{GC}/mm²	I_{polym}/μA	t_{polym}/s	Q_{polym}/mC	V_{DM}/μL	C_{LF}/μF	R_{DM}/kΩ	τ/s
3	7.07	14.14	707.2	10	25	207.88	111.41	23.16
					100	225.28	1397.86	314.91
			1414.2	20	25	298.35	78.51	23.42
					100	291.75	1093.50	319.03
5	19.6	39.26	707.2	27.8	41.7	574.92	39.10	22.48
					166.8	584.74	306.58	179.27
			1414.2	55.5	41.7	864.57	35.32	30.53

It has been proven in previous studies that increasing the electrode area with constant thickness of the CP film and low membrane resistance increases the accessibility of the redox capacitance of the solid-contact layer[10], that is why the ratio between the change in C_{LF} and in A_{GC} is close to one. It is quite the opposite when the thickness of PEDOT:PSS film is increased at constant A_{GC}. The redox capacitance in thicker CP films becomes less accessible and could be limited to those that are exposed at the surface, so it is difficult to fully utilize the material as ion-to-electron transducer. This could be the reason why

doubling the film thickness only resulted in only *ca.* 1.4 times the C_{LF} value. Lastly, since the results from the impedance spectra is dominated by the high-frequency semicircle, the C_{LF} did not have much effect on the time constant τ compared to R_{DM}.

7.3. Potentiometric measurements

7.3.1. Calibration of K^+-ISEs

The potentiometric performance of the K^+-SCISEs is an important factor in the studied novel experimental setup, since the potentiometric detection of the Δa_{K+} is the start of the coulometric transduction process. Potentiometric calibration was performed to check if K^+-SCISEs exhibit Nernstian behavior with and without the presence of 10^{-1} M NaCl as BGE. The slopes were calculated from the linear portion of the calibration curves in the range 10^{-1} M to 10^{-5} M KCl, typical for K^+-SCISEs.

Performing the calibration in the presence of a constant, high concentration of BGE did not have a great influence on the calibration results, which means that the K^+-SCISEs can be used in the new experimental setup that requires the constant presence of a BGE. As can be seen in **Table 7**, the K^+-SCISEs exhibit near-Nernstian slopes, with a good agreement in the slope values of identical electrodes. Except for the conventional K^+-ISEs, which are known to have stable standard potential *(E°)*[14,16], a large standard potential deviation was observed for the other studied electrodes. As discussed earlier, having irreproducible *E°* is one of the limitations to achieving calibration-free potentiometric ion sensors. Considering the obtained calibration parameters, all the electrodes were found to be suitable and were subjected to further experiments.

Table 7. *Potentiometric calibration data obtained for the fabricated K^+-SCISEs. s_d = standard deviation (n =3)*

K^+-SCISE	**Slope ± s_d / mV decade^{-1}**		***E°*± s_d /mV**	
	in KCl	in KCl + 10^{-1}M NaCl	in KCl	in KCl + 10^{-1}M NaCl
GC/2 mC PEDOT:PSS /50 µL K^+-ISM	56.8 ± 0.32	55.5 ± 0.4	216.3 ± 30.9	212.7 ± 30.4
GC/10 uL of 0.5wt% MWCNTs/50 µL K^+-ISM	54.8 ± 1.9	53.7 ± 1.6	258.5 ± 61.3	253.2 ± 62.2
Conventional K^+-ISE	55.5 ± 0.1	55.2 ± 0.2	255.9 ± 0.7	254.4 ± 0.6

7.3.2. Response of the PEDOT:PSS-based electrodes to changes in K^+ concentration

The use of a single electrochemical cell in the proposed novel experimental setup was made possible by the presence of a constant and high concentration of BGE in the sample solution. This eliminated the need of having separate sample and detection cells connected by a salt bridge, which is an advantage over previous studies employing the ISE as the RE[7,12]. However, since the sample and detection cells are combined in one, it is important to ensure that the analyte recognition only happens at the K^+-ISEs.

As shown in **Figure 22**, adding a dummy membrane on the GC/PEDOT:PSS electrode, with the main purpose of increasing the electrode resistance and regulating the response time and resulted signal, did not influence the sensitivity of the electrode when the measurement is done in the presence of 10^{-1} M NaCl as BGE. The electrode responses to changes in K^+ concentration is almost the same with and without the DM. As discussed in **Section 3.2.1**, the conducting polymer PEDOT:PSS film itself exhibits a sensitive but non-selective cationic response. However, the presence of a constant BGE suppressed the detection of the sequentially diluted K^+ at the GC/PEDOT:PSS electrode. In the absence of BGE, the changes in K^+ concentration are clearly detected, producing a typical potentiometric response with lower potential values for lower K^+ ion concentrations.

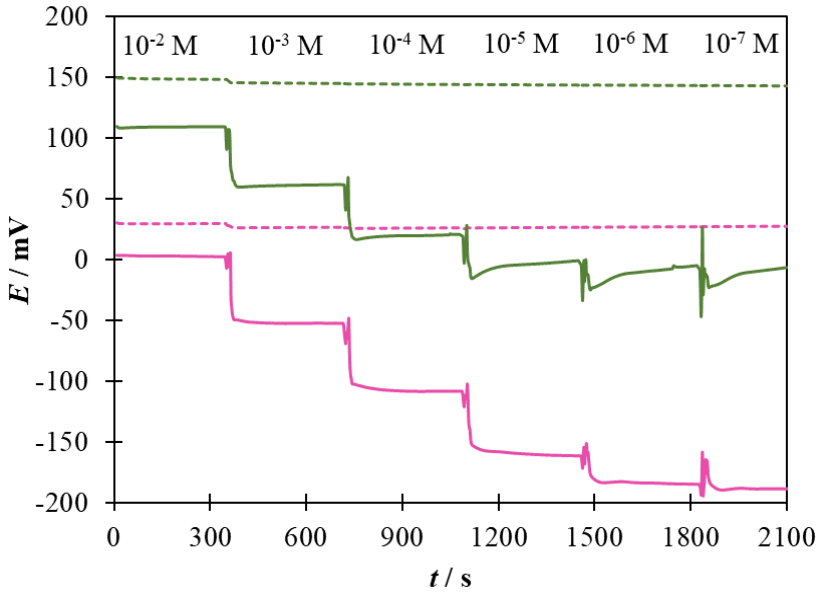

Figure 22. *Comparison between the potentiometric response of GC/10 mC PEDOT:PSS and GC/10 mC PEDOT:PSS/25 µL DM as the concentration of K^+ is changed from 10^{-2} M to 10^{-7} M with (dashed line) and without (solid line) the presence of 10^{-1} M NaCl as BGE.*

To further highlight the difference in response of K^+-ISEs and GC/PEDOT:PSS/DM electrodes to changes in K^+ ion concentration, the potential of these electrodes was measured in 10^{-2} M to 10^{-7} M KCl solutions with 10^{-1} M NaCl as BGE (**Figure 23**). It was established that the presence of a BGE does not affect the performance of the K^+-ISEs and the electrodes are selective to K^+ ion even in the presence of BGE, as expected. On the other hand, the GC/PEDOT:PSS electrodes, with and without the DM, were not sensitive to the change in K^+ ion concertation due to the high Na^+ concentration in the BGE.

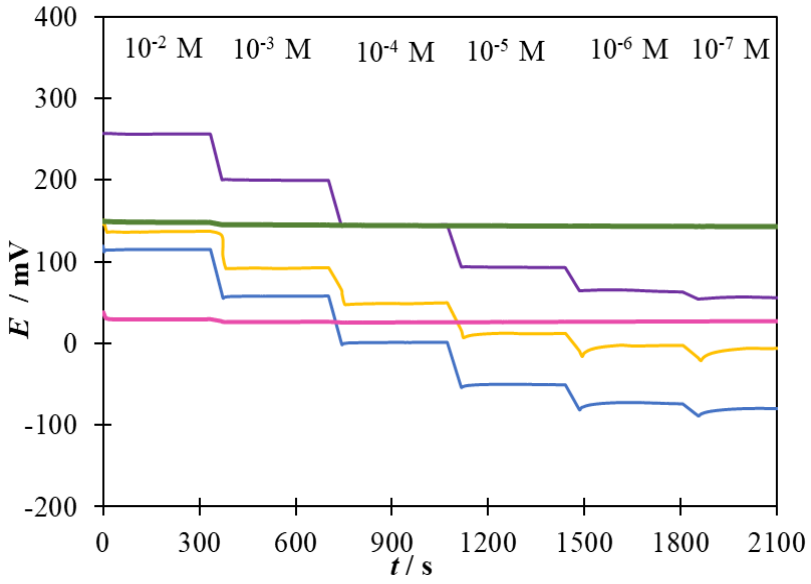

Figure 23. *Comparison between the potentiometric response of different K^+-ISEs (GC/PEDOT:PSS/50 µL K^+-ISM, GC/MWCNTs/50 µL K^+-ISM, and conventional K^+-ISE), GC/10 mC PEDOT:PSS, and GC/10 mC PEDOT:PSS/25 µL DM as the concentration of K^+ is changed from 10^{-2} M to 10^{-7} M with 10^{-1} M NaCl as BGE.*

7.3.3. Gas sensitivity

One of the conditions that should be fulfilled in order to have SCISEs with stable potential is the absence of side reactions. This includes the potential stability in the presence of gases that could pass through the plasticized PVC-based membrane and affect the potential of the solid-contact layer[20,25]. Studies on conducting polymer films as solid-contacts have reported their sensitivity to gases such as O_2 and CO_2 [25,49]. The gas sensitivity of PEDOT-based films were found to be less compared to other conducting polymers such as PPy, and were suppressed, though not completely removed, by the addition of a K^+-ISM layer[25]. In this thesis, it was shown that adding a non-selective DM in the working electrode could

further improve the electrode stability, such as insensitivity to dissolved gases in the sample, in addition to its main purpose of adding resistance to the electrodes. The measurements were done in 10^{-3} M KCl or 10^{-2} M KCl with 10^{-1} M NaCl as BGE.

The resulting chronopotentiometric plots (**Figure 24**) were found to be consistent with previous studies[25,49]. Applying a PVC-based dummy membrane made the electrode less sensitive to the presence of dissolved gases. Introducing O_2 gas in the solution resulted in *ca.* 10 mV increase in potential of the GC/PEDOT:PSS electrodes. The presence of CO_2 gas in the solution has the most distinct effect on the potential readings (*ca.* 100 mV) due to the accompanying pH change[25] as a consequence of the dissolution of CO_2 in the solution. An inert gas such as N_2 was introduced in between the reactive gases in an attempt to stabilize the potential readings. The results of this experiment confirmed that the addition of a non-selective PVC-based dummy membrane reduced the gas (and pH) sensitivity of the PEDOT:PSS films. Comparing the response GGC/PEDOT:PSS electrode, measured in KCl solution with and without BGE, shows that the presence of BGE slightly reduced the gas sensitivity of the electrode. Electrode stability in the presence of dissolved gases and fluctuating pH value is an attractive property for sensors used in the measurements carried out in real samples with more complex and variable matrices.

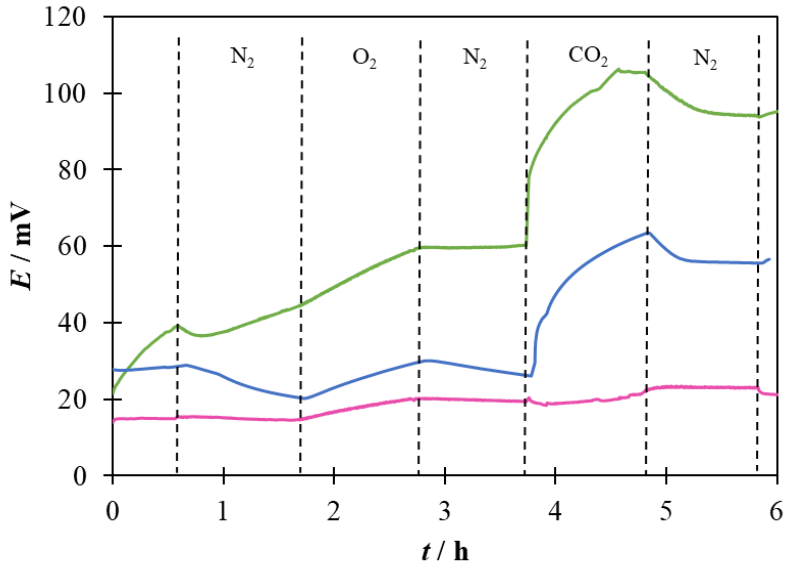

Figure 24. *Gas sensitivity of electrodes without and with the dummy membrane (GC/10 mC PEDOT:PSS and GC/10 mC PEDOT:PSS/25 µL DM) in 10^{-3}M KCl and the GC/10 mC PEDOT:PSS electrode in 10^{-2} M KCl + 10^{-1}M NaCl as BGE.*

7.4. Chronoamperometric and chronocoulometric measurements

7.4.1. Preliminary measurements

In the original setup for constant-potential coulometry where the ISE was connected as a WE, an increase in analyte activity (addition step) produces a negative current. As explained in **Section 4.2**, this negative (reducing) transient current is produced to lower the ΔE_{cp} to compensate for the increase in ΔE_{pb}. On the contrary, in the proposed novel coulometric setup studied in this thesis, where the ISE is connected as the RE, a positive current is produced in the addition step. An increase in analyte activity increases the ΔE_{pb}, and since the potential difference between the RE and WE is kept constant, a positive (oxidizing) transient current flows between the WE and CE which increases the ΔE_{cp} in the WE by the same amount.

The comparison between the chronoamperometric and chronocoulometric plots obtained using the original and the novel experimental setups is shown in **Figure 25**. The GC/2 mC PEDOT:PSS/50 µL K^+-ISM electrode was connected as the WE with a double junction Ag/AgCl/3 M KCl/1 M LiOAc as the RE in the original setup (**Figure 25a)**. Alternatively, the K^+-ISE was connected as the RE in the new setup and a GC/10 mC PEDOT:PSS/25 µL DM electrode was connected as the WE (**Figure 25b)**.

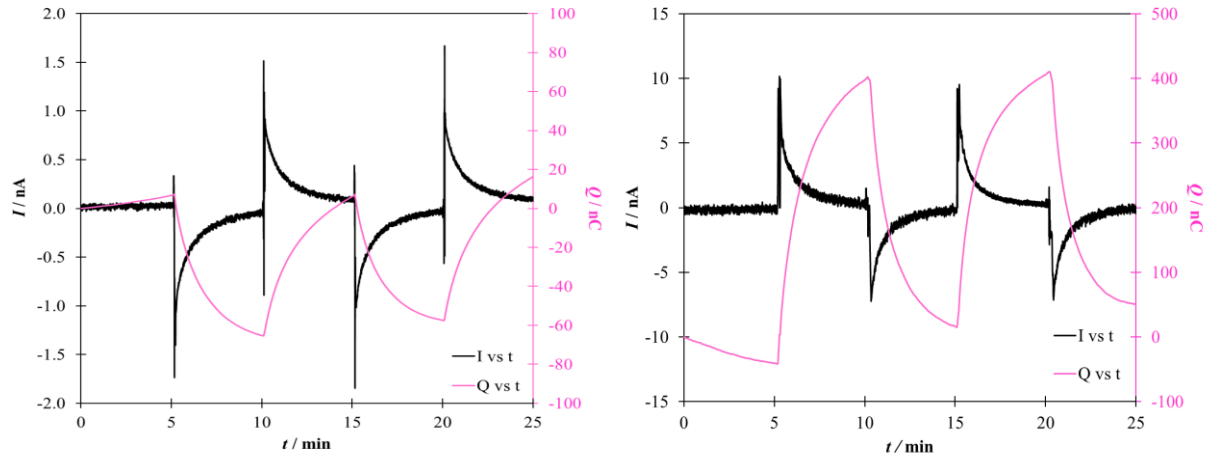

(a) WE: GC/2 mC PEDOT:PSS/50 µL K^+-ISM
RE: double junction Ag/AgCl/3 M KCl/1 M LiOAc
CE: GC rod

(b) WE: GC/10 mC PEDOT:PSS/25 µL DM
RE: GC/2 mC PEDOT:PSS/50 µL K^+-ISM
CE: GC rod

Figure 25. *Chronoamperometric and chronocoulometric response collected using the original* ***(a)*** *and the novel* ***(b)*** *experimental setups for the coulometric signal transduction. The addition/dilution steps correspond to a 5% increase/decrease of K^+ concentration in a starting solution of 10^{-3} M KCl + 10^{-1} M NaCl as BGE. Figures for the other two replicates are shown in* ***Appendix A.***

Both setups (**Figures 25a** and **25b**) showed good reversibility and signal repeatability after two consecutive addition/dilution steps. Aside from the mentioned differences in the direction of the peaks, preliminary experiments showed an improvement (*ca*. at least 5 times increase) of the current and charge signals, without sacrificing the equilibration time. It can also be noticed that the current and charge plots have good resolution, with signals detected up to the nanoscale, as compared to potential readings which are usually only down to the mV range.

Interestingly, similar results were obtained using other REs such as the GC/10 µL of 0.5 wt% MWCNTs/50 µL K^+-ISM **(Figure 26a)** and conventional K^+-ISE **(Figure 26b)**. At this point, it seems that the results are independent of the RE, as long as its Nernstian behavior was confirmed. This proves that the novel experimental setup can be used with a variety of ISEs, including the conventional ones, which is an advatnge of this setup over the original one.

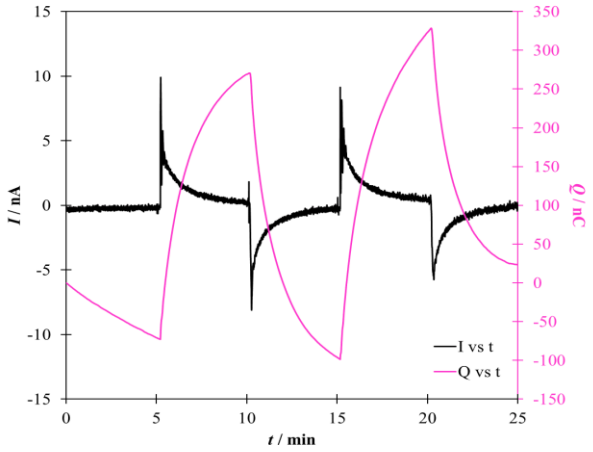

(a) WE: GC/10 mC PEDOT:PSS/25 µL DM
RE: GC/10 µL of 0.5 wt% MWCNTs/50 µL K^+-ISM
CE: GC rod

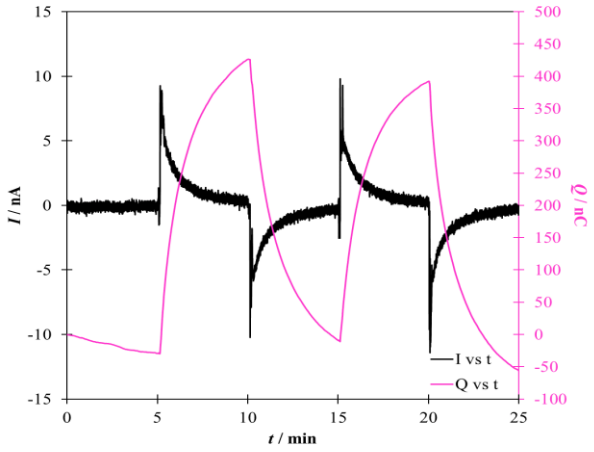

(b) WE: GC/10 mC PEDOT:PSS/25 µL DM
RE: conventional K^+-ISE
CE: GC rod

Figure 26. *Chronoamperometric and chronocoulometric response collected using the novel experimental setup for the coulometric signal transduction method using a GC/10 µL of 0.5 wt% MWCNTs/50 µL K^+-ISM* ***(a)*** *and a conventional K^+-ISE* ***(b)*** *connected as the RE with a GC/10 mC PEDOT:PSS/25 µL DM as the WE. The addition/dilution steps correspond to a 5% increase/decrease of K^+ concentration in a starting solution of 10^{-3} M KCl + 10^{-1} M NaCl as BGE.*

The estimation of the OCP to be used as the applied fixed potential is considered a pre-requisite for this experiment and is a good way of minimizing the equilibration time[10]. The significance of having adequate equilibration time has been emphasized in previous studies[11,43] to avoid the influence of residual currents

in the measurements. In some of the electrodes, the use of OCP as starting potential still gave a small initial reducing or oxidizing current, which resulted in a slightly slanted Q vs t graph upon integration of the current with time. In such cases, current baseline correction was performed, either by adding or subtracting a small amount on all the current values to bring the baseline close to zero, without affecting the magnitude of the signal peaks.

7.4.2. Effect of increasing the thickness of the dummy membrane in the WEs

The effect of increasing the thickness of dummy membrane in the WE was studied using electrodes with similar $Ø_{GC}$ and PEDOT:PSS film loading but with different DM thicknesses. As shown in **Figure 27**, electrodes with thicker DM resulted in smaller amplitude for the current peaks and longer equilibration time *ca*. greater than 15 minutes, as expected. Consequently, only one addition/dilution step was performed for the working electrodes with thicker dummy membranes.

It has been previously revealed through theoretical modelling that the peak current is inversely affected by the cell resistance[11]. From the results of the EIS measurements, it was confirmed that the addition of the dummy membrane provided a certain resistance R_{DM} to the electrode connected as WE. Moreover, it is the R_{DM} that heavily influences the time constant, τ, compared to C_{LF}. In addition to the capacitance and resistance, mass transport across the membrane could also affect the response time, which explains why thinner membranes are typically preferable[11].

Interestingly, it appears that the cumulated charge Q is independent of the DM thickness. This is a consequence of the process of integrating the current with time, removing the independence of cell resistance to Q, as reported in previous theoretical and experimental studies[4,11]. Although reversible, it can be seen in **Figures 27b** and **27d** that the current did not decay to the baseline and the residual current affected the magnitude of the reverse peak. The same results were obtained using different REs **(Appendix B)**. A summary table of the current and cumulated charge signals is also presented in **Appendix C**. For this reason, the rest of the experiments were performed only with the working electrodes having thinner DM.

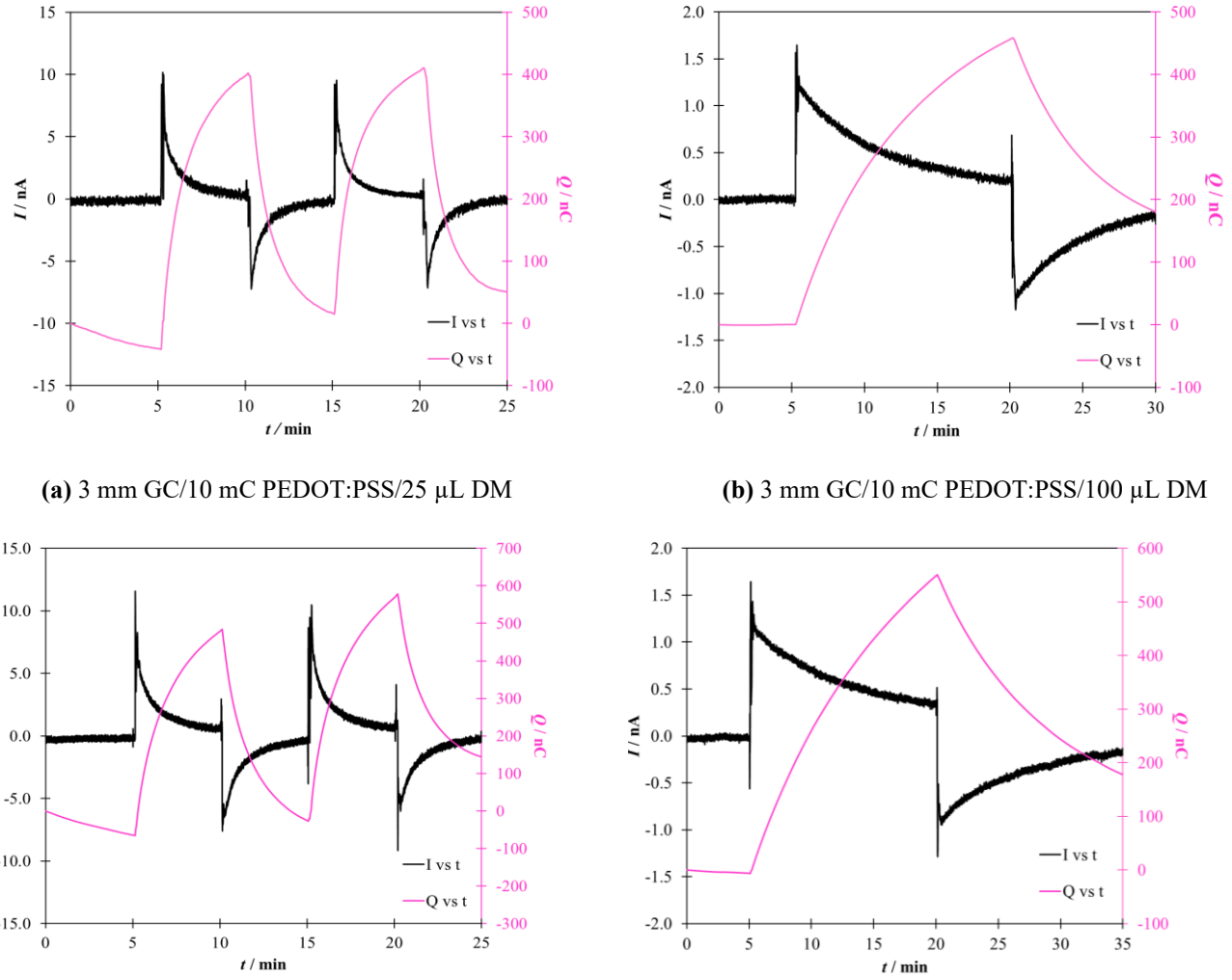

(a) 3 mm GC/10 mC PEDOT:PSS/25 µL DM

(b) 3 mm GC/10 mC PEDOT:PSS/100 µL DM

(c) 3 mm GC/20 mC PEDOT:PSS/25 µL DM

(d) 3 mm GC/20 mC PEDOT:PSS/100 µL DM

Figure 27. *Chronoamperometric and chronocoulometric response in the addition/dilution experiments using different PEDOT:PSS-based WEs and a GC/2 mC PEDOT:PSS/50 µL K^+-ISM connected as the RE. The addition/dilution steps correspond to a 5% increase/decrease of K^+ concentration in a starting solution of 10^{-3} M KCl + 10^{-1} M NaCl as BGE.*

7.4.3. Effect of increasing the redox capacitance of the PEDOT:PSS film in the WEs

The influence of the redox capacitance of the PEDOT:PSS film on signal amplification and equilibration time was investigated. Working electrodes with equivalently thin dummy membrane but with different $Ø_{GC}$ and Q_{polym} were examined through addition/dilution experiments with ΔC_{K+} = 5%. In general,

increasing the Q_{polym} (and consequently the redox capacitance) at constant $Ø_{GC}$ resulted in signal amplification. From the EIS experiments, it was observed that even though not as prominent as the effect of R_{DM}, the time constant τ is also influenced by the redox capacitance of the conducting polymer films. Increasing the amount of PEDOT:PSS means more material has to participate in the redox reaction to achieve the desired ΔE_{cp} [11,43], so a longer time was needed to reach equilibrium.

From the experimental results shown in **Figure 28**, it is notable that increasing the thickness of the PEDOT:PSS layer in WEs with the same $Ø_{GC}$ and DM thickness did not influence the amplitude of the current peak. Instead, it resulted in peak broadening and longer equilibration time, which has been consistently observed in both theoretical and experimental studies[4,10,11]. Interestingly, increasing the $Ø_{GC}$ from 3 mm to 5 mm with constant PEDOT:PSS film thickness at Q_{polym}10 mC and 27.8 mC, respectively seemed to be a better approach. Increasing the redox capacitance accompanied by larger electrode area, compared to just making the CP film thicker, allowed better access to the electroactive material. This resulted in higher and sharper current peaks without a significant lengthening of the equilibration time.

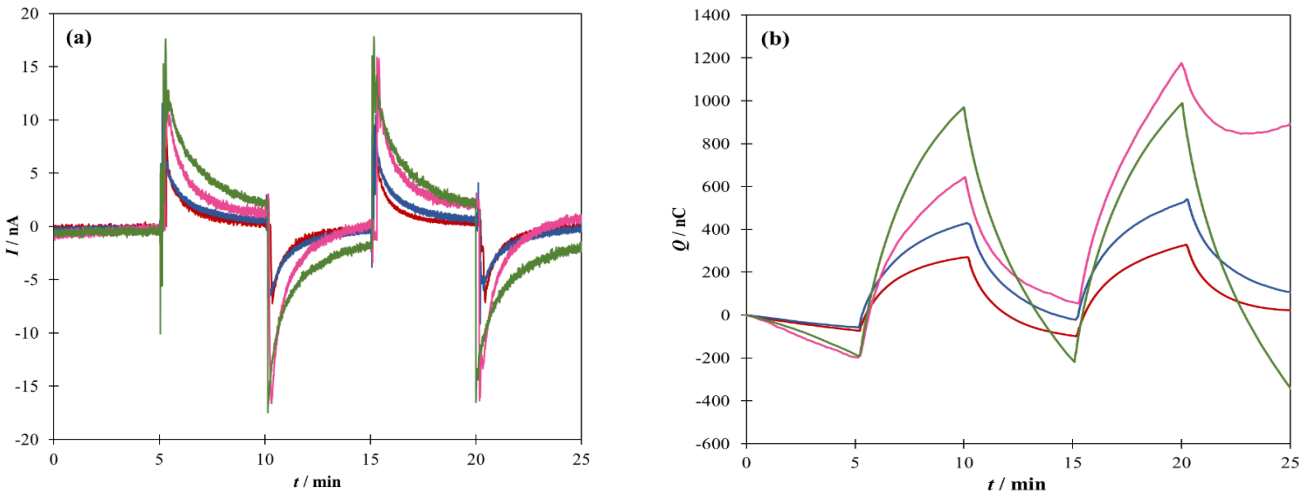

WEs: 3 mm GC/10 mC PEDOT:PSS/DM 5 mm GC/27.8 mC PEDOT:PSS/DM
3 mm GC/20 mC PEDOT:PSS/DM 5 mm GC/55.5 mC PEDOT:PSS/DM
RE: GC/2 mC PEDOT:PSS/50 µL K^+-ISM
CE: GC rod

Figure 28. *Chronoamperometric* ***(a)*** *and chronocoulometric* ***(b)*** *response during the addition/dilution experiments using different PEDOT:PSS-based WEs with equivalently thin dummy membrane and a GC/2 mC PEDOT:PSS/50 µL K^+-ISM connected as the RE. The addition/dilution steps correspond to a 5% increase/decrease in K^+ concentration in a starting solution of 10^{-3} M KCl +10^{-1} M NaCl as BGE.*

Integration of current with time resulted in a more pronounced relationship between the total cumulated charge Q and the redox capacitance of the PEDOT:PSS film. At constant DM thickness, it is expected that at higher sensitivity is achieved with increased redox capacitance, accompanied by a longer equilibration time[11]. As shown in **Figure 28b**, the change in Q values after each addition/dilution step increases with increasing the redox capacitance of the PEDOT:PSS film. Moreover, the electrode with lowest Q_{polym} (3 mm GC/10 mC PEDOT:PSS/DM), required shortest equilibration time, indicated by the appearance of a plateau-like region in the graph. Indeed, it is difficult to optimize the measurement conditions with parameters that contradict each other, but one can find a compromise between the amplitude of the current peak, response time and Q to achieve useful results. The same results and interpretations were obtained for the setups with GC/10 µL 0.5 wt% MWCNTs/50 µL K^+-ISM and conventional K^+-ISE connected as the RE (**Appendix D)**.

7.4.4. Calibration experiments

The capability of establishing a good correlation between the signal and analyte concentration using the novel experimental setup is determined using sequential dilution. For practical reasons, only the electrodes with equivalently thin dummy membranes were investigated, based on the observed equilibration times in **Section 7.4.2**. The results obtained from the successive dilution performed from 10^{-2} M to $10^{-3.4}$ M KCl with 10^{-1} M NaCl as BGE and having $\Delta \log C_{K+} = 0.2$ decade step^{-1} are summarized in **Figure 29**. The electrochemical cell is composed of a GC/2 mC PEDOT:PSS/50 µL K^+-ISM electrode connected as the RE, a GC rod connected as the CE, and GC/PEDOT:PSS WEs of similar DM thicknesses but with $Ø_{GC}$=3 and 5 mm, and various Q_{polym} used for the deposition of PEDOT:PSS.

The results of the calibration experiments were found to be consistent with the results presented in **Section 7.4.3**. Increasing the redox capacitance at constant $Ø_{GC}$ and DM thickness resulted in broader peaks and longer equilibration time. Since larger dilution steps are involved, the measurement time was extended from 5 minutes to 10 minutes for each concentration change. **Figure 29a** shows that the current peaks are quite reproducible throughout all the dilution steps. The drifting current baseline, most pronounced in the large electrode with the thicker PEDOT:PSS film and highest redox capacitance, is due to the insufficient time for equilibration in between the dilution steps. Moreover, the instability of

readings in electrodes with large area has been observed in a previous study and was explained to be the result of having larger surface for unwanted reactions to take place[10].

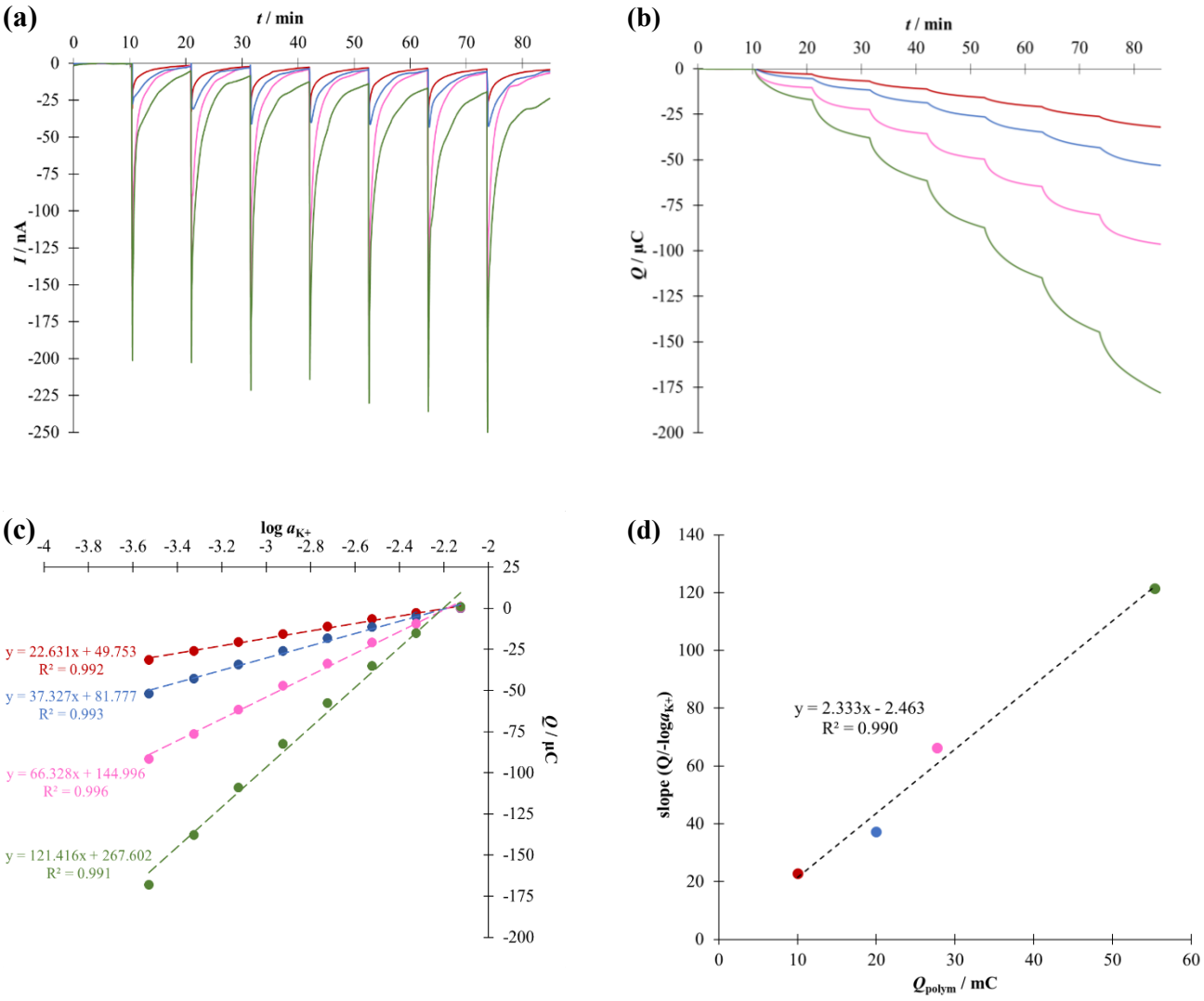

Figure 29. *Chronoamperometric* ***(a)****, chronocoulometric* ***(b)*** *response, cumulated charge Q vs loga_{K+}* ***(c)*** *during the calibration done in 10^{-2} M to $10^{-3.4}$ M KCl + 10^{-1} M NaCl as BGE with $\Delta logC_{K+}$ = 0.2 decade $step^{-1}$. GC/PEDOT:PSS electrodes with equivalent dummy membrane thickness were used as the WE and a GC/2 mC PEDOT:PSS/50 µL K^+-ISM connected as the RE. Slope values from results in* ***(c)*** *against the polymerization charge Q_{polym} of the PEDOT:PSS film in the WE* ***(d)****.*

Integration of the current-time curve was done to get the coulometric response (**Figure 29b**). Similar to the potentiometric calibration, a ladder-like plot was observed as the sequential dilution was performed.

The a_{K+} values were calculated at each step using the extended Debye-Huckel equation, considering the presence of BGE. Linear calibration plots were obtained for all working electrodes, with R^2 *ca.* 0.99 or better, indicating a good linear relationship between the Q and log a_{K+} values. Furthermore, the slopes from the calibration curves were determined and interpreted as the sensitivity to detecting changes in loga_{K+}. As dicussed earlier, it is expected that thicker PEDOT:PSS layer with higher redox capacitance would directly increase the sensitivity. The calibration curves in **Figure 29c** illustrated the increase in steepness of the line as the redox capacitance of the WE increases.

A plot of the obtained slopes against the Q_{polym} shows a direct relationship between these two values (**Figure 29d**). However, the curve is not perfectly linear, due to the difference in $Ø_{GC}$ of the electrodes. Doubling the PEDOT:PSS film thickness resulted in *ca.* 1.7 times increase in the slope value. Moreover, enlargement of working electrode area at constant PEDOT:PSS film thickness by *ca*. 2.8 times resulted in *ca.* 3.1 times increase in slope value . This supports the results from EIS measurements that spreading out the conducting polymer film in a wider area gives better accessibility to its redox capacitance as compared to depositing a thicker film on the same electrode area.

The same interpretations can be made for the calibration performed using a GC/10 µL 0.5 wt% MWCNTs/50 µL K^+-ISM WE and a conventional K^+-ISE connected as the RE **(Appendix E)**. The slopes of the calibration plots obtained from using different K^+-ISEs connected as the RE are summarized in **Appendix F**. **Figure 30** shows that the reproducibility of the results is good upon using different types of K^+-ISEs as RE, whether all-solid-state or conventional, as long as they exhibit acceptable potentiometric performance. This means that the novel experimental setup can be assembled using different electrode combinations to suit the demands of an experiment, and still get reproducible results.

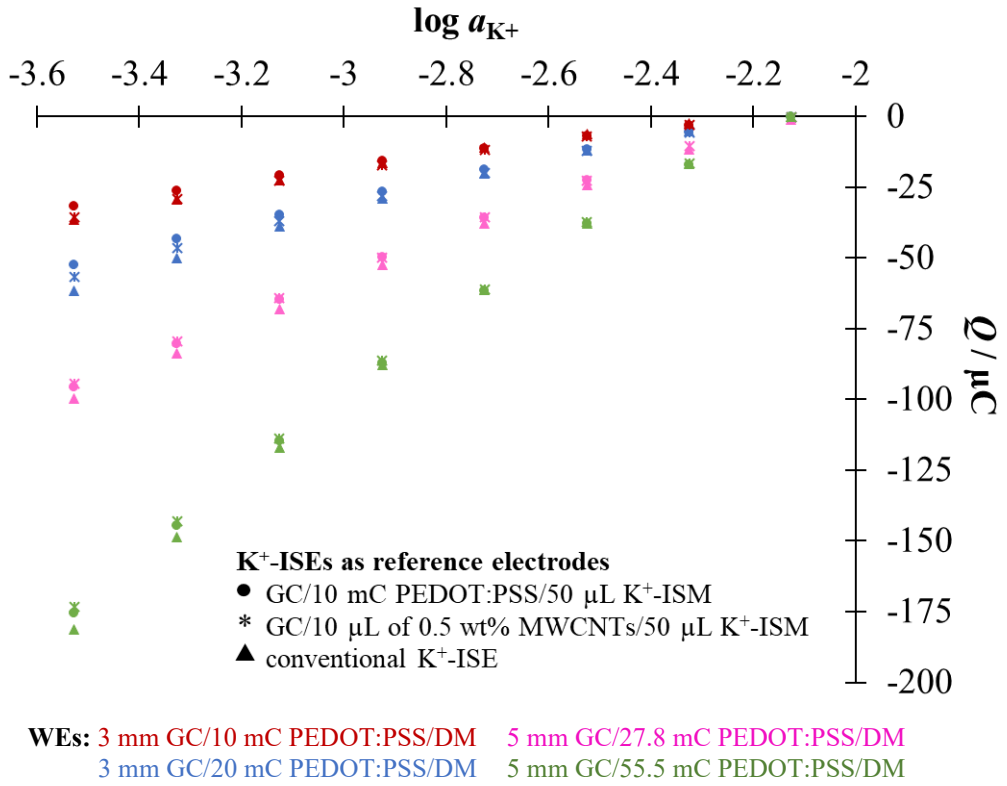

Figure 30. *Cumulated charge Q vs loga_{K+} from the calibration done in 10^{-2} M to $10^{-3.4}$ M KCl + 10^{-1} M NaCl as BGE with $\Delta logC_{K+}$ = 0.2 decade step^{-1}. GC/PEDOT:PSS electrodes with equivalent dummy membrane thickness were used as the WE with different K$^+$-ISEs as the REs.*

7.4.5. Detection of smaller concentration changes

One of the many advantages of the coulometric signal transduction method over the classical potentiometric one is its ability to detect smaller changes in concentration. The electrode response in the new setup was further investigated through addition/dilution experiments for ΔC_{K+} = 5%, 2.5%, and 1%, in the presence of 0.1 M NaCl as BGE. **Figure 31** shows results from using the 3 mm GC/10 mC PEDOT:PSS/25 μL DM electrode as the WE and GC/2 mC PEDOT:PSS/50 μL K$^+$-ISM as the RE. With smaller changes in K$^+$ concentration (ΔC_{K+}), smaller ΔE_{pb} is developed in the K$^+$-ISE. Consequently, a smaller equivalent ΔE_{cp} is needed to be established, therefore causing a smaller transient current to flow between the WE and CE. As expected, smaller ΔC_{K+} produced smaller current peaks that decay faster **(Figure 31a)** which was also observed in the chronocouolometric responses **(Figure 31b)**.

Looking closely at the results, a 1% change in concentration produced signals with magnitude that are comparable to the 5% change in concentration using the original setup in the preliminary measurements **(Section 7.4.1)**. This is in good agreement with the estimation that the novel experimental setup produced signals that are at least 5 times larger than the ones resulted from the original setup. Moreover, varying the REs did not have a huge influence on the results as can be seen in **Appendix G**.

Previous studies have shown that by using coulometric signal transduction method it is possible to detect as small as 0.1% changes in a_{K+}[4]. As a plan for the future, signal amplification could be investigated further along with electrodes having higher C_{LF} and larger $Ø_{GC}$. It is expected to obtain smaller signals with smaller ΔC_{K+} but this can be addressed by increasing C_{LF} and $Ø_{GC}$, at a longer equilibration time. Again, one can fine-tune these parameters to achieve the most suitable responses.

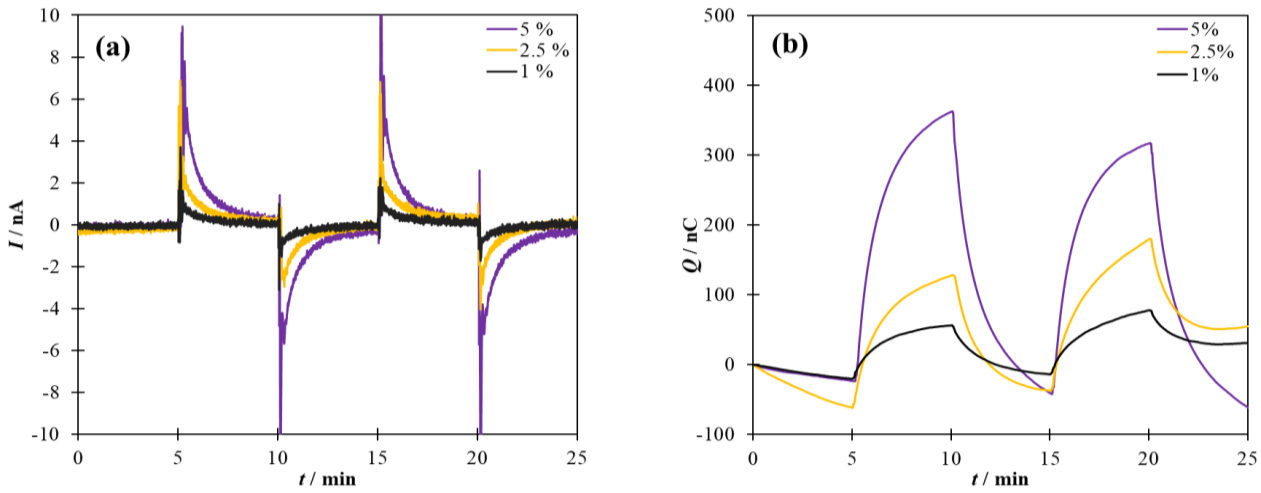

WE: 3 mm GC/10 mC PEDOT:PSS/DM
RE: GC/2 mC PEDOT:PSS/50 µL K^+-ISM
CE: GC rod

Figure 31. *Chronoamperometric* ***(a)*** *and chronocoulometric* ***(b)*** *response resulted from the addition/dilution experiments using a 3 mm GC/10 mC PEDOT:PSS/25 µL DM as the WE and a GC/2 mC PEDOT:PSS/50 µL K^+-ISM connected as the RE. The addition/dilution steps correspond to 5%, 2.5%, and 1% increase/decrease in K^+ concentration done in a starting solution of 10^{-3} M KCl +10^{-1} M NaCl as BGE.*

7.4.6. Measurements in a biological sample

The novel experimental setup for coulometric signal transduction method was found to work well in all the experiments using synthetic samples. However, it is important to know if this extends to real biological samples with more complex matrices. A human control serum sample containing 6.8 mM K^+ was used in this measurement and the addition/dilution steps were performed with ΔC_{K+} = 5% and 2.5%. As presented in **Figure 32,** the setup was able to detect the ΔC_{K+} but with an accompanying decrease in signal compared to the synthetic samples with simpler matrix. However, it is notable that the current and Q signal values resulted from measurement done in the control serum sample using the novel experimental setup are higher compared to the results from synthetic sample tested in the original experimental setup with ΔC_{K+} = 5% **(Section 7.4.1)**.

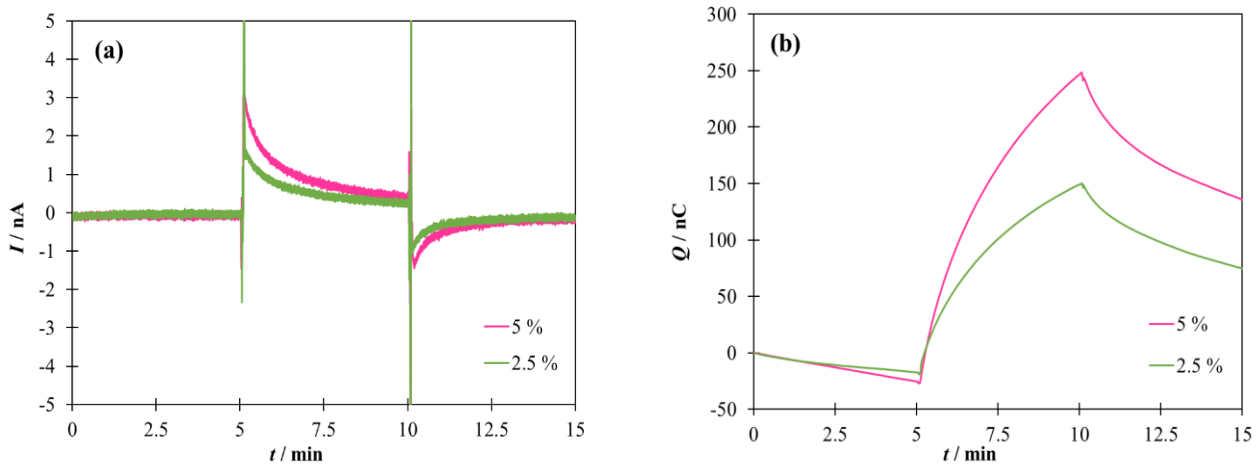

WE: 3 mm GC/10 mC PEDOT:PSS/DM
RE: GC/2 mC PEDOT:PSS/50 µL K^+-ISM
CE: GC rod

Figure 32. *Chronoamperometric* ***(a)*** *and chronocoulometric* ***(b)*** *response during the addition/dilution experiments done using a 3 mm GC/10 mC PEDOT:PSS/25 µL DM as the WE and a GC/2 mC PEDOT:PSS/50 µL K^+-ISM connected as the RE. The addition/dilution steps correspond to 5% and 2.5% change in K^+ concentration of a control serum sample containing 6.8 mM K^+.*

8. CONCLUSIONS

A novel experimental setup for the coulometric signal transduction method in ion-selective electrodes was investigated in this thesis. It is an alternative signal readout possibility based on the principle of constant potential coulometry and involves the transformation of potentiometric analyte detection into a coulometric signals. The single-compartment electrochemical cell used was composed of a K^+-ISE connected as the RE, a non-selective WE, and a GC as counter electrode. Three different types of K^+-ISEs with near Nernstian and reproducible slopes were used as the REs: one conventional and two SCISEs with either PEDOT:PSS or MWCNTs as solid contact. The WEs were prepared using GC substrates of two different sizes covered with various thicknesses of the PEDOT:PSS film and dummy membrane.

The approaches employed in this work made it possible to combine the two-compartment sample and detection cells from previous studies into a simple and convenient single-compartment cell. The PEDOT:PSS film in the WE exhibits a non-selective cationic response, but the use of a high concentration of BGE effectively masked the sensitivity of the WE to changes in K^+ concentration. This maintained the separation of potentiometric detection in the K^+-ISE from the signal transformation in the WE despite being in the same measuring cell. Furthermore, a layer of dummy membrane (without ionophore) was added on top of PEDOT:PSS in the WE to regulate the signal and measurement time. Furthermore, potentiometric tests revealed that the dummy membrane made the working electrode insensitive to the presence of gases such O_2 or CO_2 that may cause the alteration of pH in the sample solution.

Results from cyclic voltammetry measurements confirmed the successful deposition of the transducer layers with their corresponding capacitive-like currents. The electrochemical properties of the fabricated WE were investigated further through electrochemical impedance spectroscopy measurements. The addition of a dummy membrane layer to impart electrode resistance was clearly depicted on the resulting spectra that were dominated by a resistive semicircle. Moreover, the presence of the Warburg impedance line at low frequencies indicates that the ion-to-electron transduction is diffusion-limited.

Results from chronoamperometry and chronocoulometry addition/dilution experiments showed that the new setup produced results with improved current and charge signals as compared to the original setup used earlier. Good reversibility and measurement repeatability were exhibited by the current (I) and cumulated charge (Q) signals. Upon working with different types of REs, it was proven that the novel setup is compatible with both solid-contact and conventional ISEs, compared to the original setup that is limited to SCISEs. Furthermore, the performance of the WE was found to be independent of the RE, shown by the good agreement of results obtained using different types of K^+-ISEs connected as the RE. This demonstrates the versatility of the novel setup, where different types of RE and WE can be combined together, depending on the needs of the analysis.

Consistent with previous studies and with the results from electrochemical impedance spectroscopy measurements, increasing the thickness of the resistive dummy membrane in the WE resulted in longer equilibration time and smaller signals. Increasing the redox capacitance of the conducting polymer produced larger signals at the expense of longer equilibration time. Interestingly, it was observed that instead of simply depositing a thicker film, increasing the redox capacitance of the CP film is more effective when accompanied by an increase in electrode area. The calibration curves obtained during the sequential dilution experiments showed a good linear relationship between Q and $\log a_{K+}$. Moreover, the determination of smaller changes in the analyte concentration (5%, 2.5%, and 1%) was successful. Further tests showed that the setup can also be useful in samples with more complicated matrices like human serum sample.

For future studies, improvement of measurement stability should be considered especially in terms of electrode preparation such as the dummy membrane composition and the transducer layer material in the WE. In addition, there are still many factors to be studied and optimized such as the equilibration time and the electrode response in more complex matrices. Based on the presented results, it can be stated that the new setup for coulometric signal transduction that was successfully examined in this work offers a simple and versatile alternative for signal transduction in ISEs compatible for specific purposes.

9. REFERENCES

1. van de Velde, L., d'Angremont, E. & Olthuis, W. Solid contact potassium selective electrodes for biomedical applications – a review. *Talanta* **160**, 56–65 (2016).
2. Hanrahan, G., Patil, D. G. & Wang, J. Electrochemical sensors for environmental monitoring: design, development and applications. *J. Environ. Monitor.* **6**, 657 (2004).
3. Rousseau, C. R. & Bühlmann, P. Calibration-free potentiometric sensing with solid-contact ion-selective electrodes. *TrAC Trends in Analytical Chemistry* **140**, 116277 (2021).
4. Han, T., Mattinen, U. & Bobacka, J. Improving the Sensitivity of Solid-Contact Ion-Selective Electrodes by Using Coulometric Signal Transduction. *ACS Sens.* **4**, 900–906 (2019).
5. Bobacka, J., Ivaska, A. & Lewenstam, A. Potentiometric Ion Sensors. *Chem. Rev.* **108**, 329–351 (2008).
6. Wang, H., Yuan, B., Yin, T. & Qin, W. Alternative coulometric signal readout based on a solid-contact ion-selective electrode for detection of nitrate. *Analytica Chimica Acta* **1129**, 136–142 (2020).
7. Yin, T., Wang, H., Li, J., Yuan, B. & Qin, W. Translating potentiometric detection into non-enzymatic amperometric measurement of H2O2. *Talanta* **232**, 122489 (2021).
8. Shao, Y., Ying, Y. & Ping, J. Recent advances in solid-contact ion-selective electrodes: functional materials, transduction mechanisms, and development trends. *Chem. Soc. Rev.* **49**, 4405–4465 (2020).
9. Yan, R., Qiu, S., Tong, L. & Qian, Y. Review of progresses on clinical applications of ion selective electrodes for electrolytic ion tests: from conventional ISEs to graphene-based ISEs. *Chemical Speciation & Bioavailability* **28**, 72–77 (2016).

10. Han, T., Vanamo, U. & Bobacka, J. Influence of Electrode Geometry on the Response of Solid-Contact Ion-Selective Electrodes when Utilizing a New Coulometric Signal Readout Method. *ChemElectroChem* **3**, 2071–2077 (2016).
11. Jarolímová, Z., Han, T., Mattinen, U., Bobacka, J. & Bakker, E. Capacitive Model for Coulometric Readout of Ion-Selective Electrodes. *Anal. Chem.* **90**, 8700–8707 (2018).
12. Sun, X., Yin, T., Zhang, Z. & Qin, W. Redox probe-based amperometric sensing for solid-contact ion-selective electrodes. *Talanta* **239**, 123114 (2022).
13. Frant, M. S. & Ross, J. W. Potassium Ion Specific Electrode with High Selectivity for Potassium over Sodium. *Science* **167**, 987–988 (1970).
14. Cattrall, R. *Chemical sensors*. (Oxford University Press, 1997).
15. Skoog, D. A., West, D. M., Holler, F. J. & Crouch, S. R. *Fundamentals of Analytical Chemistry*. (Cengage Learning, 2014).
16. Mikhelson, K. N. *Ion-Selective Electrodes*. vol. 81 (Springer Berlin Heidelberg, 2013).
17. Lewenstam, A. Routines and Challenges in Clinical Application of Electrochemical Ion-Sensors. *Electroanalysis* **26**, 1171–1181 (2014).
18. Zdrachek, E. & Bakker, E. Potentiometric Sensing. *Anal. Chem.* **91**, 2–26 (2019).
19. K, N. & Rout, C. S. Conducting polymers: a comprehensive review on recent advances in synthesis, properties and applications. *RSC Adv.* **11**, 5659–5697 (2021).
20. Bobacka, J. & Ivaska, A. Chemical Sensors Based on Conducting Polymers. in *Electropolymerization* (eds. Cosnier, S. & Karyakin, A.) 173–187 (Wiley-VCH Verlag GmbH & Co. KGaA, 2010). doi:10.1002/9783527630592.ch9.
21. MacDiarmid, A. The concept of ‘doping’ of conducting polymers: the role of reduction potentials. *Phil. Trans. R. Soc. Lond. A* **314**, 3–15 (1985).

22. Moore, J. W. Chemistry in the News Nobel Prizes, 2000. *Journal of Chemical Education* **78**, 2 (2001).

23. Bobacka, J., Lewenstam, A. & Ivaska, A. Electrochemical impedance spectroscopy of oxidized poly(3,4-ethylenedioxythiophene) film electrodes in aqueous solutions. *Journal of Electroanalytical Chemistry* **489**, 17–27 (2000).

24. Inzelt, G. Chemical and Electrochemical Syntheses of Conducting Polymers. in *Conducting Polymers* 123–148 (Springer Berlin Heidelberg, 2008). doi:10.1007/978-3-540-75930-0_4.

25. Vázquez, M., Bobacka, J., Ivaska, A. & Lewenstam, A. Influence of oxygen and carbon dioxide on the electrochemical stability of poly(3,4-ethylenedioxythiophene) used as ion-to-electron transducer in all-solid-state ion-selective electrodes. *Sensors and Actuators B: Chemical* **82**, 7–13 (2002).

26. Crespo, G. A., Macho, S. & Rius, F. X. Ion-Selective Electrodes Using Carbon Nanotubes as Ion-to-Electron Transducers. *Anal. Chem.* **80**, 1316–1322 (2008).

27. Crespo, G. A., Macho, S., Bobacka, J. & Rius, F. X. Transduction Mechanism of Carbon Nanotubes in Solid-Contact Ion-Selective Electrodes. *Anal. Chem.* **81**, 676–681 (2009).

28. Yuan, D., Anthis, A., Ghahraman, Asfhar, M., Pankratova, N., Cuartero, M., Crespo, G. & Bakker, E. All-Solid-State Potentiometric Sensors with a Multiwalled Carbon Nanotube Inner Transducing Layer for Anion Detection in Environmental Samples. *Anal. Chem.* **87**, 8640–8645 (2015).

29. Kour, R., Arya, S., Young, S., Gupta, V., Bandhoria, P. & Khosla, A. Review—Recent Advances in Carbon Nanomaterials as Electrochemical Biosensors. *J. Electrochem. Soc.* **167**, 037555 (2020).

30. Crespo, G. A., Gugsa, D., Macho, S. & Rius, F. X. Solid-contact pH-selective electrode using multi-walled carbon nanotubes. *Anal Bioanal Chem* **395**, 2371–2376 (2009).

31. Mousavi, Z., Teter, A., Lewenstam, A., Maj-Zurawska, M., Ivaska, A. & Bobacka, J. Comparison of Multi-walled Carbon Nanotubes and Poly(3-octylthiophene) as Ion-to-Electron Transducers in All-Solid-State Potassium Ion-Selective Electrodes. *Electroanalysis* **23**, 1352–1358 (2011).

32. Mousavi, Z., Bobacka, J., Lewenstam, A. & Ivaska, A. Poly(3,4-ethylenedioxythiophene) (PEDOT) doped with carbon nanotubes as ion-to-electron transducer in polymer membrane-based potassium ion-selective electrodes. *Journal of Electroanalytical Chemistry* **633**, 246–252 (2009).
33. Eugster, R, Rosatzin, T., Rusterholz, B., Aebersold, B., Pedrazza, U., Riiegg, D., Schmid, A., Spichiger, U. & Simon, W. Plasticizers for liquid polymeric membranes of ion-selective chemical sensors. *Analytica Chimica Acta.* **289**, 1-13 (1994).
34. Armstrong, R. D. & Horvai, G. Properties of PVC based membranes used in ion-selective electrodes. *Electrochimica Acta* **35**, 1–7 (1990).
35. Bakker, E. & Pretsch, E. Lipophilicity of tetraphenylborate derivatives as anionic sites in neutral carrier-based solvent polymeric membranes and lifetime of corresponding ion-selective electrochemical and optical sensors. *Analytica Chimica Acta* **309**, 7–17 (1995).
36. Zook, J. M., Langmaier, J. & Lindner, E. Current-polarized ion-selective membranes: The influence of plasticizer and lipophilic background electrolyte on concentration profiles, resistance, and voltage transients. *Sensors and Actuators B: Chemical* **136**, 410–418 (2009).
37. Fuller, T. F. & Harb, J. N. *Electrochemical engineering*. (Wiley, 2018).
38. Bard, A. J. & Faulkner, L. R. *Electrochemical methods: fundamentals and applications*. (Wiley, 2001).
39. Palmer, B. F. & Clegg, D. J. Physiology and pathophysiology of potassium homeostasis. *Advances in Physiology Education* **40**, 480–490 (2016).
40. Hupa, E., Vanamo, U. & Bobacka, J. Novel Ion-to-Electron Transduction Principle for Solid-Contact ISEs. *Electroanalysis* **27**, 591–594 (2015).
41. Jaworska, E., Pawłowski, P., Michalska, A. & Maksymiuk, K. Advantages of Amperometric Readout Mode of Ion-selective Electrodes under Potentiostatic Conditions. *Electroanalysis* **31**, 343–349 (2019).

42. Cuartero, M., Crespo, G. A. & Bakker, E. Ionophore-Based Voltammetric Ion Activity Sensing with Thin Layer Membranes. *Anal. Chem.* **88**, 1654–1660 (2016).

43. Vanamo, U., Hupa, E., Yrjänä, V. & Bobacka, J. New Signal Readout Principle for Solid-Contact Ion-Selective Electrodes. *Anal. Chem.* **88**, 4369–4374 (2016).

44. Monk, P. M. *Fundamentals of Electro-Analytical Chemistry*. (John Wiley & Sons LTD, 2001).

45. Wang, J. *Analytical Electochemistry (Second Edition)*. (Wiley-VCH, 2000).

46. Moran, P. J. & Gileadi, E. Alleviating the common confusion caused by polarity in electrochemistry. *J. Chem. Educ.* **66**, 912 (1989).

47. Wang, S., Zhang, J., Gharbi, O., Vivier, V., Gao, M. & Orazem, M. Electrochemical impedance spectroscopy. *Nat Rev Methods Primers* **1**, 41 (2021).

48. Inzelt, G. Chronoamperometry, Chronocoulometry, and Chronopotentiometry. in *Encyclopedia of Applied Electrochemistry* (eds. Kreysa, G., Ota, K. & Savinell, R. F.) 207–214 (Springer New York, 2014). doi:10.1007/978-1-4419-6996-5_217.

49. Vázquez, M., Danielsson, P., Bobacka, J., Lewenstam, A. & Ivaska, A. Solution-cast films of poly(3,4-ethylenedioxythiophene) as ion-to-electron transducers in all-solid-state ion-selective electrodes. *Sensors and Actuators B: Chemical* **97**, 182–189 (2004).

10. APPENDICES

10.1. Appendix A

Comparison between the original and the novel experimental setup

Original setup

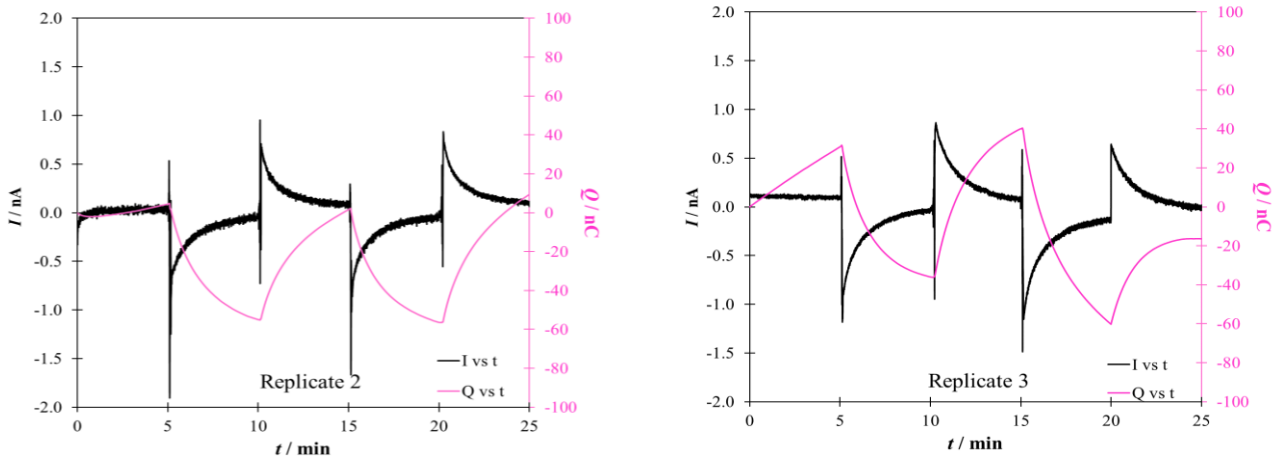

WE: GC/2 mC PEDOT:PSS/50 µL K^+-ISM
RE: double junction Ag/AgCl/3 M KCl/1 M LiOAc
CE: GC rod

Chronoamperometric and chronocoulometric response collected using the original experimental setup for the coulometric signal transduction method. The addition/dilution steps correspond to a 5% increase/decrease of K^+ concentration in a starting solution of 10^{-3} M KCl +10^{-1} M NaCl as BGE.

Novel setup

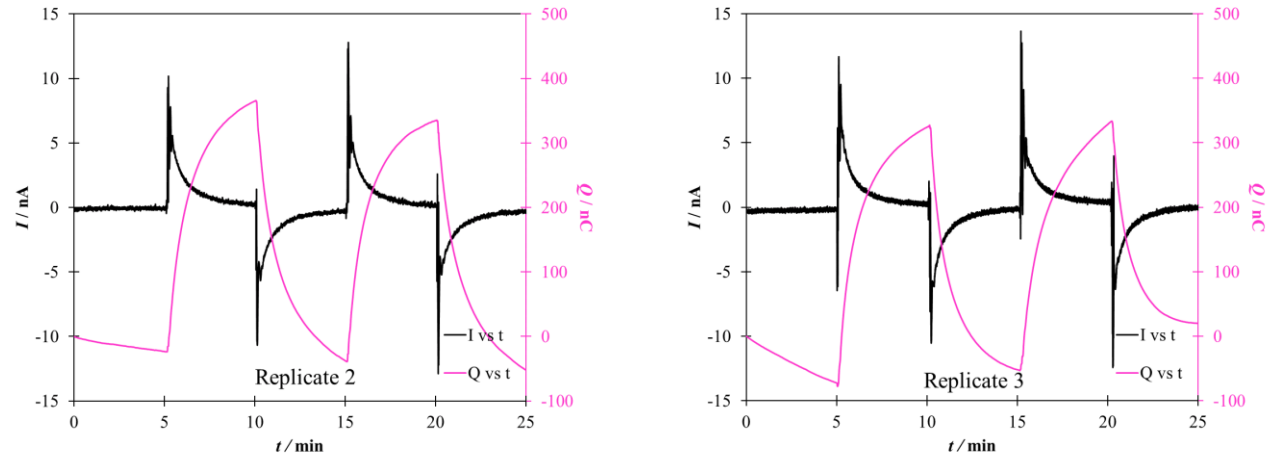

WE: GC/10 mC PEDOT:PSS/25 µL DM
RE: GC/2 mC PEDOT:PSS/50 µL K^+-ISM
CE: GC rod

Chronoamperometric and chronocoulometric response collected using the novel experimental setup for the coulometric signal transduction method. The addition/dilution steps correspond to a 5% increase/decrease of K^+ concentration in a starting solution of 10^{-3} M KCl+10^{-1} M NaCl as BGE.

10.2. Appendix B

Effect of varying dummy membrane thickness

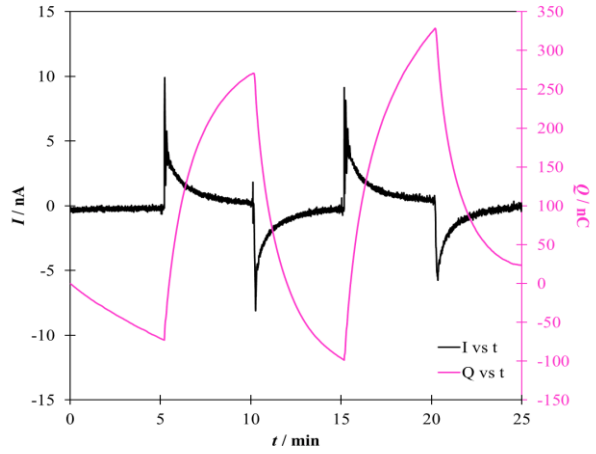

(a) 3 mm GC/10 mC PEDOT:PSS/thin DM

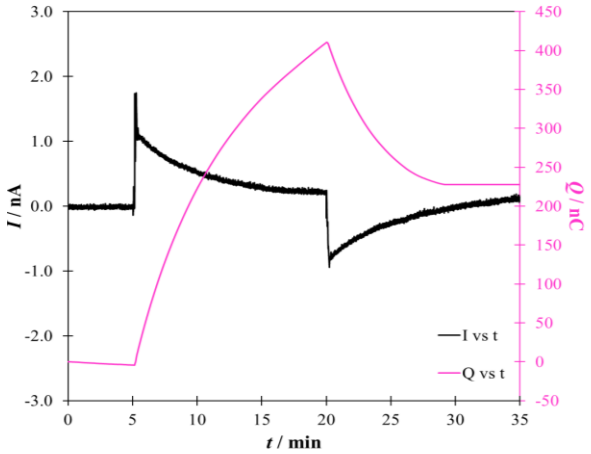

(b) 3 mm GC/10 mC PEDOT:PSS/thick DM

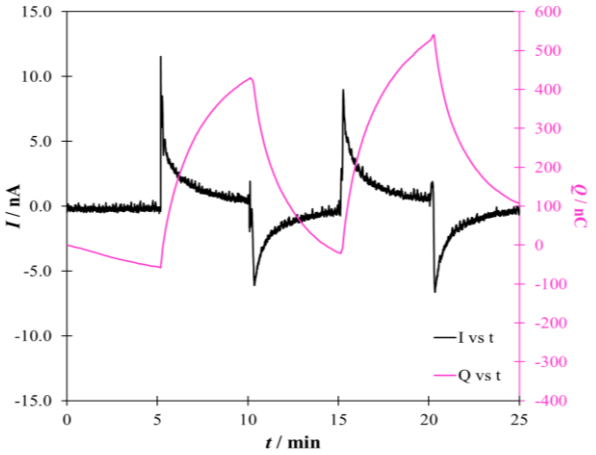

(c) 3 mm GC/20 mC PEDOT:PSS/thin DM

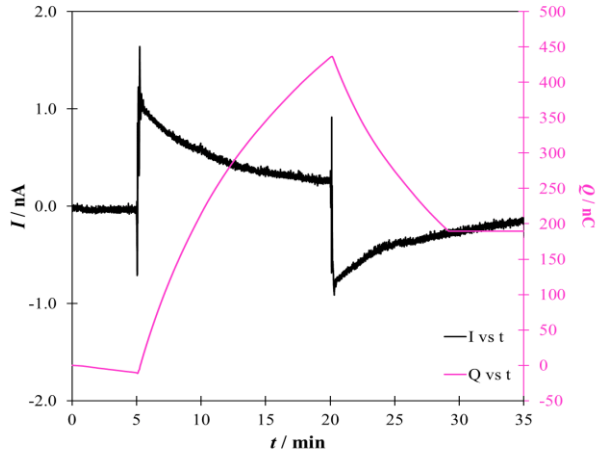

(d) 3 mm GC/20 mC PEDOT:PSS/thick DM

RE: GC/10 µL 0.5 wt% MWCNTs/50 µL K^+-ISM

CE: *GC rod*

Chronoamperometric and chronocoulometric response in the addition/dilution experiments using different PEDOT:PSS-based WEs and a GC/10 µL 0.5 wt% MWCNTs/50 µL K^+-ISM connected as the RE. The addition/dilution steps correspond to a 5% increase/decrease of K^+ concentration in a starting solution of 10^{-3} M KCl + 10^{-1} M NaCl as BGE.

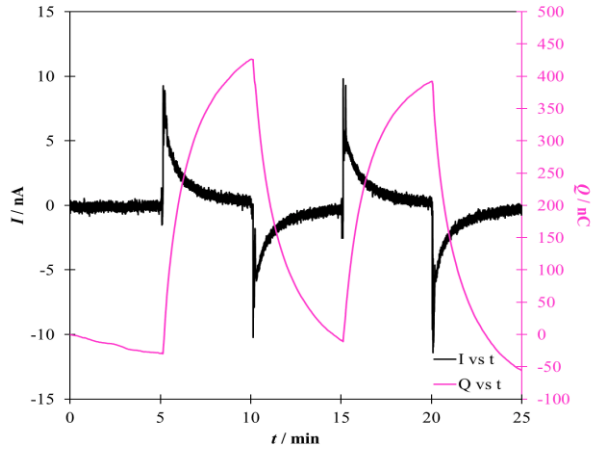

(a) 3 mm GC/10 mC PEDOT:PSS/25 µL DM

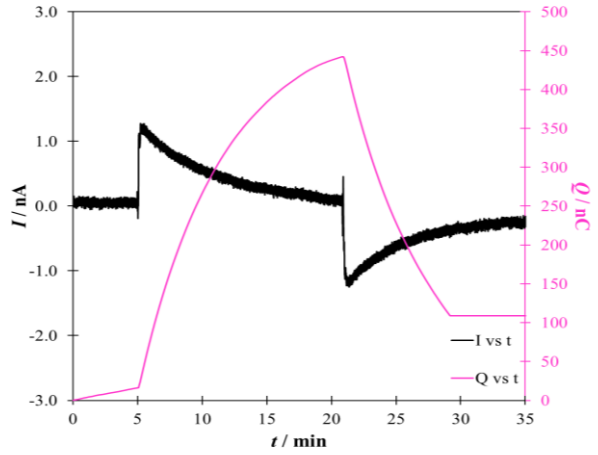

(b) 3 mm GC/10 mC PEDOT:PSS/100 µL DM

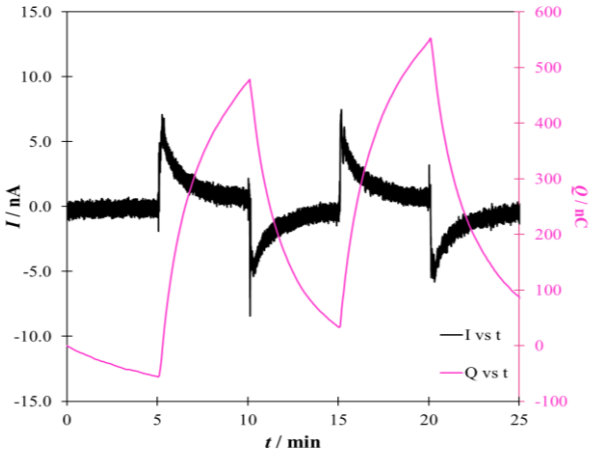

(c) 3 mm GC/20 mC PEDOT:PSS/25 µL DM

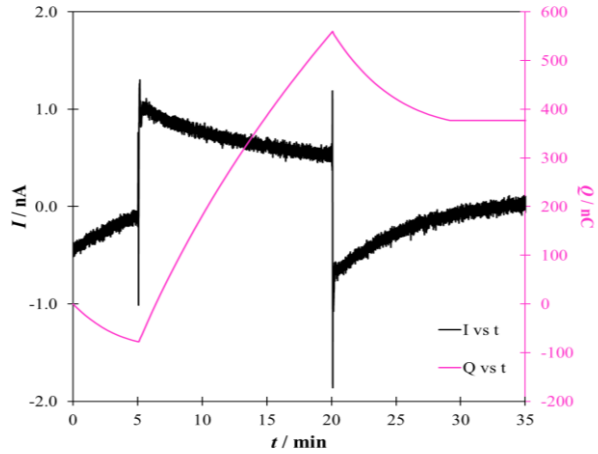

(d) 3 mm GC/20 mC PEDOT:PSS/100 µL DM

RE: conventional K^+-ISE
CE: GC rod

Chronoamperometric and chronocoulometric response in the addition/dilution experiments using different PEDOT:PSS-based WEs and a conventional K^+-ISE connected as the RE. The addition/dilution steps correspond to a 5% increase/decrease of K^+ concentration in a starting solution of 10^{-3} M KCl + 10^{-1} M NaCl as BGE.

10.3. Appendix C

Summary of the chronoamperometry and chronocoulometry responses obtained using the novel experimental setup with different PEDOT:PSS-based working electrodes and various K^+-ISEs connected as the reference electrode. The estimated current and cumulated charge signals correspond to a 5% increase/decrease in K^+ concentration in a starting solution of 10^{-3} M KCl with 10^{-1} M NaCl as BGE.

Working electrodes	**Time constant / s**	**K^+-ISEs connected as RE**		
		GC/2 mC PEDOT:PSS/ 50 µL K^+-ISM	**GC/10 µL 0.5 wt% MWCNTs/ 50 µL K^+-ISM**	**Conventional K^+-ISE**
current and cumulated charge signals of electrodes with equivalently thin dummy membrane, equilibration time *ca* 5 min				
3 mm/10 mC PEDOT:PSS/25 µL DM	23.16	*ca* 7.5 nA, *ca* 350 nC	*ca* 7.5 nA, *ca* 300 nC	*ca* 7.5 nA, *ca* 400 nC
3 mm/20 mC PEDOT:PSS/25 µL DM	23.42	*ca* 7.5 nA, *ca* 450 nC	*ca* 7.5 nA, *ca* 400 nC	*ca* 7.5 nA, *ca* 450 nC
current and cumulated charge signals of electrodes with equivalently thick dummy membrane, equilibration time > 15 min				
3 mm/10 mC PEDOT:PSS/100 µL DM	314.91	*ca* 1.5 nA, *ca* 400 nC	*ca* 1.5 nA, *ca* 400 nC	*ca* 1.5 nA, *ca* 450 nC
3 mm/20 mC PEDOT:PSS/100 µL DM	319.03	*ca* 1.5 nA, *ca* 450 nC	*ca* 1.5 nA, *ca* 450 nC	*ca* 1.5 nA, *ca* 550 nC

10.4. Appendix D

Effect of increasing the redox capacitance of the PEDOT:PSS film in the WEs

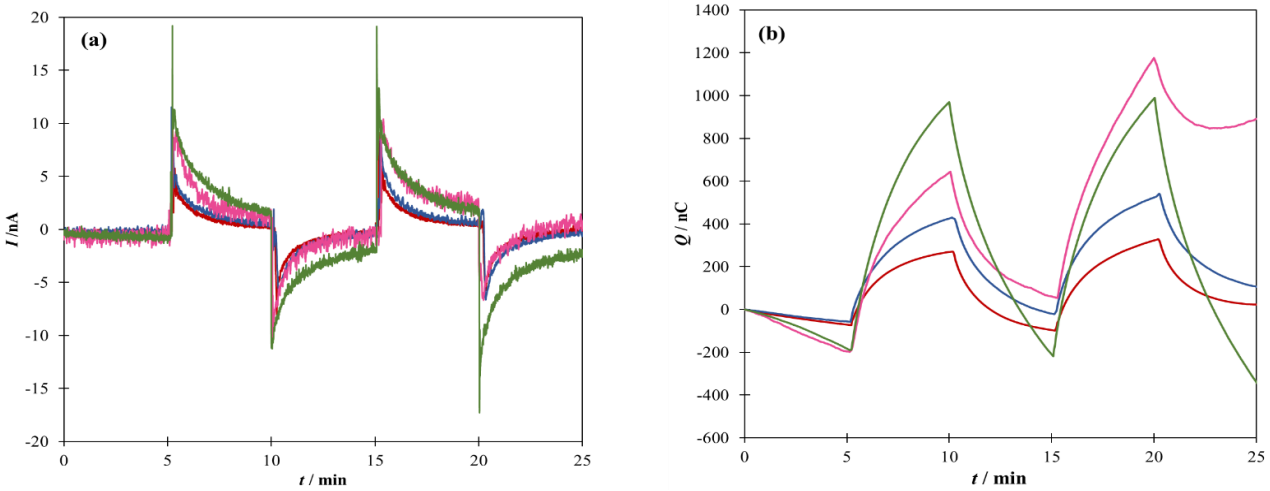

WEs: 3 mm GC/10 mC PEDOT:PSS/DM 5 mm GC/27.8 mC PEDOT:PSS/DM
3 mm GC/20 mC PEDOT:PSS/DM 5 mm GC/55.5 mC PEDOT:PSS/DM
RE: GC/10 µL 0.5 wt% MWCNTs /50 µL K^+-ISM
CE: GC rod

*Chronoamperometric **(a)** and chronocoulometric **(b)** response during the addition/dilution experiments using different PEDOT:PSS-based WEs with equivalently thin dummy membrane and a GC/10 µL 0.5 wt% MWCNTs/50 µL K^+-ISM connected as the RE. The addition/dilution steps correspond to a 5% increase/decrease in K^+ concentration in a starting solution of 10^{-3} M KCl +10^{-1} M NaCl as BGE.*

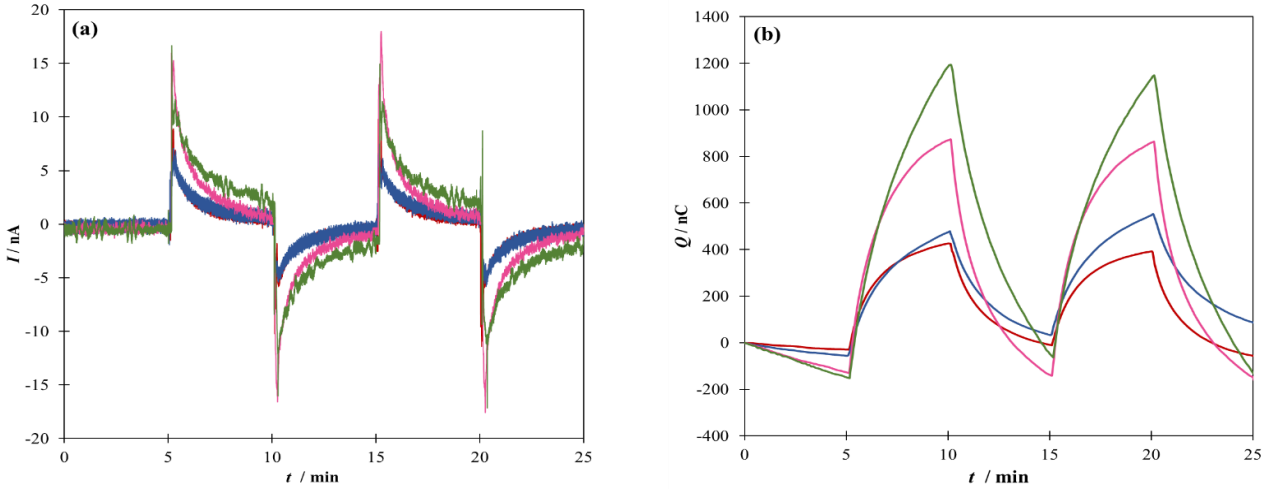

WEs: 3 mm GC/10 mC PEDOT:PSS/DM 5 mm GC/27.8 mC PEDOT:PSS/DM
3 mm GC/20 mC PEDOT:PSS/DM 5 mm GC/55.5 mC PEDOT:PSS/DM
RE: conventional K^+-ISE
CE: GC rod

*Chronoamperometric **(a)** and chronocoulometric **(b)** response during the addition/dilution experiments using different PEDOT:PSS-based WEs with equivalently thin dummy membrane and a conventional K^+-ISE connected as the RE. The addition/dilution steps correspond to a 5% increase/decrease in K^+ concentration in a starting solution of 10^{-3} M KCl + 10^{-1} M NaCl as BGE.*

10.5. Appendix E

Chronoamperometric/chronocoulometric calibration

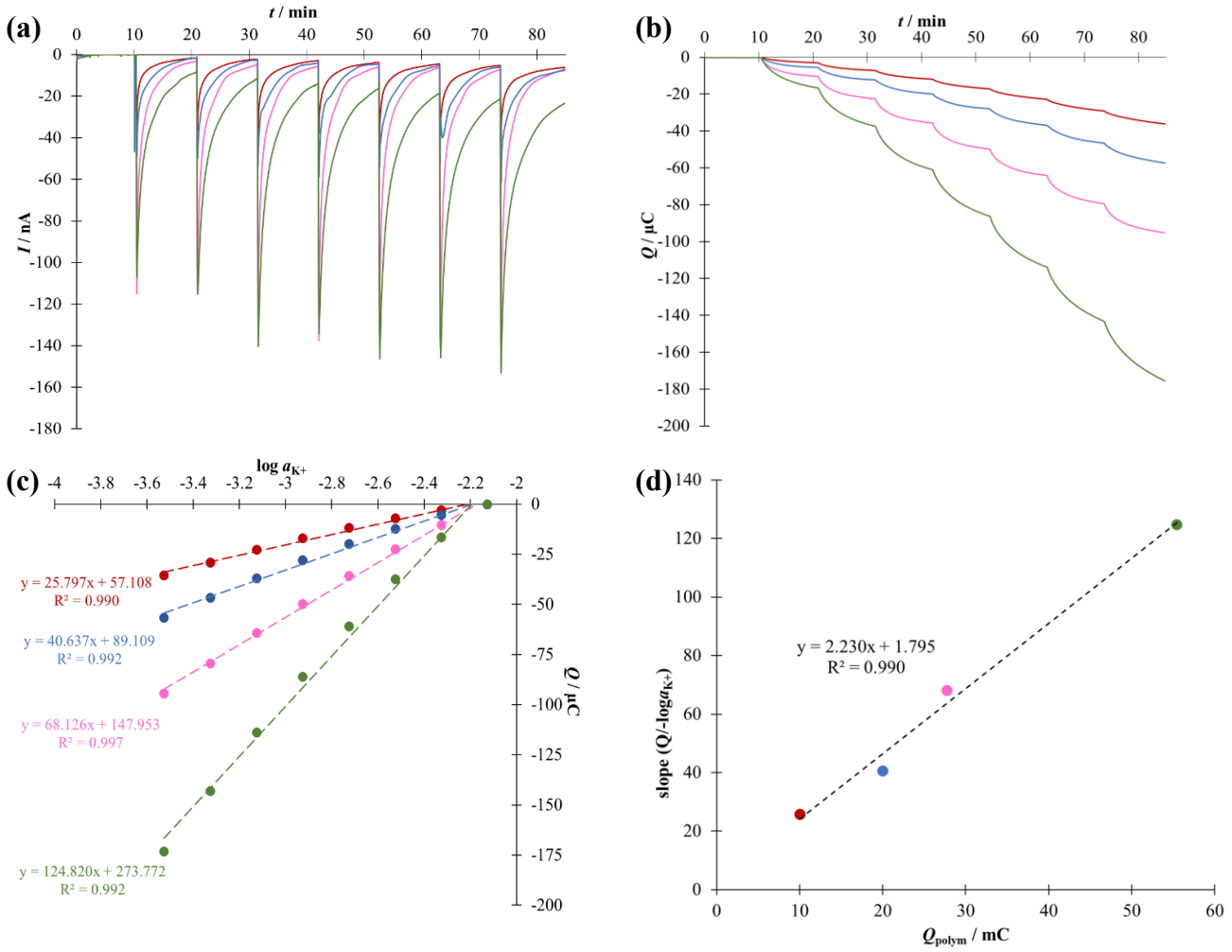

WEs: 3 mm GC/10 mC PEDOT:PSS/DM 5 mm GC/27.8 mC PEDOT:PSS/DM
3 mm GC/20 mC PEDOT:PSS/DM 5 mm GC/55.5 mC PEDOT:PSS/DM
RE: GC/10 µL 0.5 wt% MWCNTs/50 µL K^+-ISM
CE: GC rod

*Chronoamperometric **(a)**, chronocoulometric **(b)** response, cumulated charge Q vs loga_{K+} **(c)** during the calibration in 10^{-2} M to $10^{-3.4}$ M KCl + 10^{-1} M NaCl as BGE with $\Delta logC_{K+}$ = 0.2 decade step^{-1}. GC/PEDOT:PSS electrodes with equivalently thin dummy membrane were used as the WE and a GC/10 µL 0.5 wt% MWCNTs /50 µL K^+-ISM was connected as the RE. Slope values from results in **(c)** against the polymerization charge Q_{polym} of the PEDOT:PSS film in the WE **(d)**.*

Chronoamperometric/chronocoulometric calibration

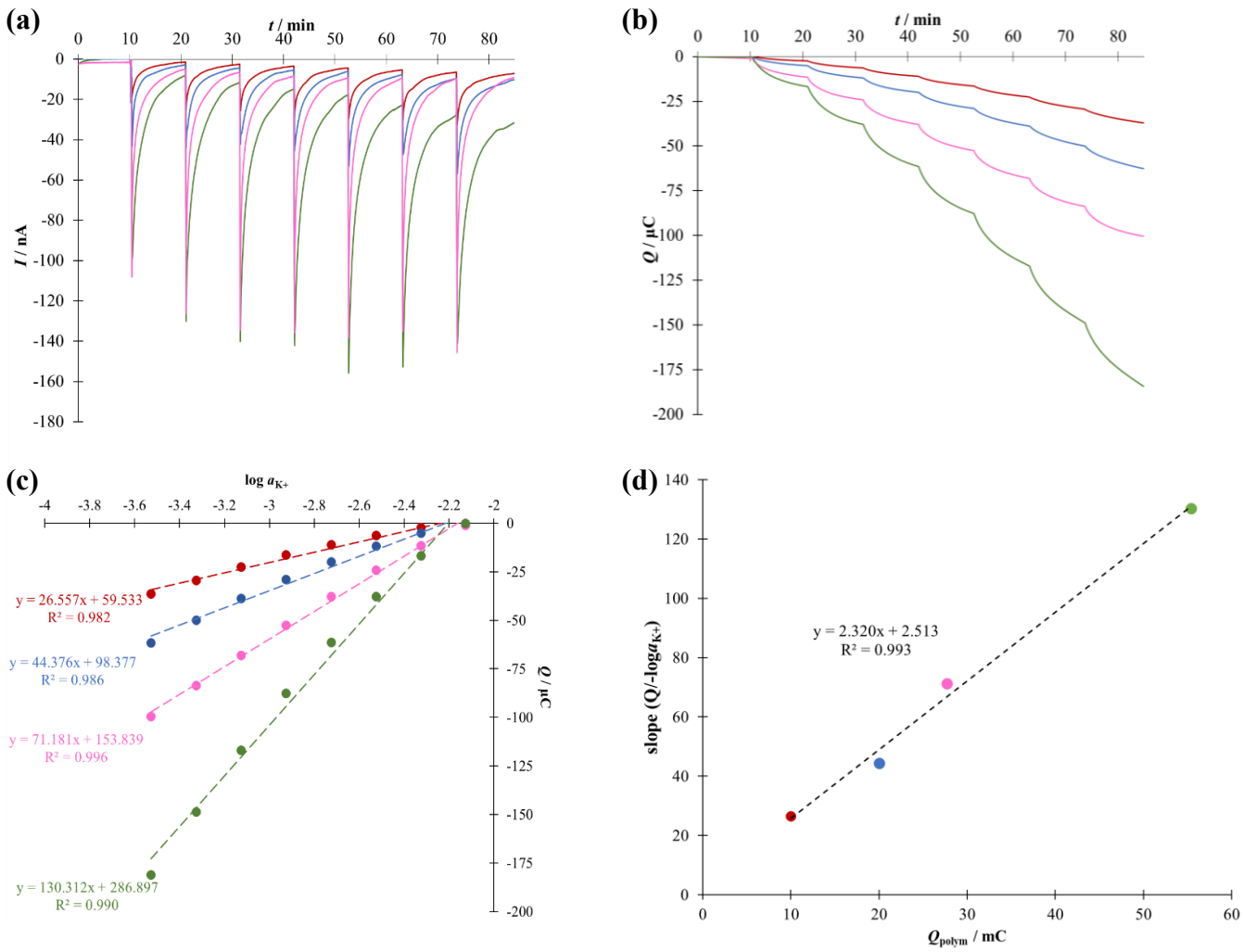

WEs: 3 mm GC/10 mC PEDOT:PSS/DM 5 mm GC/27.8 mC PEDOT:PSS/DM
3 mm GC/20 mC PEDOT:PSS/DM 5 mm GC/55.5 mC PEDOT:PSS/DM
RE: conventional K^+-ISE
CE: GC rod

*Chronoamperometric **(a)**, chronocoulometric **(b)** response, cumulated charge Q vs $loga_{K+}$ **(c)** during the calibration in 10^{-2} M to $10^{-3.4}$ M KCl + 10^{-1} M NaCl as BGE with $\Delta logC_{K+}$ = 0.2 decade $step^{-1}$. GC/PEDOT:PSS electrodes with equivalently thin dummy membrane were used as the WE and a conventional K^+-ISE was connected as the RE. Slope values from results in **(c)** against the polymerization charge Q_{polym} of the PEDOT:PSS film in the WE **(d)**.*

10.6. Appendix F

Summary of the slopes of the calibration curves obtained using the novel experimental setup with different PEDOT:PSS-based working electrodes and various K^+-ISEs connected as the reference electrode. The calibration experiments were performed from 10^{-2} M to $10^{-3.4}$ M KCl with 10^{-1} M NaCl as BGE and $\Delta \log C_{K+} = 0.2$ decade $step^{-1}$.

Working electrodes	**K^+-ISEs connected as RE**		
	GC/2 mC PEDOT:PSS/50 µL K^+-ISM	**GC/10 µL 0.5 wt% MWCNTs/50 µL K^+-ISM**	**Conventional K^+-ISE**
With equivalently thin dummy membrane	slope (Q/-loga_{k+})		
3 mm/10 mC PEDOT:PSS/25 µL DM	22.631	25.797	26.557
3 mm/20 mC PEDOT:PSS/25 µL DM	37.327	40.637	44.376
5 mm/27.8 mC PEDOT:PSS/41.7 µL DM	66.328	68.126	71.181
5 mm/55.5 mC PEDOT:PSS/41.7 µL DM	121.416	124.820	130.312

10.7. Appendix G

Smaller changes in concentration

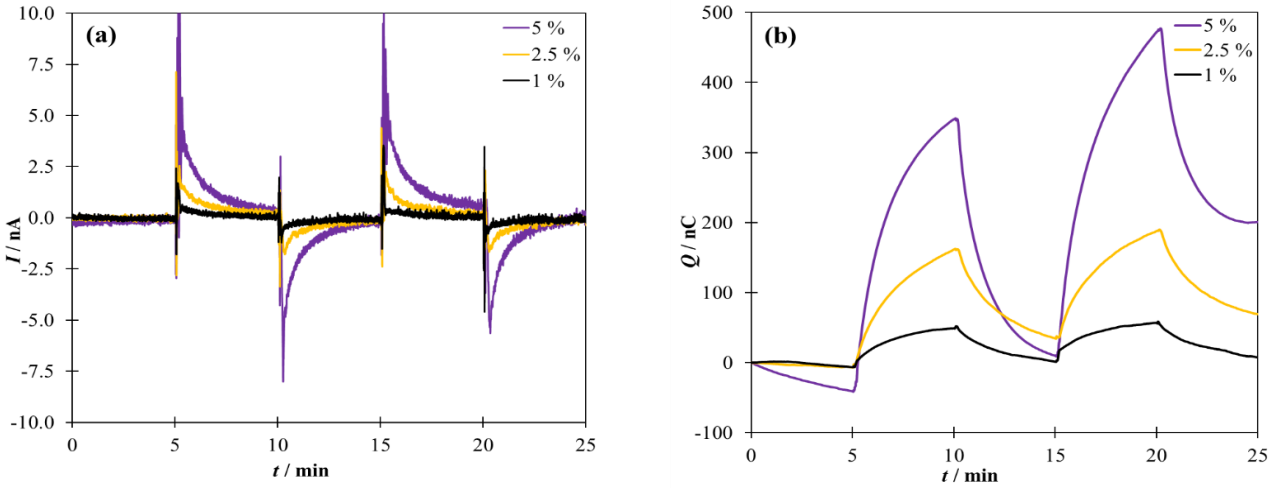

RE: GC/10 µL 0.5 wt% MWCNTs/50 µL K^+-ISM
WE: 3 mm GC/10 mC PEDOT:PSS/25 µL DM
CE: GC rod

*Chronoamperometric **(a)** and chronocoulometric **(b)** response during the addition/dilution experiments using a 3 mm GC/10 mC PEDOT:PSS/25 µL DM as the WE and a GC/10 µL 0.5 wt% MWCNTs/50 µL K^+-ISM connected as the RE. The addition/dilution steps correspond to 5%, 2.5%, and 1% increase/decrease in K^+ concentration done in a starting solution of 10^{-3} M KCl +10^{-1} M NaCl as BGE.*

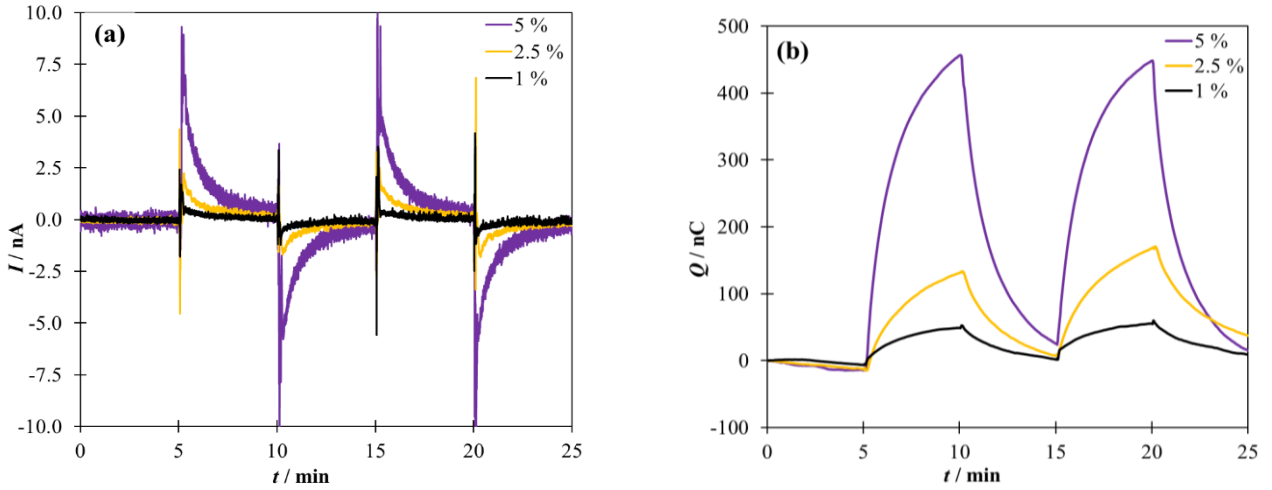

RE: conventional K^+-ISE
WE: 3 mm GC/10 mC PEDOT:PSS/25 µL DM
CE: GC rod

*Chronoamperometric **(a)** and chronocoulometric **(b)** response during the addition/dilution experiments using a 3 mm GC/10 mC PEDOT:PSS/25 µL DM as the WE and a conventional K^+-ISE connected as the RE. The addition/dilution steps correspond to 5%, 2.5%, and 1% increase/decrease in K^+ concentration done in a starting solution of 10^{-3} M KCl + 10^{-1} M NaCl as BGE.*